OCS Study
MMS 93-0032

Chemosynthetic Ecosystems Studies

Interim Report

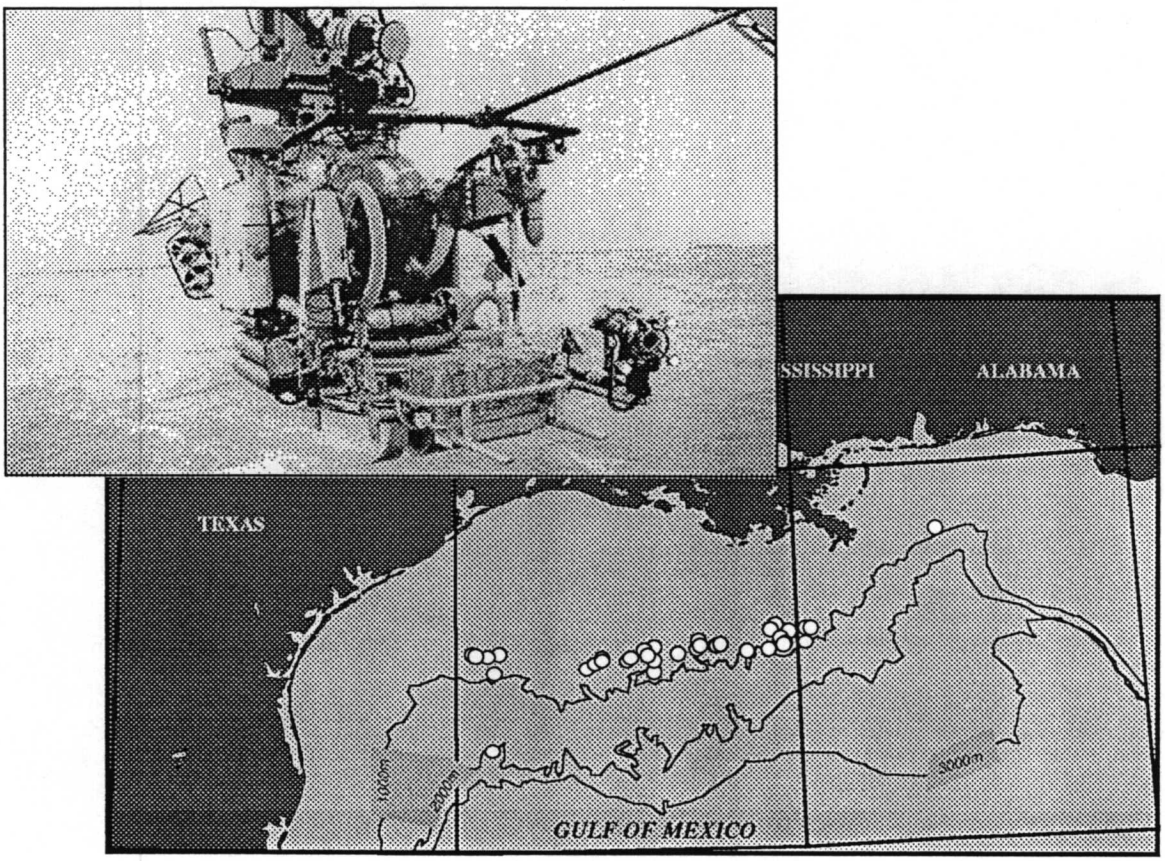

MMS
U.S. Department of the Interior
Minerals Management Service
Gulf of Mexico OCS Region

OCS Study
MMS 93-0032

Chemosynthetic Ecosystems Studies

Interim Report

Editors

Ian R. MacDonald
William W. Schroeder

Prepared under MMS Contract
14-35-0001-30555
by
Texas A&M University
Texas A&M Research Foundation
College Station, Texas

Published by

U.S. Department of the Interior
Minerals Management Service
Gulf of Mexico OCS Region

New Orleans
June 1993

DISCLAIMER

This draft report was prepared under contract between the Minerals Management Service (MMS) and Geochemical and Environmental Research Group. This draft report has been technically reviewed by the MMS and approved for publication. Approval does not signify that the contents necessarily reflect the views and policies of the Service, nor does mention of trade names or commercial products constitute endorsement or recommendation for use. It is, however, exempt from review and compliance with MMS editorial standards.

REPORT AVAILABILITY

Extra copies of the report may be obtained from the Public Information Unit (Mail Stop 5034) at the following address:

U.S. Department of the Interior
Minerals Management Service
Gulf of Mexico OCS Region
1201 Elmwood Park Boulevard
New Orleans, Louisiana 70123-2394

Attention: Public Information Unit (MS 5034)

Telephone Number: (504) 736-2519

CITATION

Suggested citation:

U.S. Dept. of the Interior, Minerals Management Service. 1993. Chemosynthetic Ecosystems Studies Interim Report. Prepared by Geochemical and Environmental Research Group. U.S. Dept. of the Interior, Minerals Mgmt. Service, Gulf of Mexico OCS Regional Office, New Orleans, LA, 110 pp.

COVER PHOTOGRAPH

The foreground photograph shows the submersible *Johnson Sea-Link I* preparing for one of its many dives to study chemosynthetic ecosystems. The map depicts the locations of known chemosynthetic ecosystems in the northern Gulf of Mexico.

ABSTRACT

The U.S. Department of Interior, Minerals Management Service (MMS), Gulf of Mexico OCS Region Office has initiated the Chemosynthetic Ecosystems Study (Contract 14-35-0001-30555) to compile management-relevant scientific information concerning the prominent biological communities of tube worms, mussels, and clams that occur at natural oil seeps on the continental slope and that derive their food supply from chemicals associated with the seeps. This is the second of three major reports that will be issued by the Study, which is sponsored by the MMS. This document is the Interim Report of the Study and is issued following the completion of all scheduled field work and data collection. The report describes the methods, techniques, and equipment used during the field program, will outline the data sets and collections collected during the field study, and will discuss the analyses and interpretations employed to treat these materials. The individual study topics covered in the report comprise the following:

Chapter 2 - Geological Studies;
Chapter 3 - Geochemical Processes;
Chapter 4 - Long-Term Change;
Chapter 5 - Community Structure and Short-Term Change;
Chapter 6 - Methods, Collections, and Status of Growth Studies of Chemosynthetic Fauna and Associated Analyses of Animals and Habitats;
Chapter 7 - Heterotrophic Megafauna of Chemosynthetic Seep Ecosystems;
Chapter 8 - Ancillary Studies: Topics Not Included in Proposal, but under Consideration for Additional Work.

TABLE OF CONTENTS

LIST OF FIGURES

LIST OF TABLES

ACKNOWLEDGMENTS

Ian R. MacDonald and William W. Schroeder, Editors

Contributors (in alphabetical order):

W. Russell Callender
Robert S. Carney
Charles R. Fisher
M.C. Kennicutt II
Changshik Lee
Ian R. MacDonald
Eric N. Powell
William S. Sager
William W. Schroeder

Technical Support:

Cheryl Hussey
Dave Martin
Joanna Fritz

1.0 Introduction

The Chemosynthetic Ecosystems Study concerns the prominent biological communities of tube worms, mussels, and clams that occur at natural oil seeps on the continental slope and that derive their food supply from chemicals associated with the seeps. This is the second of three major reports that will be issued by the Study, which is sponsored by the U.S. Department of Interior Minerals Management Service (MMS), Gulf of Mexico Region OCS Office (Contract 14-35-0001-30555).

The Study is being conducted by ten principal investigators (PIs) and four associates under the overall management of the Geochemical and Environmental Research Group (GERG) of Texas A&M University (Table 1.1 lists the names, responsibilities, and affiliations of the PIs and associates). At this juncture, the Program has completed all of the three scheduled research cruises and has completed preliminary processing of material collected on these cruises. The first report of the Study presented a review of published literature pertinent to the subject and a limited synthesis of data collected prior to commencement of the Program. This report will describe the methods, techniques, and equipment used during the field program, will outline the data sets and collections obtained during the field study, and will discuss the analyses and interpretations employed to treat these materials.

1.1. Chemosynthetic Ecosystems Study: Overview

The chemosynthetic communities associated with hydrocarbon seeps on the Louisiana/Texas continental slope are one of a series of functionally and taxonomically related assemblages in the deep-sea. These communities are characteristically associated with sources of hydrogen sulfide and/or methane in an oxygenated environment. The underlying geological processes supplyingthese reduced compounds vary from site to site. These communities are the focus of intense international research, and many of the programmatic questions being asked in the Gulf of Mexico have been identified in previous efforts elsewhere. These questions include:

1. What are the specific geological, chemical, and ecological processes whereby seeping hydrocarbons support distinct communities?
2. How do these communities persist, and to what degree do physical-chemical and biological factors interact on different spatial and temporal scales?
3. How quickly and to what degree will chemosynthetic communities recover from mechanical damage?
4. How rare or common are dense chemosynthetic communities across the Gulf of Mexico?
5. How much biomass do these communities comprise on the continental slope and what is the contribution to slope ecosystems?

Table 1.1. Principal Investigators (*) and associates for the Chemosynthetic Ecosystems Study. Affiliation abbreviations are:
TAMU *Texas A&M University*;
GERG *Geochemical and Environmental Research Group*;
OCNG *Oceanography Department*;
LSU *Louisiana State University*;
PSU *Pennsylvania State University*;
WHOI *Woods Hole Oceanographic Institution*; and
UA/DISL *University of Alabama Dauphin Island Sea Lab.*

Principal Investigator	Affiliation	Major Responsibility
Javier Alcala-Herrera	TAMU/GERG	Chemical Analyses
James M. Brooks*	TAMU/GERG	Project Management
Robert S. Carney*	LSU	Ecology
Charles R. Fisher*	PSU	Physiology
Norman L. Guinasso, Jr.*	TAMU/GERG	Data Analysis
Holgar W. Jannasch*	WHOI	Microbiology
Mahlon C. Kennicutt II*	TAMU/GERG	Geochemistry
Ian R. MacDonald*	TAMU/GERG	Ecology/Management
Eric N. Powell*	TAMU/OCNG	Taphonomy
William S. Sager*	TAMU/OCNG	Geology
William W. Schroeder*	UA/DISL	Geology/Ecology
Dan L. Wilkinson	TAMU/GERG	Field Logistics
Carl O. Wirsen	WHOI	Microbiology
Gary A. Wolff	TAMU/GERG	Data Management

In the Gulf of Mexico, these basic scientific questions assume an applied importance because of the potential impact on a fauna uniquely associated with exploitable hydrocarbon reserves. To evaluate possible impacts, it is important that we understand how these communities persist in the natural environment and the extent to which they will be resilient in the face of petroleum-related activities.

Evaluations of potential impacts depend in part on how chemosynthetic communities are defined, rather than on specific findings. If the characteristic features of seep communities (that is, authigenic carbonate substrate and the associated tubeworms, mussels, solitary corals, soft corals, etc.) are considered to be a variation of a live bottom, then regulation is comparatively straightforward; as with any live bottom, sensitivity to petroleum activities would be determined, and appropriate limits placed on the proximity of activities. In addition to the usual live bottom concerns, it is important to determine how the unique, and probably complex, linkages between geology, geochemistry, and biology might be affected by industry activities. Informed management decisions can only be made when the possible effects of petroleum activities on these critical linkages are known.

In this regard, our overall goal is to determine to what extent the Gulf of Mexico deep water petroleum seeps fit into two possible categories: a robust or fragile community.

- A Robust Community - Since these communities are naturally associated with petroleum seepage and degradation processes, then they may be uniquely adapted and resistant to impact by hydrocarbons. They may, in effect, be "weeds" capable of rapidly locating and colonizing numerous sites which afford the appropriate geological-chemical setting. In such a case, simple restrictions to prevent mechanical damage might be sufficient when combined with regulations which preserve some habitat areas.

- A Fragile Community - Alternately, it can be argued that these communities occupy a relatively rare and narrow niche associated with different phases of petroleum seepage and degradation. Being so very highly specialized, the narrow range of environmental conditions which support these communities might easily be altered by drilling and production activities. Indeed, production may result in a loss of the very energy source required to maintain these communities.

Determination of the extent to which the hydrocarbon seep communities are robust or fragile entails coordinated geological, geochemical, and ecological research efforts that will develop an understanding of the spatial and temporal linkage pattern between hydrocarbon seepage and the formation of chemosynthetic community development on the seafloor. These investigations must determine how communities are established and persist within the particular geological and geochemical environments that support them. As stated above, the key to understanding potential impacts lies in understanding how the processes of geology, geochemistry, and biology interact.

1.2. Summary of Progress to Date

The Study was initiated on 26 July 1991 (Figure 1.1 shows a project time-line). The PIs made substantial resources available to the Study at no cost to MMS. These resources included a large and diverse amount of data gathered during previous investigations of chemosynthetic ecosystems in the Gulf of Mexico. Additionally, the North Carolina NOAA National Undersea Research Center had granted the PIs a series of submarine dives with the *Johnson Sea-Link* during 1991 and 1992. Consequently, the PIs were able to offer MMS a research program that was more extensive and which commenced field activities more expeditiously than anticipated in the Request for Proposal (RFP).

The first submarine cruise (JSL-91) utilized the *Johnson Sea-Link I*, deployed from the support ship R/V *Seward Johnson* during 25, 26, and 31 August and 14-27 September 1991. Appendix A contains the post-cruise report for this cruise, which details the day-to-day activities and locations occupied. The individual sections of this report discuss in detail the techniques used and the materials collected. Briefly, the cruise occupied six sites, at locations of known chemosynthetic communities, in water depths of 500 to 750 m. Collectively, these six sites were judged by the PIs to represent the faunal and environmental diversity of the chemosynthetic communities on the mid- to upper continental slope. A base-line set of water column, sediment, carbonate, and tissue samples from chemosynthetic and heterotrophic fauna were collected at each site. Additionally, extensive photographic and video documentation was obtained,

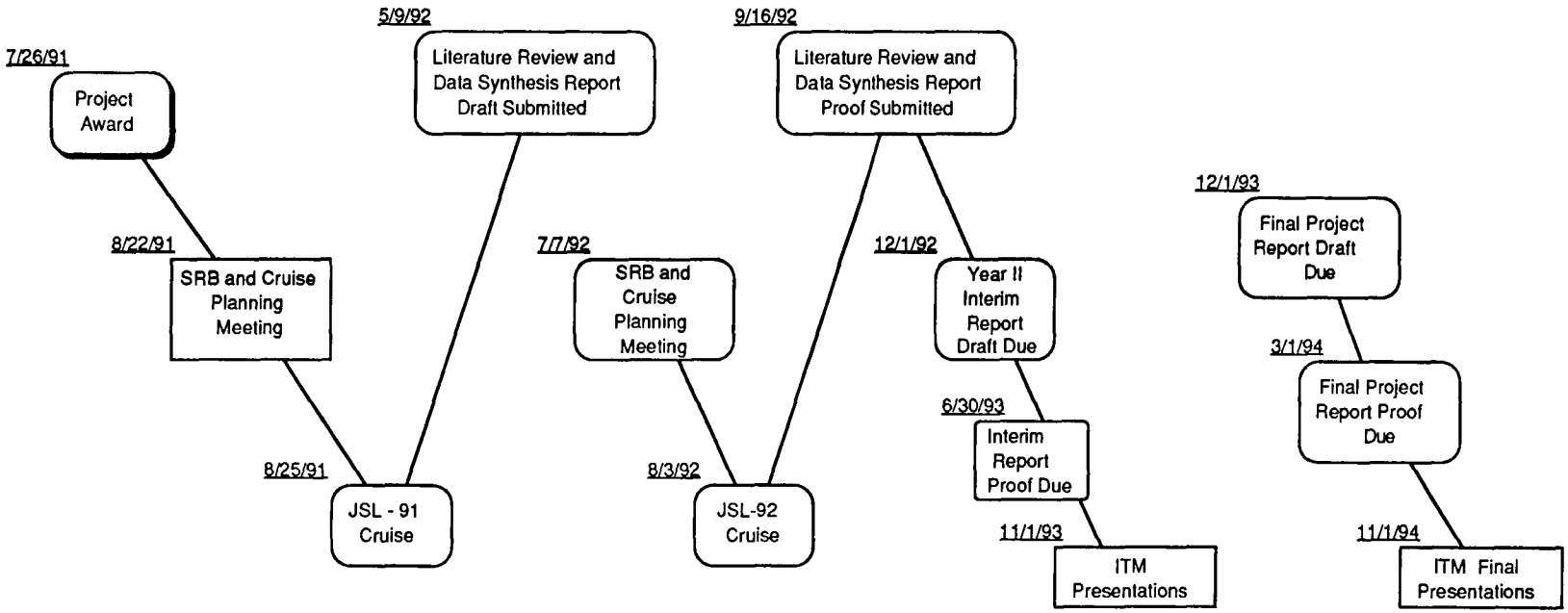

Figure 1.1. Chemosynthetic ecosystems project timeline.

particularly from stations delineated with durable sea-floor markers and floats. At selected sites, collections of tube worms, mussels, or clams were measured, marked, and returned alive to their habitats to determine *in situ* growth rates for the species. Samples of *Beggiatoa* mats were collected for shipboard experiments and laboratory assay. Several deployments of two time-lapse camera systems were carried out to determine short and long-term activity patterns within clusters of tube worms and mussels. Various markers, shell collections, and cages were also deployed for retrieval during subsequent cruises.

The second submarine cruise (JSL-92) utilized the *Johnson Sea-Link I,* deployed from the support ship R/V *Seward Johnson* during the period 3-31 August 1992. This cruise occupied the same sites as JSL-91 and successfully resampled many of the stations established previously. The long-term experiments were retrieved with uniform success, although there were some failures in performance. New techniques utilized during JSL-92 included an *in situ* pore-water sampling device and a small-diameter push-core array that made it possible to collect up to 15 sediment and bacteria samples from a 1 m^2 grid.

A limited cruise was recently completed using the R/V *Gyre* during 4-9 November 1992 (Gyre-92). This cruise collected sediment cores with a piston-corer specially designed for collecting intact shell samples from the surface strata (≤ 3 m subbottom). Two of the sites occupied during JSL-91 and JSL-92 were successfully cored. A third non-study site was also cored and subbottom profile data were collected at two sites.

An additional submarine cruise completed by some of the PIs was also noteworthy, although not formally part of the Study, because it enabled the collection of complementary samples and analyses from a seep community at 2200-m depths in the Alaminos Canyon region of the eastern Gulf. This cruise (Alvin-92) utilized the submarine *Alvin*, deployed from the support ship *Atlantis II* during 20-29 May 1992.

The first report was submitted in final form on 30 November 1992. For this report, each of the PIs wrote an independent overview of both the published literature in his topic area and of his unpublished results which are sufficiently advanced to release. In addition, a collection of the core literature pertinent to the Gulf of Mexico communities was assembled and reproduced in an appendix to this report. This collection included the discovery papers, review articles, and a series of papers entitled "Gulf of Mexico Hydrocarbon Seep Communities I through VII," which has been dispersed among a variety of journals.

2.0 Geological Studies

W.W. Sager, C. Lee, and W.W. Schroeder

2.1. Introduction

Chemosynthetic biotic communities consisting of assemblages of tube worms, mussels, clams, bacterial mats, and other associated organisms have been found widely in the Gulf of Mexico (MacDonald et al., 1990). Because they are dependent on hydrocarbon seepage, the development and distribution of the communities are constrained by geological processes and structures, especially faulting associated with salt deformation (Hessler et al., 1985). The object of this study is to better understand how geological processes constrain chemosynthetic communities on the northern Gulf of Mexico continental slope.

2.1.1. Data Description (See Table 2.1)

A. Primary data for three main areas (GC 184/185, GC 234, and GB 386)
   1. *NR-1* side-scan sonar records
   2. *NR-1* 25 kHz subbottom profiles
   3. *NR-1* bathymetry data
   4. *NR-1* video tape records

B. Other data available for these three areas
   1. Push cores (*Johnson Sea-Link*, August 1992)
   2. Piston cores (GC 234 and GB 386; R/V *Gyre*, November 1992)
   3. Proprietary oil company hazard-survey data
      a. GC 184/185 (Conoco)
         1) 3.5 kHz echo sounder records
         2) Hazard-survey map
         3) Selected multi-channel seismic data
      b. GC 234 (Exxon)
         1) 3.5 kHz echo sounder records
         2) Hazard-survey map
      c. GB 386 (Exxon)
         1) 3.5 kHz echo sounder records
         2) Hazard-survey map
         3) Selected multi-channel seismic data

C. Other data available for GB 425 (R/V *Gyre*, November 1992)
   1. 3.5 kHz and 12 kHz echo sounder records
   2. Piston cores
   3. Bathymetry data

2.2. Methods

Geophysical records including side-scan sonar data and 25 kHz high-resolution subbottom profiles were collected on parallel transects spaced 15 to 30 m apart while the submarine *NR-1* maintained 4 to 6 m altitude above the seafloor. Compared with sea-surface surveys, the submarine survey has the advantage of

Table 2.1. Data description and status of the study as of 23 November 1992.

Data	GC 184/185	GC 234	GB 386	GB 425
25 kHz Seismic Subbottom Profile	Interpreted	Interpreted	Interpreted	N/A
Side-Scan Mosaic	Completed	Needs work	Completed	N/A
Video Tape Record	Analyzed	Needs work	Needs work	N/A
3.5 kHz Echo Sounder Record	Interpreted, waiting for data from Conoco	Waiting for data from Exxon	Waiting for data from Exxon	Needs work
Multi-Channel Seismic Reflection Data	Interpreted (Conoco)	N/A	Needs work (6 lines available	N/A
Bathymetry	Completed	Completed	Completed	Completed
Push Core Sample	Analyzed (7)	Analyzed (8)	Analyzed (3)	N/A
Piston Core Sample	N/A	Needs work (2)	Needs work (4)	Needs work (4)

direct inspection of seafloor features and synoptic observations of the biological community. However, it also has some disadvantages, which are introduced by the change of submarine's altitude above seafloor, heading, and forward speed due to irregular topography.

During the submarine survey, 25 kHz subbottom profile data were continuously recorded on half-inch video tape. The records were digitized in 1.5 minute segments by use of a frame-grabber board, then digitally resized and assembled transect by transect. Changes in the submarine's altitude created artifactual variation in apparent seafloor topography. The artifact was corrected by plotting recorded water depth along transects.

Half-tone photographs of the side-scan sonar records were digitized with an eight-bit scanner. The digital files were then resampled in the along-transect axis to correct errors introduced by changes in the submarine's forward speed during the collection of the data. The corrected files were digitally mosaicked to produce an acoustic backscatter overview image of the study site.

Numerous available data, including 25 kHz subbottom profiles, side-scan sonar mosaic, features mapped from *NR-1* video tape records, hazard survey data from the oil industry, and geologic core samples were synthesized in map form and compared. Acoustic facies of 25 kHz high-resolution subbottom profiles were mapped, and compared with backscatter types of side-scan sonar records. The acoustic facies of 25 kHz subbottom profiles and the backscatter types were also correlated with geologic features and the distribution of chemosynthetic communities determined from video tape and voice records.

The returned side-scan signal depends mainly on backscattered energy from the seafloor. The backscattering of the sound is a complex function

dependent on the acoustic impedance contrast between the seafloor and seawater, the angle of incidence between the sound wave front and the surface of the seafloor, and small-scale roughness on the seafloor or subsurfaces (Johnson and Helferty, 1990). In contrast, reflections seen in subbottom profile records result mainly from differences in acoustic impedance between layers.

2.3. Results and Current Status

2.3.1. GC 184/185

Bush Hill is a mound in 540 to 570 m of water, which occurs on a terrace at the base of a relatively steep, fault-controlled slope (Fig. 2.1), and is a prolific chemosynthetic community site (MacDonald et al., 1989). The mound lies in the Green Canyon lease area and overlaps portions of blocks 184 and 185. The origin of the mound is considered to be the result of heave or diapiric processes rather than vertical accretion by a mud-volcanic process (Neurauter and Bryant, 1990). Lines of 3.5 kHz subbottom profiles show seismic wipe out features across the whole mound (Fig. 2.2), which is a characteristic acoustic indication of free gas in seafloor sediment (Anderson and Bryant, 1990). More lines of 3.5 kHz hazard-survey data will be available from Conoco in the near future, and will be used to further investigate distribution of acoustic facies.

High resolution 25 kHz subbottom profiles show four distinctive acoustic facies in Bush Hill area, caused by differences in seafloor geology (Fig. 2.3). Acoustic facies mapping using 25 kHz high resolution subbottom profiles (Fig. 2.4) matches well with that of side-scan sonar backscatter images (Fig. 2.5).

Type I acoustic facies shows strong bottom echoes with no subbottom echoes and is thought to represent rock outcrop. *NR-1* video camera data shows that the distribution of the chemosynthetic communities, especially tube worm communities, are strongly correlated with this facies, which shows the distribution of authigenic carbonate outcrops. Most gas seeps were observed in this facies. Also, gas hydrates coexisting with these authigenic carbonates were found from the research submarine, *Johnson Sea-Link*. The Type I facies is concentrated in the western half of the Bush Hill mound, and video records show uneven, hummocky, small-scale topography. The tube worm communities are probably located here because they need hard substratum for attachment or support. It is known that the migration of shallow gas through marine sediments can cause precipitation of methane-derived calcium carbonate (Jørgensen, 1992). This facies is characterized by strong backscattering on the side-scan records. Small dots on the side-scan mosaic are thought to be tube worm bushes, and the mosaic shows the concentration of the communities on the Type I facies.

Type II facies is acoustically turbid with no subbottom echoes, a characteristic indicator of gas in seafloor sediment (Anderson and Bryant, 1990). This facies is found on the slope around the mound. It shows weak backscattering on the side-scan records.

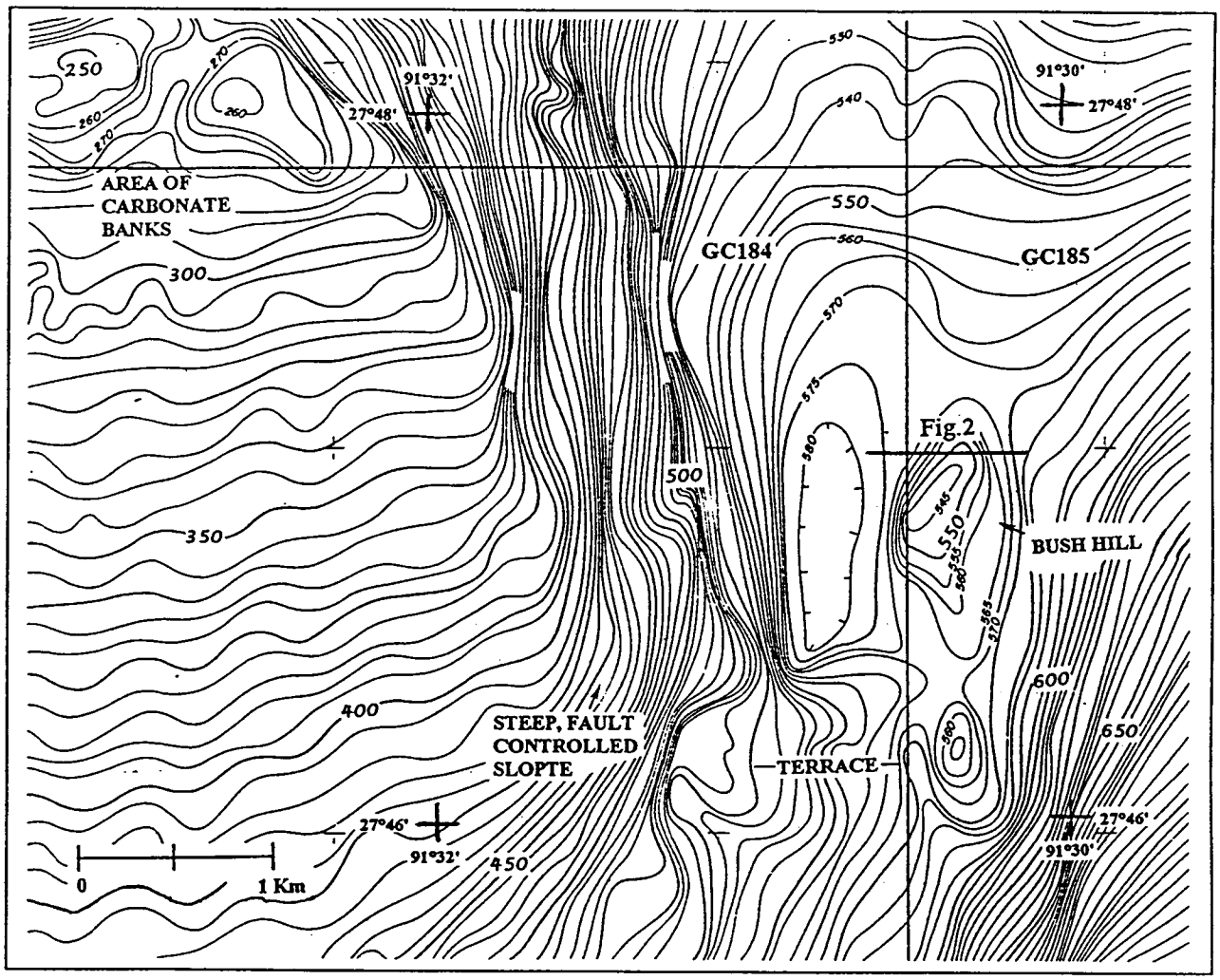

Figure 2.1. Bathymetry in the vicinity of Bush Hill. Contour interval: 5 m (after Neurauter and Bryant, 1990).

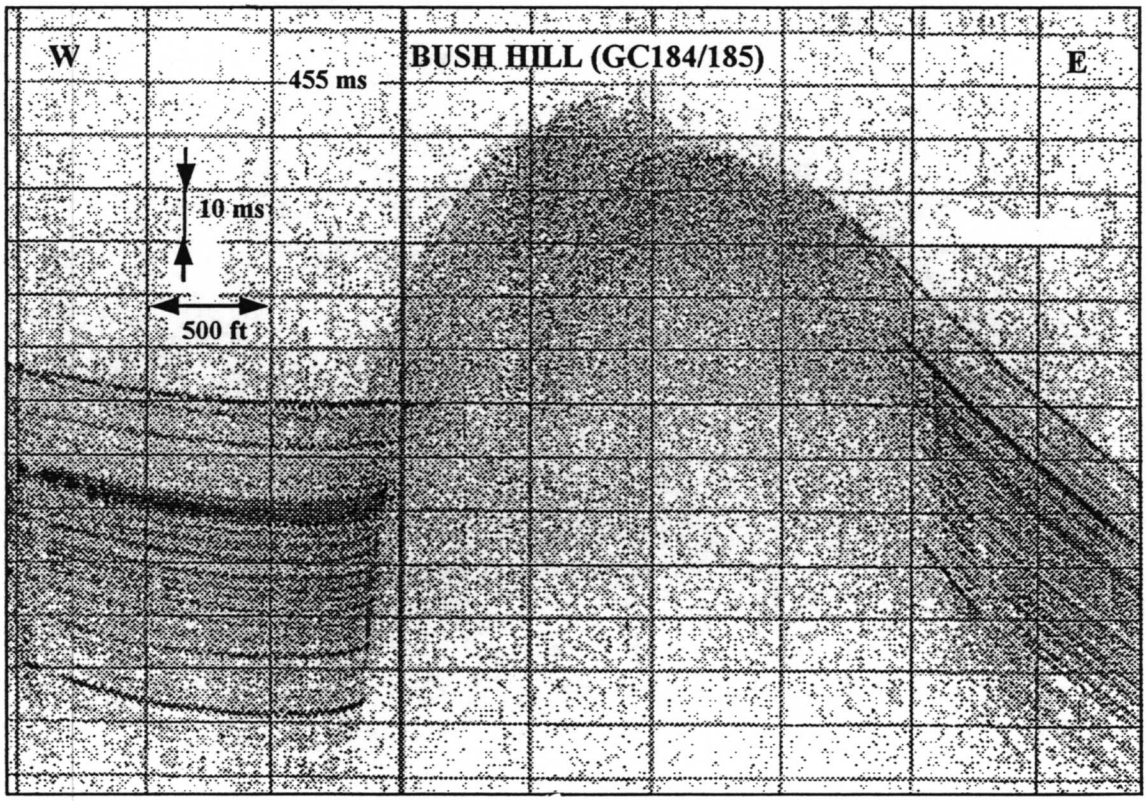

Figure 2.2. A 3.5 kHz subbottom profile across Bush Hill. See Figure 1 for location.

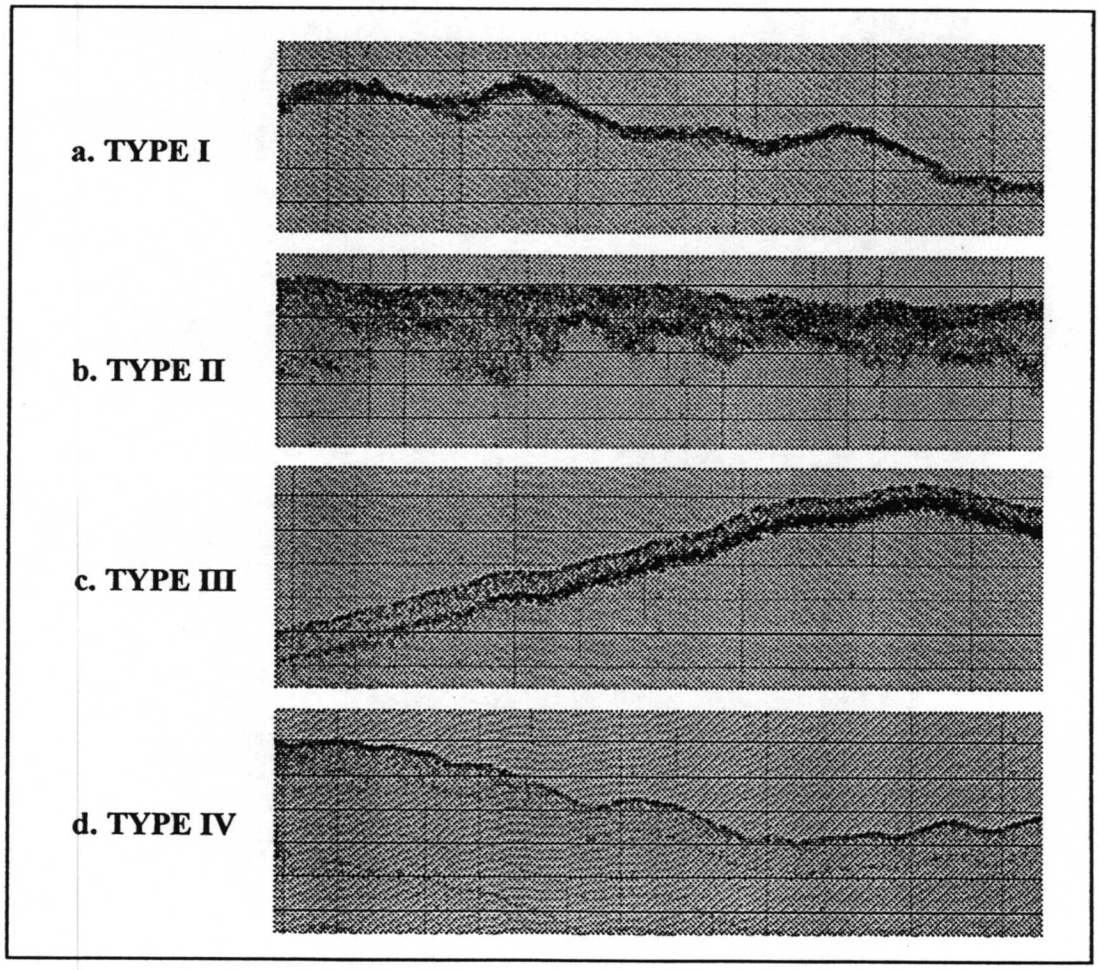

Figure 2.3. Examples of acoustic facies of 25 kHz high resolution subbottom profiles. See Figure 2.4 for profile locations.

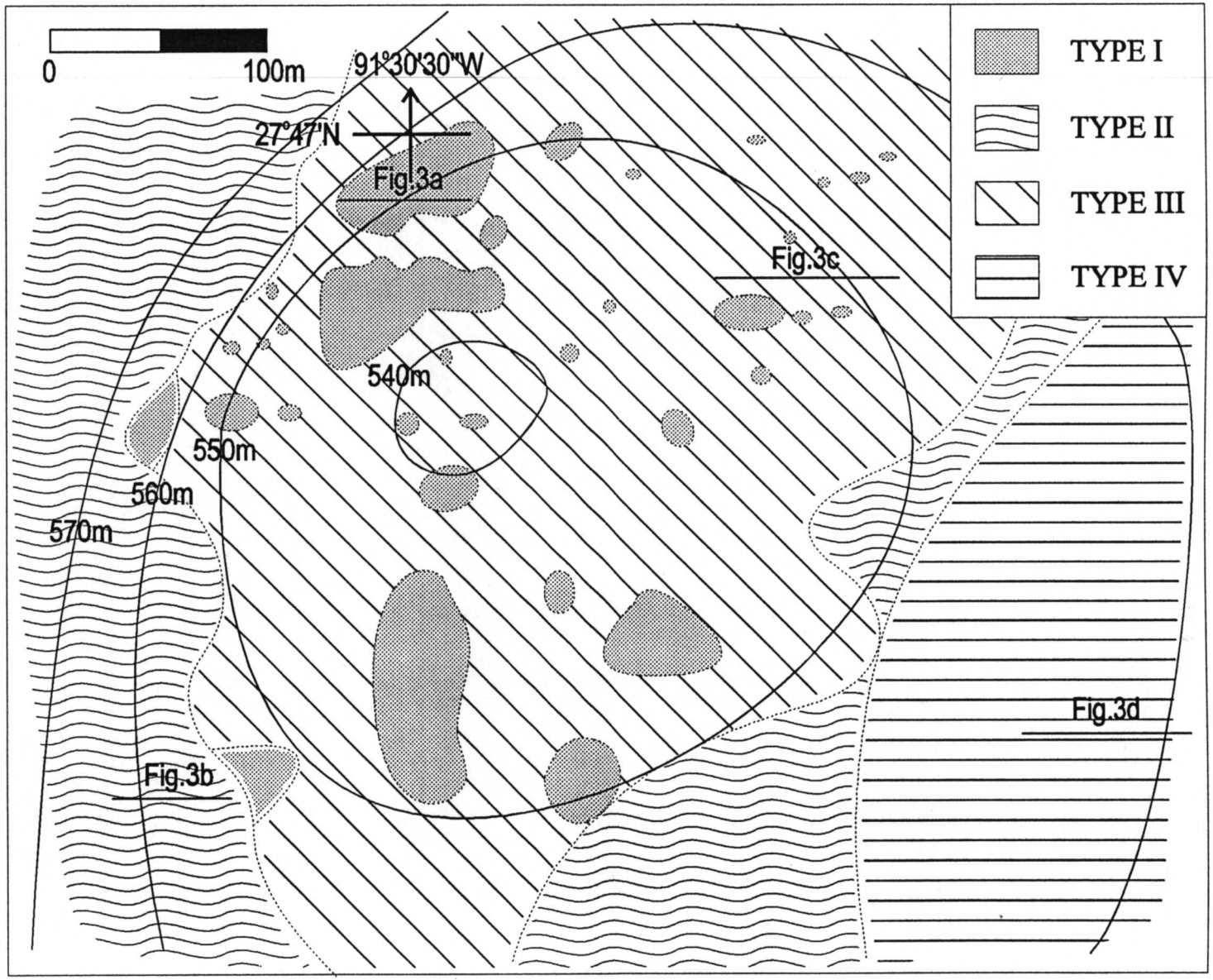

Figure 2.4. Distribution of acoustic facies of 25 kHz high resolution subbottom profiles.

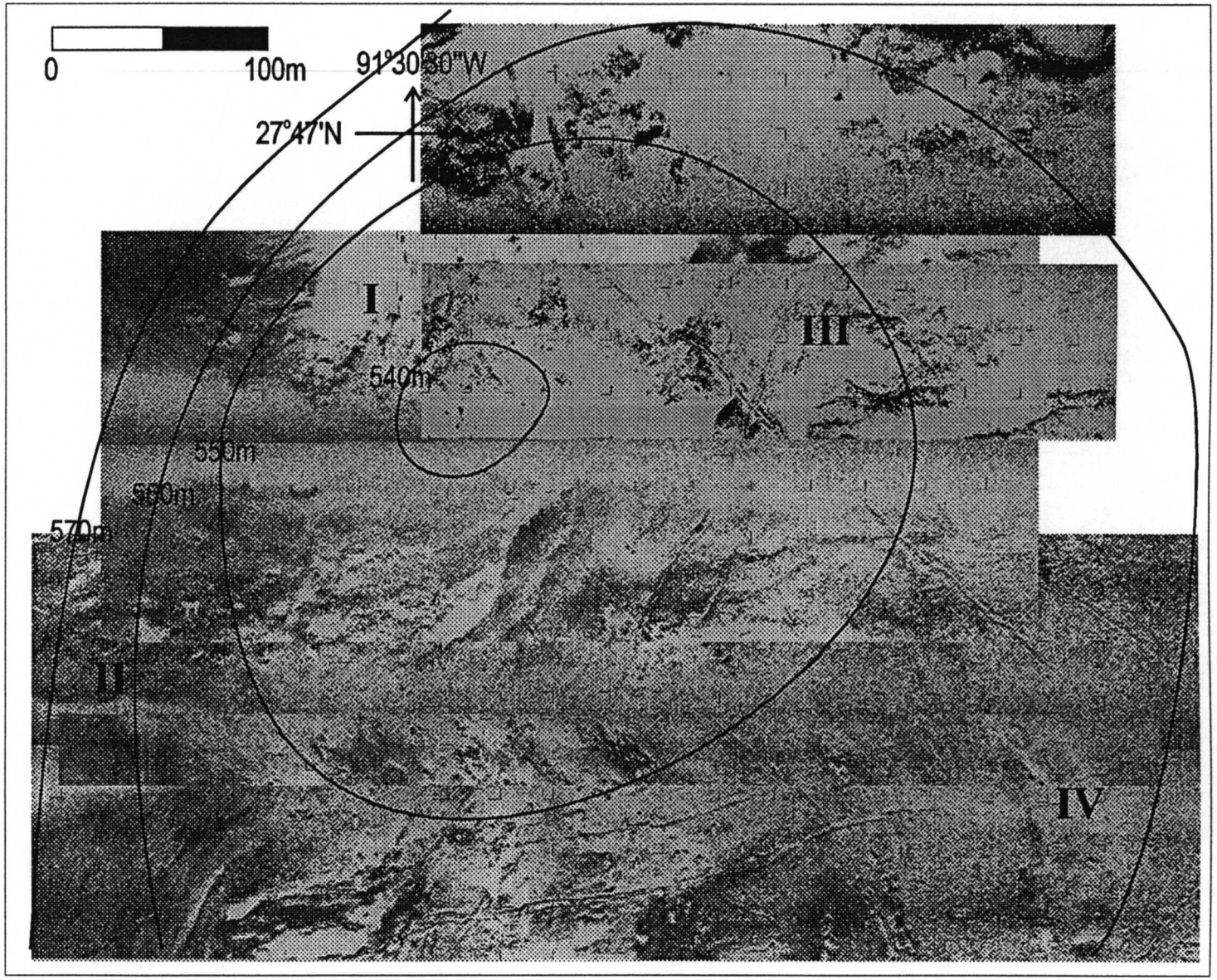

Figure 2.5. Side-scan mosaic of Bush Hill site.

Type III facies is acoustically turbid close to the seafloor, in a narrower depth range than Type II, and is often correlated with strong subbottom echoes. This facies is found all over the mound. It shows backscattering of intermediate strength on the side-scan records.

Type IV facies is acoustically transparent with parallel, continuous subbottom reflectors. This facies surrounds the Bush Hill mound, and is considered to show muddy sediments unaffected by hydrocarbon seepage. The backscattering strength is similar to or slightly stronger than that of Type II facies.

2.3.2. GC 234

Figure 6 shows three-dimensional topography of this site. Chemosynthetic communities are well developed along steep slopes. High-resolution 25 kHz subbottom profiles have been interpreted, but side-scan sonar records need more work because the mosaic was done without digital processing and artifact correction. Acoustic facies of 25 kHz subbottom profiles shows the most complex pattern among the three major study areas. Video tape records are being analyzed. Piston core samples have been collected, but still need to be analyzed.

2.3.3. GB 386

Subbottom profiles have been interpreted and the side-scan mosaic is finished. Acoustic facies of 25 kHz subbottom profiles shows the simplest pattern among study areas. The whole mound shows very strong bottom echoes with no subbottom echoes, which is thought to represent carbonate outcrop. Many carbonate rocks (size up to 14 cm) were found in piston cores from this site during cruise 92G14 of the R/V *Gyre*. Figure 2.7 shows 3.5 kHz and 12 kHz high-resolution survey track of the cruise 92G14. *NR-1* video tape records still need to be analyzed. Exxon has promised 3.5 kHz high-resolution data in the near future. Piston core samples still need to be analyzed.

2.3.4. GB 425

Only limited data is available for this study site. This site was surveyed during the piston coring cruise 92G14 of the R/V *Gyre*. Figure 2.8 shows 3.5 kHz and 12 kHz high-resolution survey track of the cruise 92G14. The bathymetry map (Fig. 2.9) and corresponding three-dimensional topography (Fig. 2.10), made from echo sounder records, show several mounds at the site. More analysis is needed on the 3.5 kHz and 12 kHz high-resolution data and piston core samples.

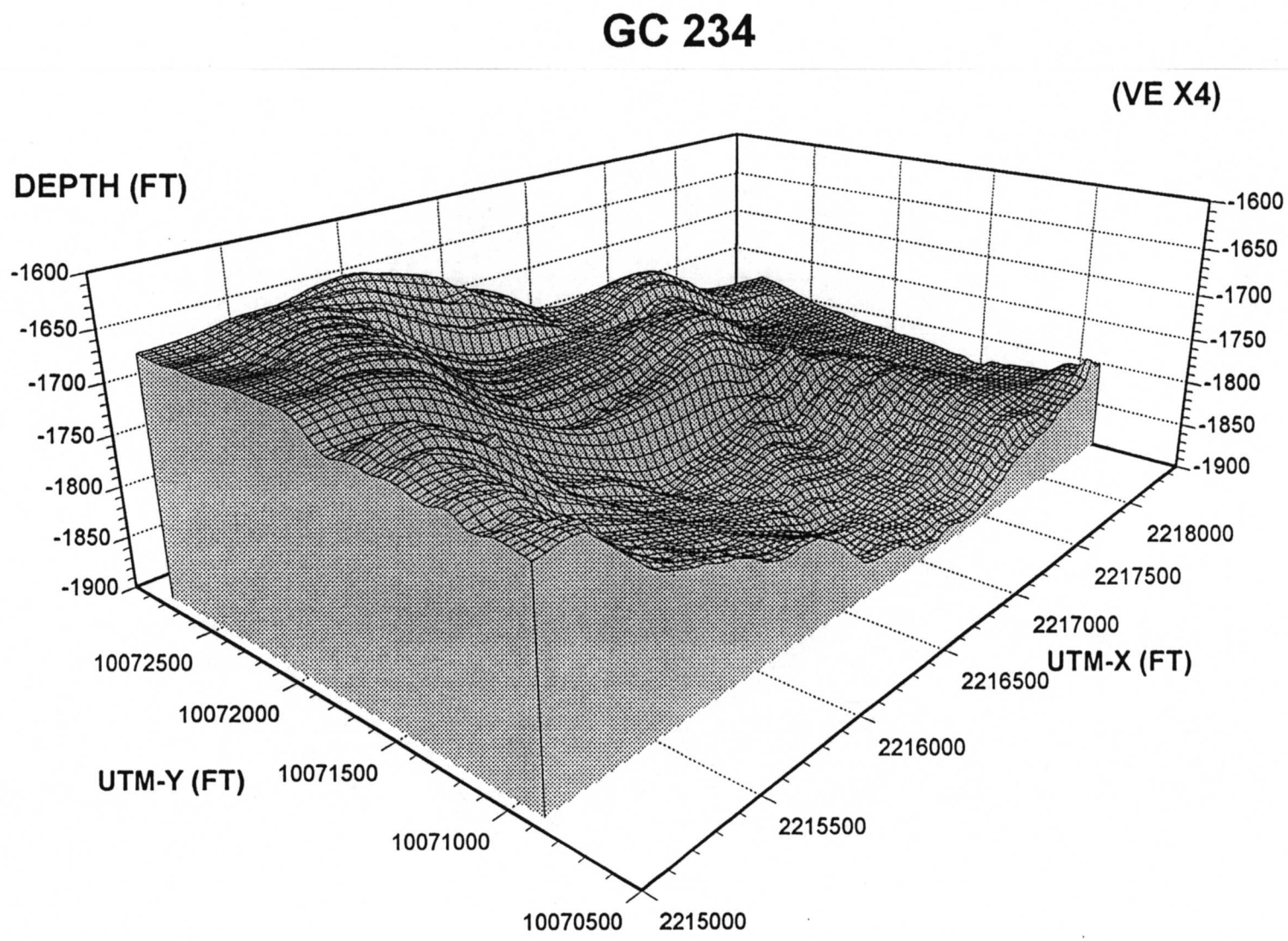

Figure 2.6. Three-dimensional topography of Site GC 234.

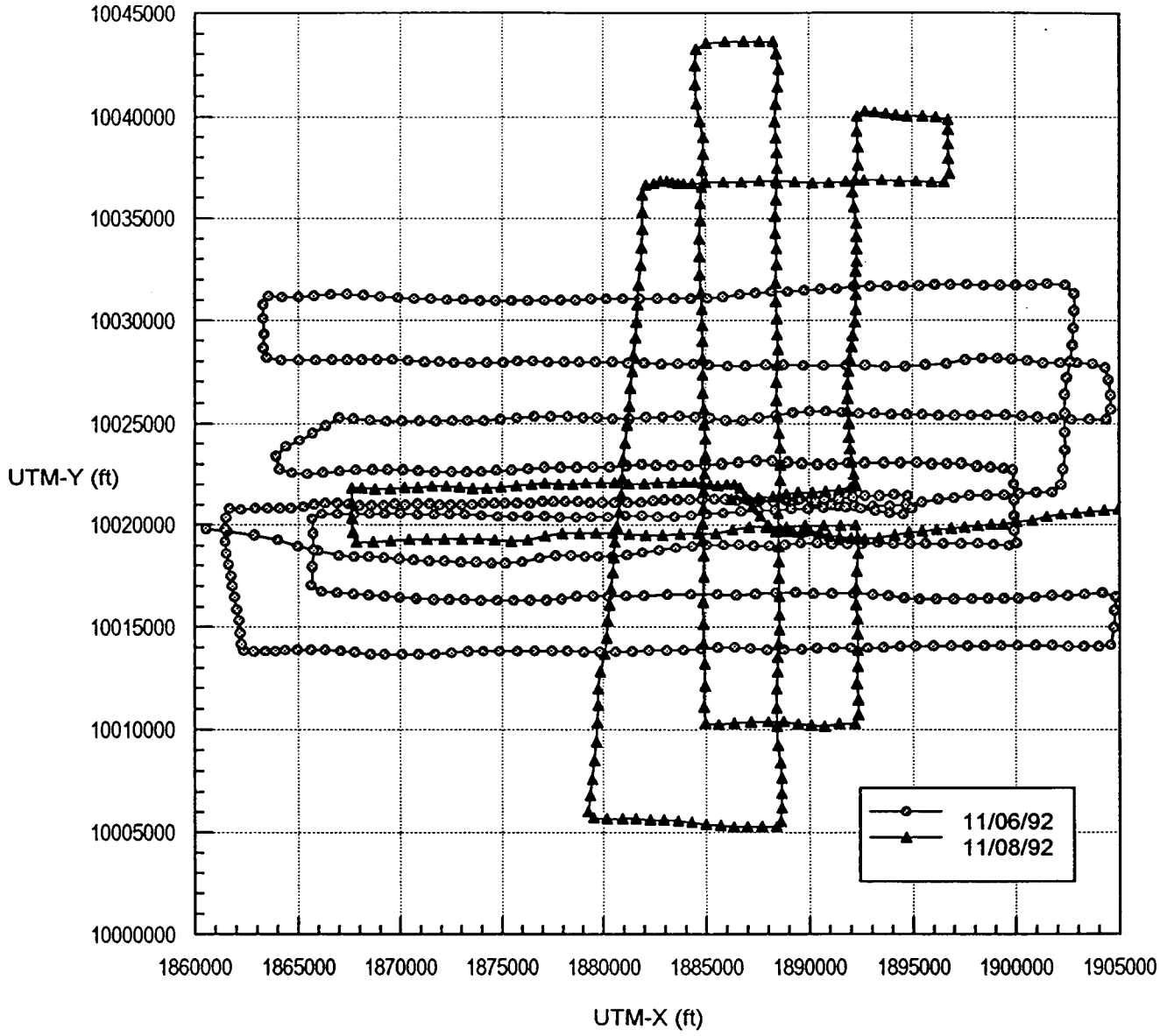

Figure 2.7. High resolution seismic survey track of the cruise 92G14 at Site GB 386.

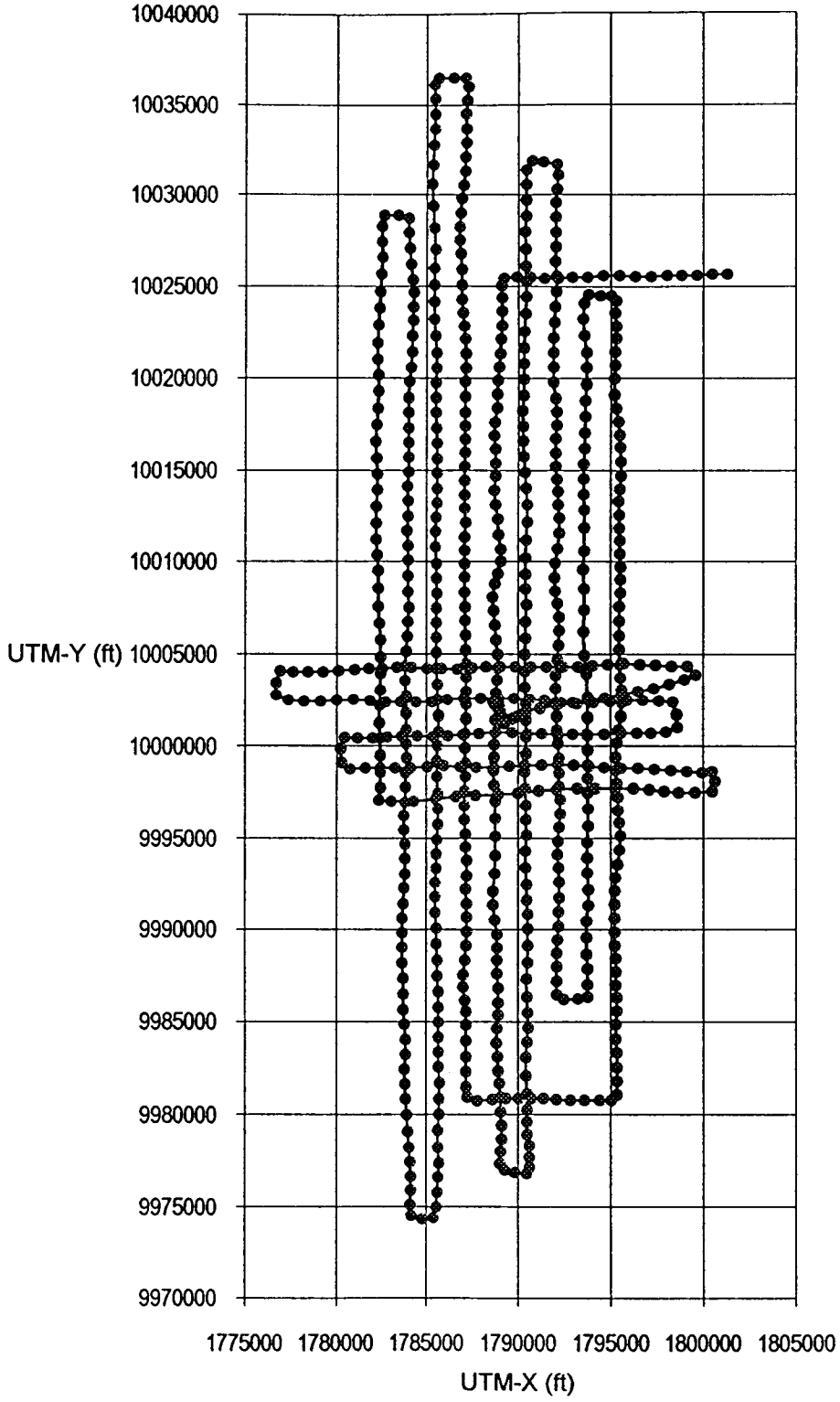

Figure 2.8. High resolution seismic survey track of the cruise 92G14 at Site GB 425.

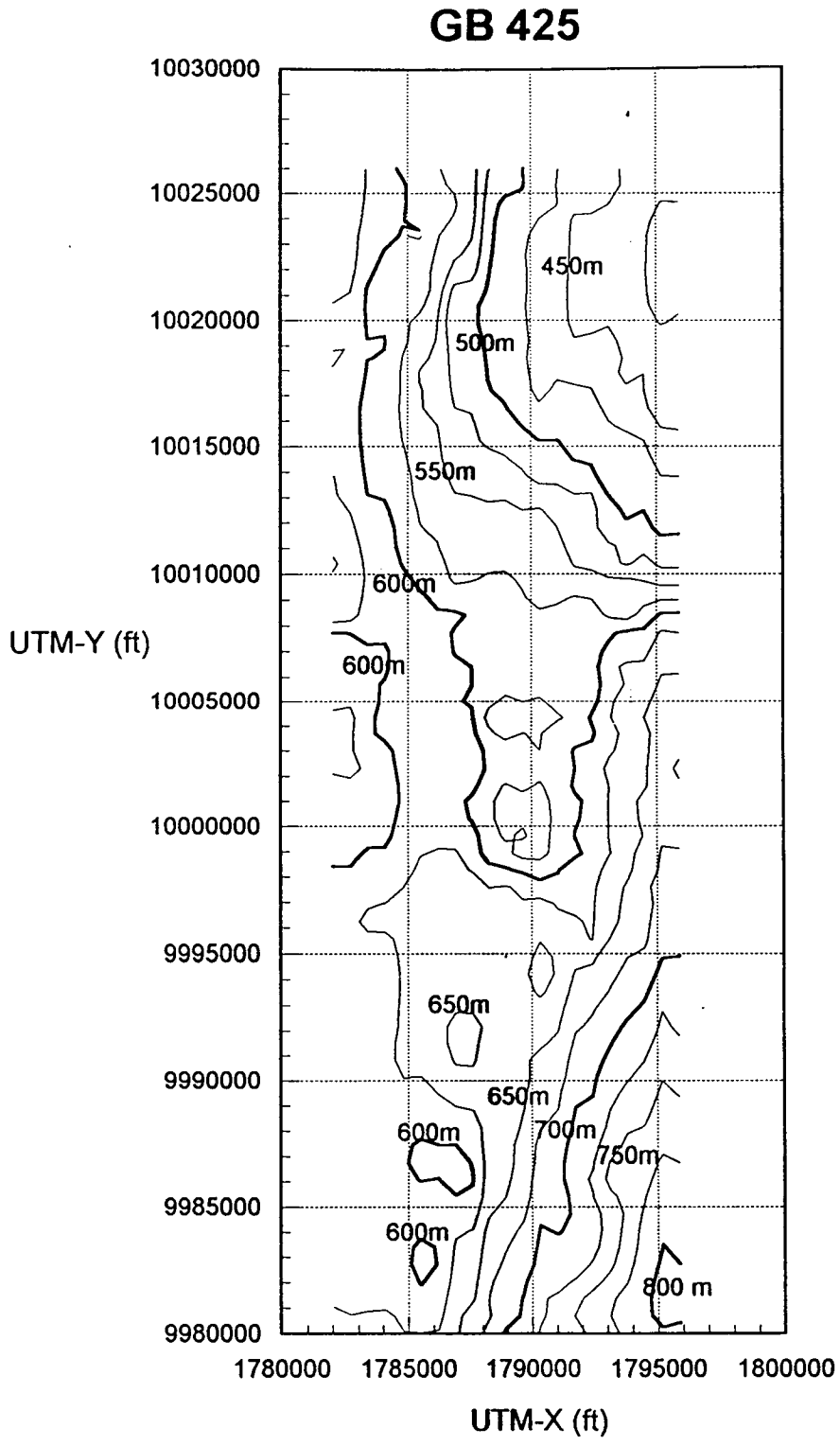

Figure 2.9. Bathymetry map of Site GB 425.

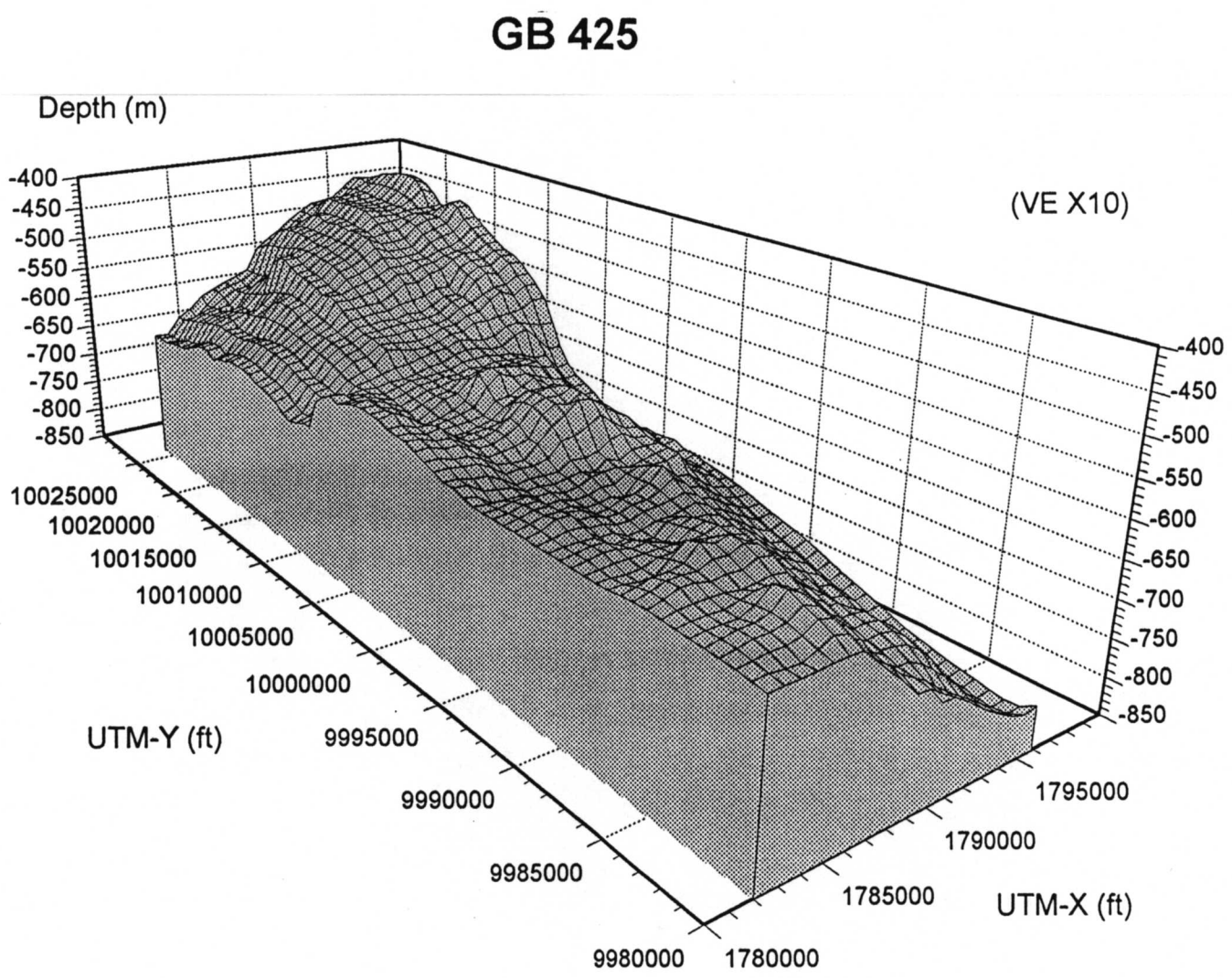

Figure 2.10. Three-dimensional topography of Site GB 425.

3.0 Geochemical Processes

Mahlon C. Kennicutt II

3.1. Introduction

Chemosynthetic communities are closely linked to a number of geochemical phenomena or processes. Directly or indirectly, these processes are primarily the result of oil and gas seepage. Historically, the recognition of oil seepage, gas-charged sediments (seismic wipeout zones), and hydrates lead to the discovery of seep communities. This fundamental coupling of biochemical processes and the chemical environment is at best incompletely understood. A common feature at both cold seeps and hot vents is the co-occurrence of anoxic and oxic conditions that allow for the storage of reduced compounds in close proximity to oxygenated waters. This dynamic system can only be maintained through an active supply of reduced compounds. The supply of these reduced compounds can result from seepage or venting (a deep source) and/or bacterial processes (aerobic and anaerobic). The seepage of oil and gas provides an unconventional source of carbon as well as some portion of the hydrogen sulfide needed for the community's energy and nutrition requirements. Oil and gas are readily available to hydrocarbon oxidizing bacteria that naturally occur in the marine environment. Microbial processes form the basis of the ecosystem and provide the mechanism to transform chemical energy into biochemical energy, mediated by free-living as well as endosymbiotic bacteria.

3.1.1. Bottom Waters

Bottom waters generally containing several ml/L of O_2 (Kennicutt et al., 1989) and low concentrations of H_2S have been measured in close proximity (< 1 m) to the sediment/water interface. Discrete bubble plumes of methane are often evident and highly elevated levels of dissolved methane are measurable in these plumes. At some locations, elevated salinities are present directly above brine seeps due to advection and diffusion. However, bottom waters in general are typical of slope waters in temperature, salinity, oxygen content, and nutrient concentrations.

3.1.2. Pore Waters

In contrast to bottom waters, sediment pore waters in the vicinity of chemosynthetic ecosystems contain elevated concentrations of many chemicals. In many areas, the presence of subsurface or exposed salt diapirs provides a source of highly saline water that often moves to near-surface sediments. This process is ultimately manifested in the accumulation of brine in pools, elevated pore water chlorinities, and anoxia (Kennicutt et al., 1989; MacDonald et al., 1989). Large accumulations of brine have been noted on the Louisiana continental shelf (MacDonald et al., 1990). Pore water chlorinities exceeding 1,500 mM and salinities in excess of 200‰ have been reported (Behrens, 1988; Kennicutt et al., 1989). Other pore water constituents, including H_2S, ammonia, phosphate, and silicate, are also elevated in seepage-influenced pore waters.

Extensive bacterial mats are generally a widespread feature in seep areas and appear to overlie anoxic, H_2S-rich pore waters (Brooks et al., 1987, 1989; Montagna et al., 1987 and references therein; MacDonald et al., 1989). The anoxic environment may result from oxygen depletion during microbial reduction of sulfate and/or addition of reduced compounds from the seeping fluids (Bauer et al., 1988; Montagna et al., 1986). A decrease in pore water sulfate has also been noted that may result from an infusion of salt-rich, sulfate-free brine. The ^{13}C depleted ΣCO_2 isotopic values observed in pore waters at seeps indicate that oil and/or CH_4 oxidation is occurring at the present time.

3.1.3. Sediments

A primary feature of sediments at several chemosynthetic communities is the presence of oil and gas. Oil seepage has been extensively documented in the offshore regions of the northern Gulf of Mexico over the last decade. Sediment containing as much as 4% oil, by weight, were recovered on the northwestern continental slope in 1983 by Anderson et al. (1983). Subsequently, extensive seepage was reported at several locations in the Green Canyon lease area (Brooks et al., 1984). On calm days, oil slicks can be seen forming at the seawater surface in these areas. Extensive analyses of reservoired oils, shallow sediments, sea slicks, and tar balls document a direct link between natural seepage, sea slicks and tar ball formation (Kennicutt et al., 1988a). The near-surface fluids (gases and liquids) were definitively matched with petroleum reservoired at 2,000-3,000 m deep in the subsurface. Other studies have found a clear relationship between seismic wipeout zones (areas of chaotic acoustic returns) and oil and gas seepage (Kennicutt et al., 1988b). Of thirty-three locations known to exhibit wipe-out zones, oil stained cores were retrieved at nine sites. Some sediments contained more than 15% oil by weight. Surface geochemical prospecting surveys have confirmed the presence of macroseepage of oil from offshore Brownsville, Texas, to offshore Panama City, Florida, in water depths ranging from 300 to 3000 m. In areas of massive oil seepage, the organic content of the sediments is increased by the addition of petroleum. In these cases, the *in situ* sediment biological lipids are overprinted by the oil and carbon isotope ratios tend to reflect the isotopic composition of the petroleum. The oil, in general, is highly altered by microbial processes and dissolution (Kennicutt et al., 1988b).

Methane hydrates are ice-like inclusion compounds that form at high pressures and low temperatures when methane exceeds its solubility. Until the discoveries in the Gulf of Mexico, most hydrates were associated with permafrost areas or deep in the sediment column (i.e., DSDP drill sites). The first thermogenic hydrates were recovered in shallow cores as part of a study of oil seepage on the northern Gulf of Mexico continental slope (< 6 m; Brooks et al., 1984). Subsequent regional surveys have documented more than a dozen hydrate locations in the Gulf of Mexico in water depths from 530 to 2400 m (Brooks et al., 1986). Hydrates occur as nodules, interspersed layers, and solid masses, and contain both biogenic and thermogenic methane. The thermogenic hydrates are often associated with oil staining, large amounts of C_{2+} hydrocarbons, and seismic wipe-out zones. Discrete bubble streams are often observed in areas where hydrates exist, suggesting that hydrate decomposition as well as formation is occurring.

Many of the sediments in areas associated with chemosynthetic communities contain large accumulations of calcium carbonate (Brooks et al., 1986). Although these areas are below the photic zone, on a passive margin, and remote from other hard bottom areas, significant accumulations of carbonate are present. The oxidation of hydrocarbons produces excess CO_2, which ultimately combines with calcium to form authigenic (in place) calcium carbonate. These carbonate deposits can be nodules, layers, large pieces (tens of cm) or extensive ridges (up to tens of meters long). The stable carbon isotopic composition of carbonates from several seep locations varied from +2.0 to -47.5‰, reflecting various admixtures of carbonates formed from seawater SCO_2 and oil and CH_4 oxidation products. In general, sediment $CaCO_3$ contents increase as the $\delta^{13}C$ value decreases, reflecting authigenic formation of carbonate.

3.1.4. Stable Isotopic Composition of Tissues

The isotopic analysis of organisms' tissues has been especially useful in understanding the dynamics of chemosynthesis-based communities (Childress et al., 1986; Brooks et al., 1987; Kennicutt et al., 1992). The stable carbon isotope composition of hydrothermal vent animals was one of the first indications that non-photosynthetic food sources were being utilized (Rau and Hedges, 1979; Rau, 1981). Since then, this technique has been applied to the study of more than 30 symbioses between marine invertebrates and chemoautotrophic bacteria (reviewed by Fisher, 1990). Carbon isotope ratios differentiate three distinct nutritional strategies: (1) heterotrophic, (2) thiotrophic (sulfide-based), and (3) methanotrophic (methane-based). Chemoautotrophic bacteria (generally thiotrophic) discriminate by ~25‰ against ^{13}C during the incorporation of inorganic carbon into organic compounds (Ruby et al., 1987). This discrimination results in biomass $\delta^{13}C$ values that are more negative than those originating from photosynthetically-fixed carbon by ~10‰, if the discrimination is fully expressed. The $\delta^{13}C$ values of heterotrophic marine invertebrates normally range from -12 to -24‰ (reviewed by Fisher, 1990; Kennicutt et al., 1992). Most bivalves with thiotrophic symbionts have $\delta^{13}C$ values that range from -22 to -47‰. Studies at hydrocarbon seeps have shown that clam and tube worm tissues are isotopically light, with $\delta^{13}C$ values indicative of sulfide-utilizing endosymbionts, i.e., thiotrophs. Seep tube worms are strikingly more ^{13}C-depleted than hydrothermal vent tube worms (Kennicutt et al., 1992). This difference is as yet unexplained, though CO_2 limitation is strongly suggested as a possible cause for the ^{13}C enrichment observed (Rau, 1981 and 1985; Fisher et al., 1990).

Methanotrophic bacteria do not express discrimination against ^{13}C during incorporation of methane into cellular components, most likely due to complete consumption of the methane. Therefore methanotrophic mussels generally reflect the isotopic composition of the source of the methane. Methane in reservoirs and marine sediments are very ^{13}C-depleted and can range from -35 to -90‰ (Silverman and Oyama, 1968; Ovsyannikov et al., 1973; Bernard et al., 1976; Burke and Sackett, 1986). Invertebrates with methanotrophic symbionts have tissue $\delta^{13}C$ values which range from -40 to -75‰. Enzymatic, electron microscopic and $^{14}CH_4$-uptake studies have conclusively demonstrated the

presence of a methane-based endosymbiotic relationship between a bacterium and a mollusk (Childress et al., 1986; Brooks et al., 1987). The symbiosis may be able to satisfy the mussels' entire carbon needs solely from methane oxidation (Childress et al., 1986; Cary et al., 1988). Mussels, clams and tube worms also contain mostly "dead" carbon (by ^{14}C measurements), indicating that their dietary carbon is largely derived directly or indirectly from seeping oil and/or gas.

3.2. Methods

3.2.1. Bottom and Pore Waters

Samples of bottom water were collected during *Sea-Link* submersible dives by syringe with the articulated manipulator arm and by drawing water into the submersible's aft chamber through capillary tubing placed at the end of the manipulator arm. The use of the arm allows for the placement of the inlet at specific points of interest (e.g., inside tube worm clumps, various distances above the bottom, etc.). The entire length of the sample line is flushed before each sampling. Pore water samples were collected in syringes that form air tight seals. Salinity was analyzed with either a Plessey® Environmental Systems Model 6230N Laboratory Salinometer, a Guildline® Model 8400 Autosal Laboratory Salinometer or AGE® Instruments Inc. Model 2100 salinometer. The Plessey system utilizes an inductively-coupled conductivity sensor to establish a conductivity ratio between an unknown sample and standard seawater (~35 Practical Salinity Unit [PSU] salinity). A dual-element platinum thermometer senses the temperature of the sample and applies appropriate corrections. The specifications of the system are as follows:

Range:	0 to 51 PSU
Accuracy:	±0.003 PSU
Temperature Compensation:	±0.0007 PSU/°C

The Autosal system uses conductivity directly and has better accuracy and precision than the Plessey. The AGE® Instrument is a portable, battery-operated salinometer which needs less than 10 ml of sample and employs a method directly applicable to the Practical Salinity Scale 1978 Defining Equation. It has an accuracy better than 0.003 PSU (salinity) and provides a direct readout of the salinity values. IAPSO Standard Sea Water was used as a standard reference material.

Samples for oxygen analysis were taken using a length of tygon tubing with the tip of the tube near the bottom of the flask, allowing slow filling without agitation. The flask was rinsed and air bubbles were removed from the tubing with a small amount of sample before the flask was filled. The flask was overflowed one full volume and the stopper inserted to avoid trapping air bubbles. The technique used for analysis of oxygen is a modified Winkler technique (Carpenter, 1965). As soon as possible after collection, divalent manganese solution was added, followed by strong alkali. The precipitated manganous hydroxide was dispersed evenly throughout the seawater sample, which completely filled the stoppered oxygen flask. Any dissolved oxygen rapidly oxidizes an equivalent amount of divalent manganese to basic hydroxides. When

the solution is acidified in the presence of iodide, the oxidized manganese again reverts to the divalent state, liberating iodine equivalent to the original dissolved oxygen content of the water.

Water samples were collected in 60 cc syringes for analysis of H_2S. The water sample was immediately fixed with zinc acetate to minimize losses due to degassing or reaction with atmospheric oxygen. The process used was a modification of the sulfide technique of Cline (1969), as enhanced by Goldhaber et al. (1977). A diamine reagent is prepared by dissolving Eastman Kodak No. 1333 and ferric chloride in 500 mL of cool 50% (v/v) reagent grade hydrochloric acid. The concentrations of Eastman Kodak and ferric chloride are adjusted depending upon the sulfide content of the samples (Cline, 1969). Five mL of sample are added to 1.4 mL of diamine reagent. After 20 minutes the absorbance is measured at 670 mμ using an HP 8451A Diode Assay Spectrophotometer. Concentrations were determined using the equation:

$$C_{\Sigma S} = F(A-A_b)$$

where $C_{\Sigma S}$ is the concentration of sulfide, F is the extinction coefficient determined by standards, A is the absorbance of the sample, and A_b is the absorbance of the blank. F is calculated by standardizing at multiple sulfide concentrations. Oxygen-free water is prepared by purging distilled water with nitrogen gas for approximately 20 minutes. A known amount of sodium sulfide is added. Four standards were prepared daily and calibration curves created. To assure the quality of the results, a standard sample was analyzed prior to and at the completion of each set of samples processed daily.

3.2.2. Sediments

Total carbon concentrations were determined on freeze-dried subsamples of push cores using a LECO Model 523-300 induction furnace (or equivalent) to burn samples in an oxygen atmosphere. The resulting CO_2 is swept through a dust trap and two reaction tubes for purification. The carbon dioxide is detected and quantified with a Horiba PIR-2000 non-dispersive infrared detector. Total organic carbon is determined after sample acidification and carbonate carbon is calculated as the difference between total carbon and total organic carbon. A daily standard curve was determined prior to sample analyses. The standard curve is generated by combusting various combinations of LECO standard rings and pins that span the range of expected carbon concentrations in samples.

Extractable organic matter was gravimetrically determined with a Cahn Electrobalance after a 12-hour hexane Soxhlet extraction. The extracts were blown dry with a purified air stream, brought up in 100 μl of methylene chloride and injected onto an HP 5880 gas chromatograph equipped with a 25 m fused silica capillary column. The gas chromatograph was interfaced with an HP-1000 computer for data storage and subsequent data analysis using Laboratory Automation Software (LAS).

Table 3.1. Summary of analytical results for the Green Canyon Block 272 site.

Sediments

Sample		TOC (%)	δ^{13}Com (‰)	$\delta^{13}C_{CaCO_3}$ (‰)	$CaCO_3$ (%)	EOM (ppm)	GC/FID
C3489	CF01	1.2	-25.4	-20.1	21.9	1269	yes
C3491	CF01	1.5	-24.5	-7.2	10.9	816	yes
C3492	CF03	0.6	-25.0	-10.2	10.5	690	yes
C3493	CF03	0.4	-27.6	-10.3	7.1	541	yes
C3494	CF05	0.4	-26.3	-5.2	8.4	897	yes
C3495	CF05	0.8	-25.1	-2.9	7.3	763	yes
C3496	CF08	2.5	-29.1	-17.6	26.7	29,748	yes
C3497	CF90	1.7	-27.3	-15.7	12.1	880	yes
C3498	CF90	0.8	-27.8	-10.4	12.6	1114	yes
C3499	CF08	4.5	-27.1	-18.6	32.7	30,024	yes
C3490	CF04	0.2	-27.3	-15.8	9.1	983	yes

Pore Waters

Sample	Identifier	Salinity (‰)	$\delta^{13}C\Sigma CO_2$ (‰)	H_2S (µg-at/L)	ΣCO_2 (mM/L)
C3656	910917CF0133	35.2	-39.9	< 1.0	6.39
C3657	910917CF0434	37.8	-13.5	379.1	2.19
C3658	910917CF0134	30.6	-34.1	3.3	2.90
C3659	910918CF0335	37.3	-39.0	26.3	4.28
C3660	910918CF0536	35.5	-24.6	45.3	3.29
C3661	910919CF0838	34.6	-29.7	242.9	3.30
C3662	910919CF0838	35.4	-31.5	10.6	3.88
C3663	910918CF9036	35.2	-48.9	56.1	4.39

Microwater Samples

Sample	Identifier	Salinity (‰)	$\delta^{13}C\Sigma CO_2$ (‰)	ΣCO_2 (mM/L)
C3676	910918CF0335	33.2	NS	1.17
C3677	910918CF9036	32.1	NS	1.32
C3678	910918CF9036	32.9	NS	1.64
C3680	910919CF0838	33.7	-41.8	1.28
C3681	910919CF0838	22.4	NS	1.15

Comments:
No bottom waters

δ^{13}C Organisms (‰):

Seep Mytilid	-60.8, -61.1, -61.9, -58.2, -60.5, -57.6, -58.4, -62.2, -55.2, -62.2, -55.6, -60.8, -60.3, -60.6, -63.0, -62.1, -59.7, -54.7, -59.0, -56.0		
Urchin, sp.1	-20.1	Escarpia	-35.3, -39.6, -39.6, -40.1
Starfish	-51.5	Brachiurin	-25.8, -32.1
Urchin, sp.2	-22.7	Munidopsis	-29.7
O. pictus	-18.7	Worm	-31.6
Caridian	-34.1		
Polychaete	-12.7, -32.1, -47.0		

salinities and ΣCO_2 slightly lower than seawater concentrations, suggesting that freshwater from hydrate decomposition was emanating from the sediments.

Intense localized sampling at GC-272 during 1992 *JSL* dives confirmed the presence of extensive hydrates at this site. An excess of isobutane over n-butane is consistent with a hydrate origin for the gases at one location, whereas at a second location, normal butane was most abundant. The hydrate preferentially concentrates isobutane over normal butane due to size exclusion of the larger normal butane molecule. Sediment gases contained very high concentrations of methane. Hydrocarbon gas concentrations dramatically increase with depth in the core. Large amounts of C_{2+} gases were present, suggesting a thermogenic origin for at least a portion of the gas. $\delta^{13}C$ values for methane suggests that significant amounts of biogenic gas are also present (-48.1‰, -55.7‰).

Seep mussels at this site were very ^{13}C-depleted, suggesting the uptake of biogenic methane by the symbiont (-54.7 to -63.0‰). Escarpia tube worms $\delta^{13}C$ values ranged from -35.3 to 40.1‰. A variety of background organisms (polychaetes, crustaceans etc.) were also ^{13}C-depleted reflecting transfer of chemosynthetic carbon to heterotrophic organisms (Table 3.1).

3.3.2. Green Canyon Block 184

GC-184 is a location of known seepage and hydrates. Sediment organic carbon contents were extremely elevated (5.6 to 20.8%) with $\delta^{13}C$ values indicative of typical Gulf of Mexico oil (~ -27.0‰; Table 3.2). Calcium carbonate content varied from 4.2 to 10.6%. The $CaCO_3$ was depleted in ^{13}C carbon (-2.2 to -21.5‰). Extractable organic matter (EOM) concentrations were as high as 106,036 ppm. GC/FID patterns of the EOM showed the oil to be highly biodegraded. Pore waters contained elevated levels of H_2S and ΣCO_2. ΣCO_2 was ^{13}C-depleted, reflective of active methane and oil oxidation by bacteria. Salinities were near or below seawater values, suggesting that decomposition of hydrates was occurring at this site. Bottom waters contained traces of H_2S and appeared to be freshened by pore water emanating from the sediments. Lamellebrachia tube worms collected at the site had $\delta^{13}C$ values from -19.5 to -23.1‰. Other heterotrophic organisms were slightly depleted in ^{13}C, indicating some transfer of chemosynthetic carbon into background fauna.

Intensive localized sampling in 1992 revealed large increases in CH_4 concentrations with depth in the sediment. A thermogenic origin for the gas was suggested by the presence of significant amounts of C_{2+} hydrocarbon gases.

3.3.3. Garden Banks Block 386

Only a few samples were collected at Garden Banks 386. Sediments contained oil and authigenic carbonate (Table 3.3). Pore waters were close to seawater salinity and contained ^{13}C-depleted ΣCO_2, indicative of hydrocarbon oxidation. Seep mussels were unusually ^{13}C-enriched in stable isotopic composition (-34.7 to -38.1‰). Bivalves had an isotopic composition of -34.3‰, typical of thiotrophic organisms. Lamellebrachia tube worms $\delta^{13}C$ values for tissues varied from -23.1 to -25.9‰.

Table 3.2. Summary of analytical results for the Green Canyon Block 184 (Bush Hill) site.

Sediments

Sample	Station	Dive	Core	TOC (%)	$\delta^{13}C_{om}$ (‰)	$\delta^{13}C_{CaCO_3}$ (‰)	$CaCO_3$(%)	EOM(ppm)	GC/FID
C3483	BH11	30	1	8.6	-27.1	-14.5	6.4	80,289	√
C3484	BH11	30	2	9.6	-27.1	-13.6	7.5	106,036	√
C3485	BH11	30	3	6.6	-26.3	-4.3	4.2	51,060	√
C3486	BH11	30	4	5.6	-26.3	-2.2	6.9	41,376	√
C3501	BH03	39	2	9.2	-27.7	-17.6	10.6	51,868	√
C3487	BH20	29	1	10.0	-26.4	-12.0	8.7	78,775	√
C3500	BH20	39	1	20.8	-27.9	-21.5	5.1	55,259	√
C3502	BH20	41	4	8.9	-27.0	-11.2	4.8	76,091	√
C3503	BH20	40	1	9.0	-27.7	-9.7	6.9	74,324	√
C3504	BH20	40	2	10.6	-27.3	-9.6	7.2	93,548	√
C3505	BH20	40	3	10.7	-27.9	-6.3	8.7	84,396	√

Pore Water

Sample	Field ID	Salinity (‰)	H_2S (µg-at/L)	$\delta^{13}C_{\Sigma CO2}$ (‰)	ΣCO_2 (mM/L)
C3653	910915BH2029	31.2	43.4	-18.4	5.26
C3654	910915BH1130	33.3	10.7	-12.9	2.37
C3664	910921BH2039	34.2	37.8	-11.5	1.86
C3665	910921BH0339	35.8	20.5	-17.3	2.76
C3666	910922BH2040	29.3	<1.1	-12.6	1.64
C3667	910922BH2041	32.2	<1.1	-8.0	2.85

Bottom Water

Sample	Dissolved O_2 (ml/l)
910915BH1130	3.8
910915BH1130	4.5
910922BH2040	3.3

Microwater Samples

Sample	Field ID	Salinity (‰)	H_2S (µg/L)	ΣCO_2 (mM/L)	$\delta^{13}C_{\Sigma CO_2}$ (‰)
C3683	910922BH2041	23.6	1.1	1.28	NS

Comments:

Munida sp. -20.7, -27.3
Barnacles -21.3
Rochinia crassa -18.4
Gastropod -19.8
Geryon sp. -19.4, 16.6, -19.9, -20.4, -23.6
Isopod -16.5, -18.0
Scarpaenid -21.5
Urophysis -16.5
Lamellibrachia -20.2, -19.5, -22.1, -23.1, -22.4, -20.3
Ophiuroid -19.0

Table 3.3. Summary of analytical results from the Garden Banks Block 386 site.

Sediments

Sample	Station	Dive	Core	TOC (%)	$\delta^{13}C_{om}$(‰)	$\delta^{13}C_{CaCO_3}$(‰)	$CaCO_3$(%)	EOM(ppm)	GC/FID
C3488	GB12	32	1	2.2	-26.1	-27.5	17.1	562	√

Pore Waters

Sample	Field ID	Salinity (‰)	H_2S (µg-at/L)	ΣCO_2 (mM/L)	$\delta^{13}C_{\Sigma CO_2}$ (‰)
C3655	910916GB1232	35.4‰	1.16	2.19	-9.0‰

Comments:
No bottom water samples
$\delta^{13}C$ Organisms (‰):

Acesta bullisi	-21.1
Vesycomia	-34.1
Mussels	-34.3, -37.4, -38.1, -37.2, -36.2, -37.7
Lamellabrachia	-25.9, -23.1

3.3.4. Green Canyon Block 234

The $\delta^{13}C$ value of the organic carbon reflected the amount of oil present as indicated by the elevated EOM values (up to 43,325 ppm). The oil was biodegraded and authigenic carbonate was present (Table 3.4). Salinities were low in pore waters, H_2S was not detected, and ΣCO_2 isotopic compositions suggested active hydrocarbon oxidation was occurring. Bottom water chemistry suggested that brine seepage was occurring. Elevated levels of ^{13}C depleted ΣCO_2 were also present in bottom waters. Bottom water oxygen levels were 3-4 ml/l.

Intensive localized sampling in 1992 revealed the presence of hydrates at the locations sampled. Methane values were extremely high suggesting the presence of hydrates. High levels of C_{2+} hydrocarbon gases and the stable isotopic composition of the methane suggested a mixture of biogenic and thermogenic gas.

Mussels collected at a brine pool in the GC-234 area had very ^{13}C-depleted tissues (-61.9 to -65.9‰) indicative of a primarily biogenic source of CH_4 for the symbionts.

3.4. Summary

All locations sampled have a number of common features including oil seepage; gas charged sediments; hydrates; authigenic carbonate; active hydrocarbon oxidation; chemosynthetic biomass (not only in the symbiotic organisms but also in background fauna); elevated EOM, TOC, and salinity; and biodegraded oil. While it is still not clear which of the features are essential, it is clear that all of these attributes are closely related. A supplementary source of carbon is provided by oil and gas seepage. The oxidation of hydrocarbons contributes to maintaining anoxic conditions. Most, if not all, carbon and energy

Table 3.4. Summary of analytical results from the Green Canyon Block 234 site.

Sediments

Sample	Station	Dive	Core	TOC (%)	$\delta^{13}C_{om}$ (‰)	$\delta^{13}C_{CaCO_3}$ (‰)	$CaCO_3$ (%)	EOM(ppm)	GC/FID
C3506	GC01	42	4	4.0	-26.3	-9.2	9.1	13,576	√
C3507	GC02	43	1	7.3	-27.0	-10.6	7.6	43,325	√
C3508	GC02	43	2	5.4	-26.8	-14.9	8.5	25,139	√
C3509	GC02	43	3	5.3	-26.9	-12.0	11.7	37,976	√
C3510	GC02	43	4	5.2	-27.1	-16.5	16.7	28,813	√
C3511	GC98	44	2	1.1	-24.2	-6.2	13.9	307	√
C3512	GC98	44	1	3.2	-24.6	-0.4	13.5	424	√

Pore Waters

Sample	Field ID	Salinity (‰)	H_2S (µg at/L)	ΣCO_2 (mM/L)	$\delta^{13}C_{\Sigma CO_2}$ (‰)
C3669	910923GC0243	31.3	--	2.56	-16.4
C3670	910923GC0243	27.9	<1.1	2.52	-5.7
C3671	910924GC9844	30.0	<1.3	1.53	-6.4
C3672	910924GC9844	30.4	<1.1	1.97	-6.8

Bottom Water

Sample	$[O_2]$
910923GC3143	3.38 ml
910923GC3143	3.38 ml
910923GC3142	3.69 ml
910924GC9844	3.81 ml

Microwater Samples

Sample	Field ID	Salinity (‰)	ΣCO_2 (mM/L)	$\delta^{13}C_{\Sigma CO_2}$ (‰)
C3687	910923GC0243	31.3	7.78	-8.6
C3689	910923TC0243	30.3	4.58	-10.9, -4.8
C3690	910923GC0142	27.5	11.21	-10.9
C3693	910923GC9844	41.1	1.32	-4.1

Comments:

$\delta^{13}C$ Organisms:

Callogorgia sp. -34.9, -17.5, -17.3, -20.1, -17.3, -18.3, -16.3, -16.3, -14.6, -16.8

Brine Pool Bottom Water

Field ID	$[O_2]$
910924BP0045	NS
910924BP0045	3.17 ml/L

Comments:

No sediment samples

$\delta^{13}C$ Organisms:

Seep Mytilid -62.9, -66.1, -62.5, -63.9, -65.9, -61.2, -63.9, -63.3, -63.4, -63.1, -64.8, -64.0, -63.8, -64.2, -62.0, -61.9, -65.3, -63.6, -62.5, -62.2, -62.2

Lamellibrachia -23.6

Acesta -24.6

transformations are mediated by bacteria. Sulfur, an important element, and hydrate formation/decomposition are intimately associated with the continuous supply of natural gas. It is also clear that pore waters are the main repository of reduced compounds and bottom waters supply oxygen. Steep gradients are present in almost all chemical properties and areal (including vertical) patchiness and heterogeneity are extremely high.

While it may not be clear what critical, or essential, geochemical requirements are needed for proliferation of communities, the presence of oil and gas seepage is a fundamental process in creating the chemical environment that fosters these unusual accumulations of biomass in the deep ocean.

4.0 Long-Term Change

E.N. Powell

4.1. Introduction

Our tasks are: (1) to complete a taphonomic study of the seep sites; (2) to evaluate the persistence of the seep biotas; and (3) to describe the history of the seep sites in terms of community structure. Many of the taphonomic studies have now been published. The single important exception is the *in situ* measurement of taphonomic rates which will be presented below. Objectives 2 and 3 depend on a good model for the interpretation of assemblage composition from cores. That model has also been developed and will be discussed in a subsequent section.

4.1.1. *In Situ* Measurement of Taphonomic Rates

Eight nylon net bags (1x2 cm mesh) were filled with shells of a lucinid, *Codakia orbicularis*, and a mytilid, *Mytilus edulis*. The lucinid shell is constructed of prismatic and crossed-lamellar aragonite; the mussel of mixed fibrous and prismatic calcite and aragonitic nacre (Majewske, 1969; Alexandersson, 1979). Actual shells from the continental slope petroleum seeps were not used because only a small number of these shells were available and also because the majority of shells collected from this region of the slope were already severely taphonomically altered (Callender and Powell, 1992). We chose these two shell types because they have a similar microstructure to the dominant petroleum seep species.

In mid-August, 1988, seven shell bags were deployed at Bush Hill (27°46.9'N, 91°30.4'W) by the *Pisces II* submersible. Each bag was deployed on the sedimentary surface at 550 m. One bag was stored in the laboratory as a control. Three shell bags were recovered during a series of *Johnson Sea-Link* dives in late September, 1991. (Another shell bag was collected in August, 1992, but has not yet been analyzed). Shell bags number 4 and 6 were placed and collected immediately adjacent to each other near a live mussel bed. Shell bag 2 was deployed and collected near another live mussel bed approximately 10 m from the location of the other two bags.

All three bags had remained in their original location over the three-year period; however, each had become buried by 1 to 2 cm of sediment. Sedimentation rates are thought to range from 0.01 to 0.06 cm yr^{-1} (Behrens, 1988) on this portion of the slope, a range that would add 0.03 to 0.18 cm of sediment to the site during the three-year period. Our observed sediment accumulation is well above this range; presumably, the shell bags acted as baffles to trap sediment. Degassing craters, the relatively deep burial of vestimentiferan tubes, and our recent evidence for catastrophic burial of mussel beds, point to active sediment movement and more rapid local burial in some areas. Regardless, burial of the shell bags gradually placed them lower in the taphonomically-active zone, possibly below it, so that taphonomic alteration was unlikely to have been constant throughout the three-year time frame.

Upon recovery of the shell bags, each individual shell was gently washed to remove attached sediment, dried, weighed, measured, and assessed for taphonomic alteration using the method described in Davies et al. (1990). Taphonomic attributes noted for each shell include anterior-posterior length, weight,

periostracum condition, degree of dissolution, abrasion, edge rounding, shell color, degree of fragmentation, and the presence of carbonate precipitates.

Both mussel and lucinid shells left on the sea floor for three years were radically altered by a variety of taphonomic processes (Table 4.1). Significant dissolution and edge-rounding occurred on nearly all shells. Carbonate crusts occurred on some mussel shells. Discoloration was a common feature on both species. Periostracal breakdown occurred in all of the mussels. Some fragmentation and biological alteration was also observed. These alterations occurred despite burial. By three years' time, all three bag samples were covered with 1 to 2 cm of sediment. Many of these taphonomic processes are expected to occur most rapidly while the shells are still exposed on the sea floor; therefore, the rates we observed after three years must represent minimal values.

Among the taphonomic processes affecting the shells, dissolution was the process most likely to affect their long-term preservation. Callender and Powell (1992) showed that dissolution is an important process at all petroleum seep sites studied off Louisiana. Dissolution may be important because elevated concentrations of H_2S typical of most seep sites (Lutz et al., 1988; Roux et al., 1989; Callender et al., 1990) are oxidized to the corrosive H_2SO_4 at the oxic/anoxic interface. This acid production drives carbonate dissolution (Boudreau, 1991). Dissolution not only resulted in loss of shell weight and shell sculpture, but also produced much of the edge-rounding we observed. The two processes, dissolution and edge-rounding, affected the same species and sites to roughly the same degree. Dissolution produced feathered or rounded edges on most mussel shells, but did not affect the edges of lucinid shells. Feathered or rounded edges were also noted by Flessa and Brown (1983) in a laboratory study of shell dissolution.

Powell and Davies (1990) observed that discoloration was a good indication of the relative age of shells on beaches. Discoloration is known to occur rapidly in many environments (Pilkey et al., 1969). Mussel shells generally took on a faded appearance. Lucinid shells were more frequently stained yellowish-brown, sometimes with gray, probably due to exposure to liquid hydrocarbons and H_2S. An alternative explanation is that the yellowish brown color came from the oxidation of sulfide minerals. Orange stains of obvious hydrocarbon origin have been found frequently on lucinid shells from most seep sites. Blackened mussel shells collected from an anoxic brine pool at nearby Green Canyon lease block 233 turned reddish orange in less than one hour when brought to the surface.

A number of mussel shells were fragmented. Callender and Powell (1992) suggested that some fragmentation at petroleum seeps was due to loss of shell integrity as dissolution proceeded rather than any physical or biological breakage. In our study, mussel shells had been so weakened by dissolution that only the continuing presence of periostracum maintained the shell in a recognizable condition. The selective preservation of protein coats and loss of shell carbonate has also been described for some foraminifera (De Vernal et al., 1992). The life span of a recognizable mussel shell on the sea floor, certainly less than ten years, is probably controlled in large measure by the rate of degradation of the periostracum.

Authigenic carbonate production is an important feature of seep sites (e.g., Han and Suess, 1989). This process obviously can occur rapidly. About 25% of the mussel shells had recognizable carbonate crusts. None of the lucinid shells did. As the lucinid shells were much less affected by dissolution, the implication is that the carbonate crust required a surface affected by dissolution. However, carbonate

Table 4.1. Taphonomic attributes for the control shells and the altered shells from the two locations. Data are expressed as percentages within samples. Some percentages may not add to 100% due to rounding errors. The attributes are as defined in Davies et al. (1989) and Powell and Davies (1990) except that precipitation present includes all degrees of precipitation, fragmentation includes all degrees of fragmentation except chipped edges, original color is the lifelike condition, faded includes shells still retaining some original coloration and those with no original color remaining (white), and stained includes all types of stains from gray to orange.

	Mussels			Lucinids		
Attribute	Control	Bags 4,6	Bag 2	Control	Bags 4,6	Bag 2
Number	28	39	25	14	32	16
Periostracum						
Entirely present	28.6	0.0	0.0	--	--	--
Partially present	71.4	97.4	100.0	--	--	--
Absent	0.0	2.6	0.0	--	--	--
Dissolution						
None	46.3	0.0	0.0	85.7	46.9	31.3
Minor	42.9	0.0	12.0	14.3	40.6	50.0
Major	10.7	100.0	88.0	0.0	12.5	18.8
Edge Rounding						
Unaltered edges	78.6	69.2	0.0	100.0	68.8	18.8
Chipped edges	7.1	10.3	0.0	0.0	31.2	81.3
Sharp edges	7.1	0.0	0.0	0.0	0.0	0.0
Slightly worn edges	7.1	2.6	68.0	0.0	0.0	0.0
Smooth edges	0.0	18.0	32.0	0.0	0.0	0.0
Precipitation						
Absent	100.0	92.3	76.0	100.0	100.0	100.0
Minor	0.0	7.7	24.0	0.0	0.0	0.0
Color						
Original Color	100.0	0.0	0.0	92.9	37.5	6.3
Faded Color	0.0	74.4	96.0	0.0	25.0	18.7
Stained	0.0	25.6	4.0	7.1	37.5	75.0
Abrasion						
None	21.4	25.6	100.0	14.3	31.3	81.3
Minor	78.6	74.4	0.0	85.7	68.8	18.8
Fragmentation						
Whole	100.0	87.2	96.0	100.0	100.0	100.0
Fragmented	0.0	12.8	4.0	--	--	--
Biologic alteration						
Absent	96.4	87.2	76.0	92.9	81.3	25.0
Present	3.6	12.8	24.0	7.1	18.8	75.0

crusts were only observed on the inner shell surface where dissolution was less severe and most commonly in the shell center rather than around the margin. Consequently, microenvironment was important in authigenic carbonate formation. Dissolution and precipitation occur within microenvironments of close proximity since all shells with carbonate crusts also showed clear evidence of dissolution. The deployment site where carbonate crusts occurred most frequently was also characterized by mussel shells that had lost the most weight through dissolution.

With the exception of staining and some aspects of biological alteration, mussel shells were degraded significantly more rapidly than lucinid shells in three years. Mussels were more heavily dissolved, lost more weight (Figures 4.1 and 4.2), had more altered edges, were more prone to fragmentation, and exhibited greater weight loss (=carbonate loss) than did the lucinids. Mussels have a higher surface-to-volume ratio which should make them more susceptible to rapid degradation (Aberhan and Försich, 1991); however, the rate of degradation of mussel shell was much faster than what might be expected based on a simple relationship with surface area. Probably some other aspect of shell construction, such as organic content, was important. The estimate of the life span of a mussel shell was three to 15 years at the most affected site, whereas a lucinid shell was indefinitely preserved on the scale we could measure.

Although the mussel shells were significantly more degraded, the process of degradation was similar in many respects between the two species. In both cases, the dorsal and umbonal area of the shell's outer surface was most seriously affected, as was the ventral margin. The ventral and inner surfaces were less seriously affected (Tables 4.2, 4.3, and 4.4). Precipitation was an obvious exception (Table 4.4). The differences, then, were more in degree than in kind and probably represent those areas first affected by taphonomic processes during life. The dorsal, umbonal area of the shell's outer surface is likely to be the site of periostracum degradation during life and, thus, the shell surface is likely to be more exposed to taphonomic assault in this area after death.

Mussel shells, being of epifaunal origin, should stand a lesser chance of preservation than shells from the infaunal lucinid. Differences in life habit and the more rapid deterioration of the mussel shells that occurred when placed under equivalent conditions with the clams lends credence to the belief that the species composition of seep death assemblages is biased in favor of the more robust clams. Furthermore, the relatively good preservation of the clams should not be taken as an indication of an unbiased preservation of the assemblage as a whole any more than should its autochthonous nature (Callender and Powell, 1992). Some lucinid shells were still in mint condition after three years on the sea floor. All of them would have been described as well preserved, yet most mussels had suffered significant taphonomic decay.

Callender and Powell (1992) suggested that one of the important characteristics of autochthonous assemblages, like those at petroleum seeps, was the importance of small-scale variability in the preservational process. In our case, shells deployed within 10 m of each other suffered considerably different degrees of taphonomic attack. The source of this local variation is unclear. Processes as divergent as discoloration, dissolution, and biological alteration were more important in bag 2 than in bags 4 and 6. One likely explanation is that bag 2 was buried more slowly than the bags at the other deployment site; however, we have nothing but circumstantial evidence associated with the shells to support this belief.

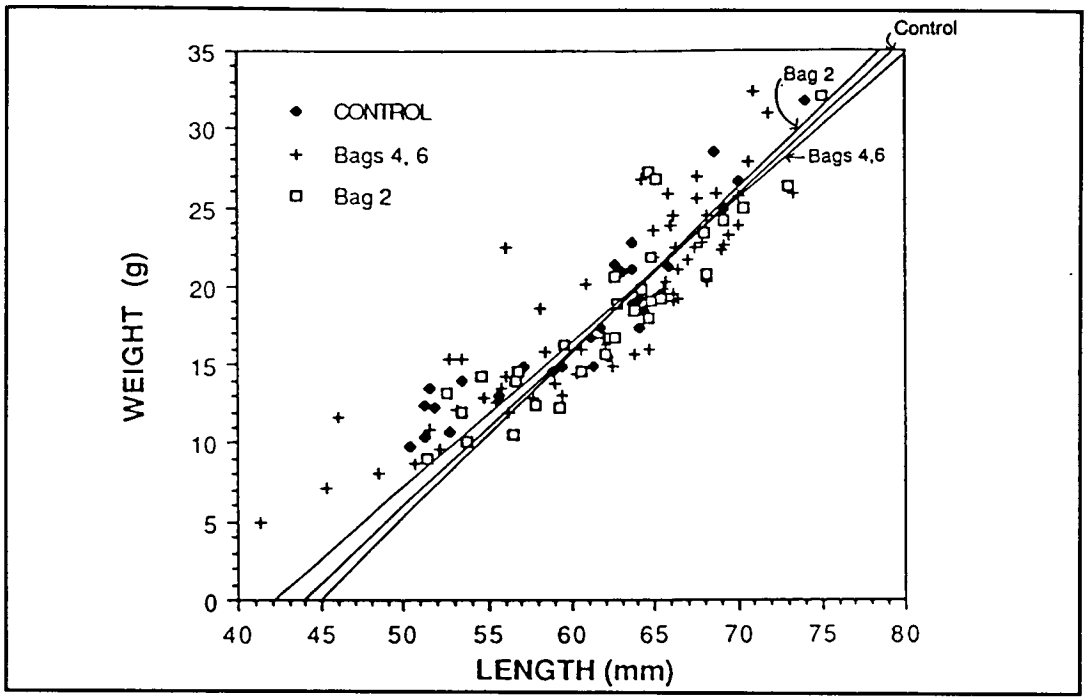

Figure 4.1. A plot of shell weight vs. length for the control lucinids and the two deployed sets of lucinid samples after three years on the sea floor. The regression lines were obtained from a least normal squares analysis (Williams and Troutman, 1987; Troutman and Williams, 1987).

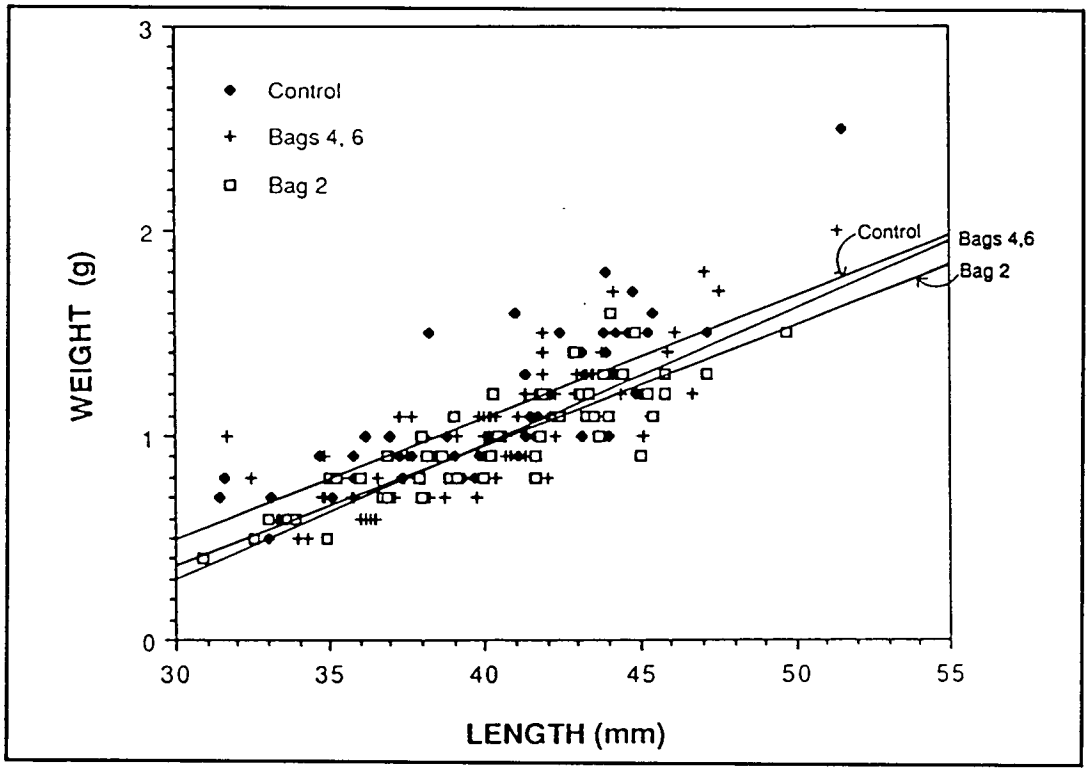

Figure 4.2. A plot of shell weight vs. length for the control mussels and the two deployed sets of mussel samples after three years on the sea floor. The regression lines were obtained from a least normal squares analysis (Williams and Troutman, 1987; Troutman and Williams, 1987).

Table 4.2. The locations of dissolution on the mussel shells. Data are presented as percentages of the total number of observations of dissolution. For example, if five shells showed evidence of dissolution, each at two of the possible eight locations, the number of observations of dissolution would be ten. The percentage of those for each standard shell area would then be recorded. The degrees of dissolution are defined in Davies et al. (1989) and Callender and Powell (1992). Minor dissolution includes chalkiness and minor pitting. Major dissolution was divided into extreme dissolution, a deeply eroded shell surface, and less extreme, but still major, dissolution such as heavy or generalized pitting and the loss of surface sculpture.

	All Dissolution			Minor Dissolution Only			Major Dissolution Only			Extreme Dissolution Only		
Shell Location	Control	Bags 4,6	Bag 2	Control	Bags 4,6	Bag 2	Control	Bags 4,6	Bag 2	Control	Bags 4,6	Bag 2
Dorsal Margin	26.8	12.3	13.1	25.0	0.7	2.6	--	6.2	29.4	--	30.6	27.9
Upper Posterior	19.5	12.3	12.6	16.7	2.2	5.3	--	13.9	26.5	--	24.1	20.9
Upper Anterior	22.0	12.3	12.6	22.2	2.2	4.4	--	13.9	23.5	--	24.1	25.6
Middle Posterior	17.1	12.6	12.0	19.4	11.0	16.7	--	30.8	8.8	--	3.7	2.3
Middle Anterior	14.6	12.6	12.0	16.7	11.0	16.7	--	30.8	8.8	--	3.7	2.3
Posterior Margin	0.0	12.6	12.6	0.0	24.3	18.4	--	1.5	0.0	--	4.6	7.0
Ventral Margin	0.0	12.6	12.6	0.0	24.2	18.4	--	1.5	0.0	--	4.6	7.0
Anterior Margin	0.0	12.6	12.6	0.0	24.3	17.6	--	1.5	2.9	--	4.6	7.0

Table 4.3. The locations of dissolution, abrasion, and edge rounding on the lucinid shells. Data are presented as percentages of the total number of observations. Further details are in Table 4.2.

Shell Location	Dissolution			Abrasion			Edge Rounding		
	Control	Bags 4,6	Bag 2	Control	Bags 4,6	Bag 2	Control	Bags 4,6	Bag 2
Dorsal Margin	100.0	34.9	19.5	0.0	3.7	0.0	-	0.0	0.0
Upper Posterior	0.0	20.9	17.1	0.0	0.0	0.0	-	0.0	0.0
Upper Anterior	0.0	20.9	14.6	0.0	0.0	0.0	-	0.0	0.0
Middle Posterior	0.0	7.0	12.2	0.0	14.8	40.0	-	0.0	0.0
Middle Anterior	0.0	7.0	12.2	0.0	13.0	40.0	-	0.0	0.0
Posterior Margin	0.0	4.7	7.3	40.9	25.9	0.0	-	31.8	34.5
Ventral Margin	0.0	2.3	9.8	22.7	16.7	0.0	-	36.4	24.1
Anterior Margin	0.0	2.3	7.3	36.4	25.9	20.0	-	31.8	41.4

Table 4.4. The locations of abrasion, precipitation, and edge-rounding on the mussel shells. Data are presented as percentages of the total number of observations. Further details are in Table 4.2.

Shell Location	Abrasion			Precipitation			Edge Rounding		
	Control	Bags 4,6	Bag 2	Control	Bags 4,6	Bag 2	Control	Bags 4,6	Bag 2
Dorsal Margin	20.7	0.0	-	-	0.0	15.8	0.0	5.1	20.9
Upper Posterior	13.8	0.0	-	-	14.3	21.1	0.0	5.1	0.0
Upper Anterior	13.8	0.0	-	-	14.3	15.8	0.0	10.3	1.1
Middle Posterior	5.2	0.0	-	-	28.6	10.5	0.0	10.3	1.1
Middle Anterior	5.2	0.0	-	-	28.6	10.5	0.0	5.1	0.0
Posterior Margin	6.9	33.3	-	-	0.0	5.3	16.7	20.5	26.4
Ventral Margin	31.0	34.5	-	-	0.0	5.3	83.3	20.5	25.3
Anterior Margin	6.9	32.1	-	-	14.3	15.8	0.0	23.0	25.3

Accordingly, petroleum seep assemblages on the continental slope are significantly and rapidly altered by taphonomic processes just as are their shallow-water counterparts. Most of the processes are the same and the biases imposed by them are not surprising, although the rates certainly differ. The presence of carbonate encrustation and the relative absence of abrasion are the salient exceptions. The principle bias introduced is produced by dissolution and periostracal degradation. The rates of these processes are species- and size-dependent, so that the final assemblage is heavily biased against juveniles and selected species.

4.1.2. Community-Structure Model

Samples from the Louisiana petroleum seeps were collected by submersible and by remote-sampling using a surface vessel. Twenty samples were collected with a submersible-operated grab during a series of *Johnson Sea-Link* dives in June, 1987. An additional 17 samples were collected using a 45 x 45-cm, 1-m deep box core during three separate R/V *Gyre* cruises in March of 1987. All samples were sieved onboard using a 1-mm mesh screen and preserved in 70% EtOH. Each specimen was identified to the lowest taxonomic level possible and its dimensions measured (anterior-posterior length for bivalves; apex-adapical tip length for gastropods).

Biomass-at-death, or upon collection if alive, was estimated from shell dimensions using the equations derived by Powell and Stanton (1985). For bivalves,

$$\log_{10}B = 0.95761 \log_{10}V - 4.8939 \quad (1)$$

where

B = biomass in g ash-free dry weight and
V = biovolume (in mm^3).

For bivalves, $V = L^3$ where L is the maximum anterior-posterior length (in mm). For gastropods,

$$\log_{10}B = 0.77081 \log_{10}V - 3.2421 \quad (2)$$

where V is an operational equivalent of shell volume derived, for most gastropods, from the equation for a cone:

$$V = \frac{1}{3}\pi\left(\frac{W}{2}\right)^2 L \quad (3)$$

where

W = the maximum width in mm and
L = the maximum apex-adapical length in mm.

For some cylindrical species, such as *Dentalium* sp., alternative equations were used (Staff et al., 1985; Powell and Stanton, 1985).

Biomass was calculated for each whole individual. Whole shells were defined using the criteria of Davies et al. (1990): > 90% of the original form for which an anterior-posterior length in bivalves or the apex-adapical length in gastropods could be accurately measured.

Estimation of paleoenergetics followed the approach described by Powell and Stanton (1985):

$$A_{lt} = P_{glt} + P_{rlt} + R_{lt} \quad (4)$$

where

A_{lt} = the energy assimilated over the individual's life span,
P_{glt} = the portion of net production devoted to somatic growth over the individual's life span,
P_{rlt} = the portion of net production devoted to reproduction over the individual's life span, and
R_{lt} = the amount of energy respired over the individual's life span.

The amount of energy consumed over the animal's life span is, then, the assimilated energy divided by the assimilation efficiency.

$$I_{lt} = A_{lt}\left(\frac{A}{I}\right)^{-1} \tag{5}$$

The parameters of equation (4) are estimated as follows:

$$P_{rlt} = 18 \text{ or } 6.8\% \text{ of } \left[\int_{t_o}^{t_n} RdR - \int_{t_o}^{t_m} RdR\right] \tag{6}$$

where

t_0 = age at birth,
t_m = age at maturity, and
t_n = age at death.

The values of 18% or 6.8% are for bivalves and gastropods respectively.

$$P_{glt} = B \tag{7}$$

where B = biomass at death in calories.

$$R_{lt} = \int_{t_o}^{t_n} \left[\left(s_T^{3m_r m_b}\right)\left(10^{m_r b_b + b_r}\right)\left[\log_{10}(T+1)\right]^{3m_r m_b}\right] dT \tag{8}$$

The constants in equation (8) come from three equations: (a) biomass versus respiration at 10°C

$$\log_{10}R = m_r \log_{10}B + b_r \tag{9}$$

(b) size (biovolume) versus biomass

$$\log_{10}B = m_b \log_{10}V + b_b \tag{10}$$

(c) size versus age

$$V = S^3 = [S_T \log_{10}(T+1)]^3 \quad (11)$$

where S (in mm) is a linear measurement of size. The values of b_b and m_b are given in equations (1) and (2). The values of m_r and b_r were taken from the equation relating biomass to respiration at 10°C given by Powell and Stanton (1985): m_r = 0.8573; b_r = 1.4984. The constant S_T was obtained by solving equation (11) using a known maximum size and maximum age for each species.

Maximum size was obtained from Odé (1975-1988) and our unpublished data. Maximum ages were obtained from Powell and Cummins (1985), Powell and Stanton (1985), Comfort (1957), Heller (1990), and others. In cases where a maximum age could not be obtained from the literature, either through reference to the species in question or a closely related taxon, we assigned a maximum age of two years. This resulted in an underestimation of paleoenergetics for these species. The most egregious of such was the estimation of lucinid maximum age at two years. No maximum age data are available for Lucinidae. Likely, this is a factor of 4 or more underestimated and, consequently, so too would be energy flow.

Six distinct biofacies are present at the petroleum seeps; mytilid mussels, vesicomyid clams, Lucinoma clams, thyasirid clams, vestimentiferan tubeworms and the normal slope fauna (hereafter termed non-seep biofacies) (Callender et al., 1990; Callender and Powell, 1992).

As Simberloff and Dayan (1991) eloquently point out, guild structure is a powerful tool for characterizing and comparing community structure. In paleoecology, guild structure has a long history not only for the reasons forwarded by Simberloff and Dayan (1991), but also because guild structure is better preserved than other trophic characteristics of the community (Staff et al., 1985; Powell et al., 1989). Guild structure is complicated in many seep communities. Besides the ever present deposit feeding guild and predator guild, the suspension feeders can be divided into low and high-level forms, the grazing guild, or herbivore, is well represented, and a chemoautotrophic guild dominates many assemblages. Accordingly, we used two types of guild structure, one based on the actual feeding information present for seep organisms and a simplified guild structure based on the more common feeding type associated with the lebensform of the organism.

The more complicated set comprised six guilds: herbivores, chemosynthetic species, low- and high-level suspension feeders, predators and deposit feeders. Parasites and predators were combined into one feeding category. The simplified set comprised four guilds: high- and low-level suspension feeders, predators and deposit feeders. In simplifying, we partition the chemoautotrophic guild between the low- and high-level suspension feeders. These taxa would certainly be considered suspension feeders if symbiosis went undetected, with one exception. Vesicomyids are classified as deposit feeders because of their umbo-up life habit and the finding of small amounts of algal detritus and sediment in the gut, indicating a rudimentary deposit-feeding capability (Le Pennec and Fiala-Médioni, 1988; Hilly et al., 1986). We combine the herbivores with the deposit-feeders, as both are likely grazing in one way or another on bacteria. Finally, we note the absence of the conveyor-belt, head-down group of deposit feeders. Both the herbivores and classic deposit feeders feed near or on the surface of the sediment in all of these biofacies.

We divided the fauna into four habitat tiers based on the location of their body mass and also their feeding structure: infauna, semi-infauna, low-level epifauna, and high-level epifauna. Rather than distinguishing habitat by mobility [e.g., vagrant, as used by Scott (1978) and Miller (1982)], we use the high and low level epifaunal categories of Ausich and Bottjer (1982) to distinguish position. Semi-infauna were those animals whose body mass straddles the sediment-water interface, such as many clams. The vesicomyids are good examples (Rosman et al., 1987). Low-level epifauna were species whose bodies rested on or just off the sediment surface and whose feeding structures were confined to near sediment-surface water. Mussels are good examples. The high-level epifaunal tiers comprise species which could raise their feeding structures significantly above the surrounding sediment either by being erect forms, forms attached to other taxa, or mobile forms which typically climbed on top of other species. Most vagrant benthos, such as herbivores grazing on mussels, tubeworms, and brachiopods, were included in the high level epifauna because they normally feed on top of the shelled chemosynthetic fauna.

The assemblage, as preserved below the depth of final burial, may not resemble the surface, actively-accumulating component normally studied by researchers. Size-selective taphonomic loss is an important process in the formation of death assemblages at petroleum seeps (Callender and Powell, 1992) (Figure 4.3). In addition, mussels of any size are poorly preserved (Callender and Powell, submitted). [Farrow and Fyfe (1988) also comment on the rapid loss of mussels from death assemblages.] Accordingly, we estimate the guild and tier structure of these biofacies as they might appear in the fossil record by removing the mussels and the smallest size classes. Biofacies size-frequency distributions were based on the largest shell collected in the biofacies. Specimens were placed into ten size classes, defined as 10, 20, 30%, etc. of the maximum size. Table 4.5 shows that these maximum sizes varied from 31.6 to 108.2 mm. In each cases, we deleted shells less than 30% of the maximum size.

Table 4.5. Biofacies size-frequency distribution based on largest shell collected in the biofacies.

Biofacies	Maximum Size
Non-seep	31.6
Tubeworm	71.9
Mussel	108.2
Vesicomyid	92.4
Lucinid	92.3
Thyasirid	59.9

Analyzing community structure by trophic guild reveals that all of the seep communities were dominated by primary consumers, namely suspension feeders, whereas the non-seep biofacies was dominated by carnivores. Interestingly, Kammer et al. (1986) found a trophic structure dominated by small deposit feeders and carnivores for dysaerobic biofacies which resemble the non-seep biofacies in

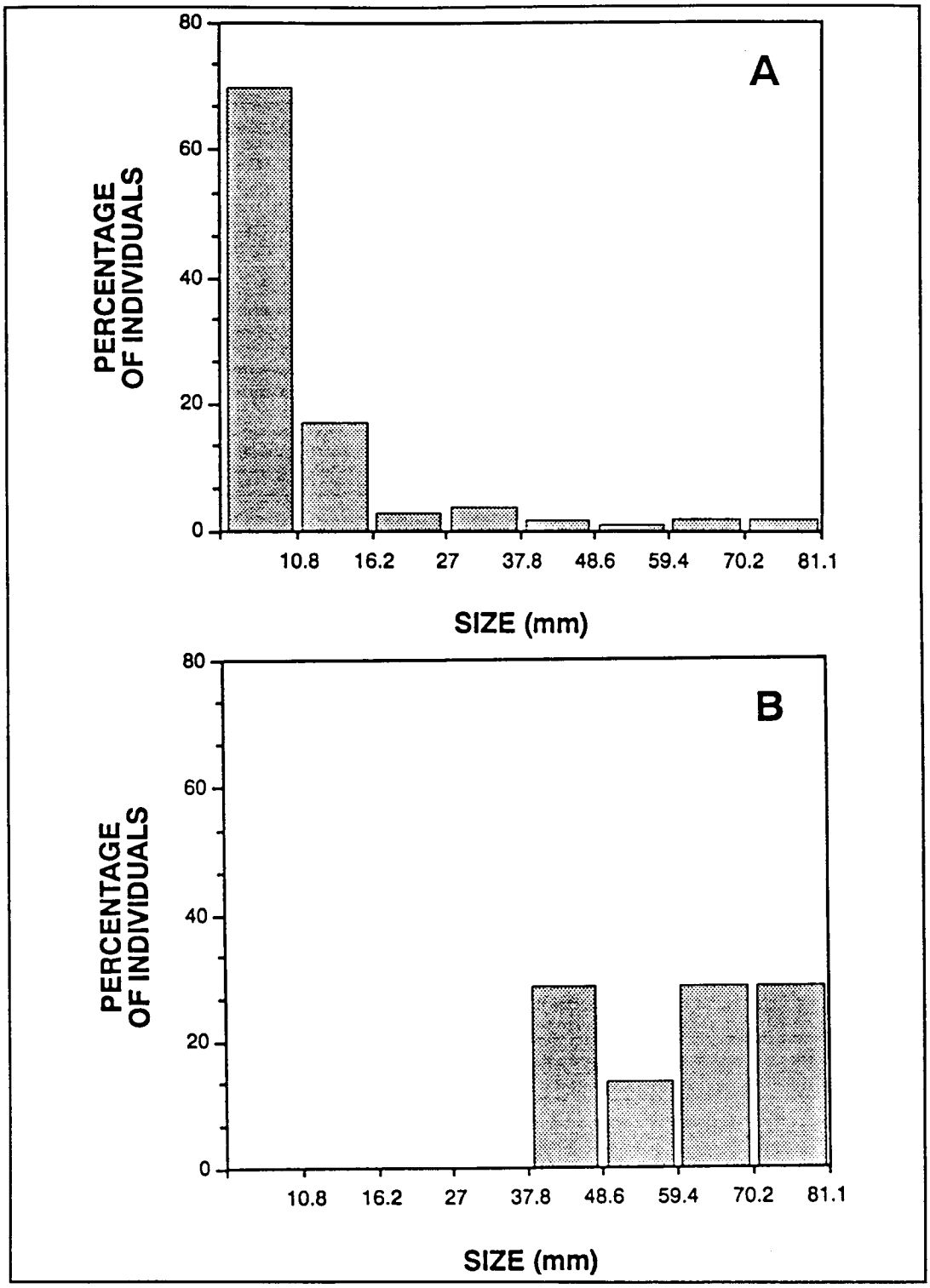

Figure 4.3. (a) Size frequency distribution of mussel shells from the mussel biofacies described by Callender and Powell (1992) and (b) the size frequency predicted after 10 years, given a rate of weight reduction of 0.11 g yr^{-1}, in percent of total. Lengths are the central values of the size class.

many respects. In recent, living communities, ecological conversion efficiencies between trophic levels typically vary between 10 and 20% (Powell and Stanton, 1985). Accordingly, carnivores should make up about 10 to 20% of the biomass of the primary consumer trophic level. The study of death assemblages, however, deals with animals that have died and, as such, have completed their life spans. A predator, then, requires not the standing crop necessary to meet its immediate or even yearly needs, but enough prey to meet its needs over its lifetime (Powell and Stanton, 1985). Accordingly, carnivores, if equivalently represented, would be very rare in death assemblages in comparison to the primary consumer level which, by definition, must have had shorter life spans.

Insufficient data are available to determine how frequently death assemblages contain an unexpectedly high representation of the predator guild. Biomass and energy flow estimates have rarely been conducted. Scott (1978) reviews a set of literature which suggests that predator dominance might be an expected attribute of shelf communities, as opposed to bays, where predators typically comprise a lower fraction of the biota. Miller's (1982) bay to inner shelf transect shows suspension feeder dominance by number in all cases; however predators make up over 10% of Miller's shelf association, high by paleoenergetics standards. Carnivore percentages in death assemblages on the Texas shelf are also high and range from approximately 35% nearshore to 12% further offshore (Staff, pers. comm.). Most of these case histories represent data derived from numerical abundance. Hoffman (1977) provides a series of examples, based on biovolume, of overrepresentation of predators and parasites in the fossil record. Stanton et al. (1981) and Stanton and Nelson (1980) present an example discussed further by Powell and Stanton (1985) in which the trophic inequality was demonstrated both in terms of biomass and at the paleoenergetics level. The data presently available suggest, then, that the proportional inequality biased in favor of carnivores might be typical of shelf (or euhaline) assemblages.

In that case, the presence of an unusually large fraction of carnivores in an assemblage is not unusual for shelf and slope death assemblages. A high fraction of carnivores in these assemblages must indicate that a large fraction of non-preserved, probably soft-bodied taxa exist in these communities. This is likely the composition of the non-seep biofacies which appears to be rather typical in its overabundance of carnivores. The seep biofacies, in contrast, is dominated by shelled biota and retains the theoretically-expected rarity of predaceous forms, a clear exception to the standard overrepresentation of carnivores. Callender et al. (1990) remark on the low abundance of soft-bodied infauna in seep communities, which might support a shelled carnivore guild but not be preserved. Table 4.5 compares the biomass requirements of the predators with that present as preserved prey. The non-seep biofacies is a factor of 100 out of balance whereas preserved prey are 10 or more times more plentiful than required to support the preserved predators in all seep biofacies. One possible explanation for the guild structure of seep assemblages is that the rarity of carnivores requires the dominance of shelled biota among the primary consumer guilds in the living community and this dominance marks a significant difference between the seep biofacies and the non-seep biofacies and the shelf communities previously considered.

The lucinid and thyasirid assemblages were dominated by infauna. The tubeworm and mussel biofacies were dominated by epifauna, and when fossilized would likely also be dominated by epifauna. The non-seep biofacies was dominated

by semi-infauna (when fossilized). Epifauna were also well represented, particularly by biomass, and, numerically, infauna were also important. The vesicomyid biofacies was dominated by semi-infauna. Once again the non-seep biofacies presents an unusual community structure among these slope biofacies in having most tiers well-represented. Once again, the literature does not contain adequate quantitative analyses of these tier structures. However, epifaunally-dominated assemblages are predominant in the recent and fossil record (Staff et al., 1985). The infaunal tier was well represented in most petroleum seep biofacies because a large fraction of the shelled biota were epifauna or semi-infauna. Dominance by infaunal suspension feeders is unusual; the dominance of the non-seep biofacies by epifauna/semi-infauna and carnivores is much less unusual.

One important concern is the understanding of the trophodynamics of the community. What was the productivity of the community over time? Death assemblages rarely preserve good evidence of ecological productivity. Firstly, much of the net production of the community is housed in small, frequently soft-bodied taxa. Secondly, even if shelled, these small individuals will rarely be adequately preserved. Dissolution is an important taphonomic process in most habitats (Powell et al., 1989; Denne and Sen Gupta, 1989; Callender and Powell, 1992).

Callender and Powell (1992) documented the decrease in species diversity and right-skewing of the size-frequency distribution across the transition from the actively accumulating assemblage to the assemblage below the depth of final burial in the lucinid biofacies, caused by the gradual taphonomic loss of small-sized individuals. They suggested that the same processes could be applied to all seep biofacies (see Figure 4.3). Few juveniles are present in the thyasirid assemblages. From Callender and Powell (1992), we believe the size-frequency distribution present documents the poor preservation of small-sized individuals, particularly juveniles. No living individuals were collected in this biofacies; it may, therefore, have been relatively old, on a taphonomic time scale. Accordingly, the net production of the community is unlikely to be preserved well enough to be deciphered in the death assemblage.

In contrast, community ingestion (energy consumption of the biota) is much better preserved. Large long-lived animals contribute disproportionately to community ingestion. They contribute little of the net production as measured by growth of somatic tissue. Large long-lived animals tend to be shelled or have preservable skeletal parts (Staff et al., 1985). Accordingly, community ingestion is normally a relatively well preserved attribute of the community and carbonate production will normally be correlated with it. Unfortunately, this attribute, community ingestion, is a lifetime attribute complete only at the end of the individuals' life spans. This type of time averaging makes comparison to the ecological literature difficult and necessitates the consideration of the attribute on a different scale. We have used the prefix "paleo-" to distinguish time-averaged attributes from ecological attributes. We disagree with those using the term "paleoproduction" to refer to the ecological attribute in the fossil record. As equation (7) shows, paleoproduction, the net production of somatic tissue, is also a lifetime attribute. All of our calculations of biomass, in fact, are true paleoproduction estimates for these species.

Paleoingestion provides a vehicle for addressing questions about paleoenergetics in a way analogous to net production in ecological usage. Both measure aspects of energy flow through the community. Inherently, this approach

requires modeling as well as data collection. A number of modeling efforts aimed at estimating paleoenergetics have already occurred (Lapenis et al., 1990; Lyle and Pisias, 1990; Herguera and Berger, 1991). The difficulty of measuring primary productivity in the fossil record (Herbert et al., 1989) suggests that hindcasting models based on the preserved assemblage may be most successful. That is the approach chosen here.

A primary clue for the recognition of seep assemblages is the considerable biomass production relative to adjacent non-seep settings. The deep sea represents a food-limited situation (Rowe et al., 1991). Any sort of enhanced nutrient input can have a profound impact on the community structure of the benthos. Standard attributes of the slope and shelf assemblages of the northwestern Gulf of Mexico include low density and small size (our unpubl. data). Low food supply is generally associated with small size (Hofmann et al., submitted). The non-seep biofacies had the least nutrient enrichment, the lowest biomass, and the smallest individuals. The extensive biomass production at cold seeps in an otherwise depauperate setting is a direct result of localized nutrient enrichment. Calculations of paleoingestion per m^3 confirm that the non-seep biofacies has considerably less paleoproduction. The size and numbers of individuals present in the various seep biofacies suggest a high productivity.

Seep communities are communities for which regional phytoplankton productivity is inadequate for their support. That is, the assemblage's size frequency contains individuals larger than would be expected from the regional level of primary production and, hence, food supply. In the case of the Louisiana slope, carbon flux, including the loss of food during planktonic rain [carbon flux declines with depth indicating ever decreasing food content (Rowe et al., 1991)], is about 20 mg C m^{-2} d^{-1} at petroleum seep depths (Rowe et al., 1991). This comes to 186 cal m^{-2} d^{-1} [using Parsons et al. (1984) g C to cal conversion]. The actual food concentration present at these seeps cannot be determined easily. Near-hydrothermal vent data for food flux indicate no difference from the normal bottom typical of non-seep biofacies (Khripounoff and Alberic, 1991), so we assume that the above calculation is adequate for all sites. Some fraction of the food reaching the bottom is utilized in bacterial and meiofaunal respiration and thus not available to the macrofauna. From measurements of benthic oxygen demand (see Powell et al., 1989), this likely accounts for 80% or more of the total. Accordingly, the value of 186 cal m^{-2} d^{-1} probably overestimates food availability by a large factor.

An estimate of food demand can be made as follows: we take the ingestion requirements represented by the preserved assemblage, from Table 4.5, for the lucinid and vesicomyid biofacies, assume a 40-cm deep sampling depth for the lucinid biofacies and a 10-cm deep sampling depth for the vesicomyid biofacies, and using a sedimentation rate of 0.3 cm yr^{-1} from Behrens (1988), we calculate the ingestion demand per m^2 per year. We raise the lucinid value by one-third to approximate the densest lucinid beds found and correct for the fragment-to-whole ratio (Callender and Powell, 1992) assuming four fragments per whole shell. Ingestion demand so calculated is 2940 cal m^{-2} d^{-1} for the vesicomyid biofacies and 31 cal m^{-2} d^{-1} for the lucinid biofacies. The lucinid estimate is likely to be very conservative because a two-year maximum age was used for these species. If a 10+ year maximum age had been used (vesicomyids live for 30+ yr), the final estimate would be at least 150 cal m^{-2} yr^{-1} higher.

The same calculation can be made for the non-seep biofacies. However, the carnivore values of the non-seep biofacies indicate that few primary consumers were preserved. Accordingly, we increase the values calculated proportionately by taking the carnivore demand to predict the expected biomass of the primary consumers not preserved and use the ratio between biomass and energy flow for the primary consumers that were preserved to calculate the energy demand of the unpreserved primary consumers. We assume that this ratio holds over all species. We again correct for fragments. This yields an ingestion of 33 cal m^{-2} d^{-1}.

Estimated food demand for the non-seep, lucinid, and vesicomyid faunas and food supply, as a flux, from Rowe et al. (1991) compare as follows: 33, > 31, 2940 cal m^{-2} d^{-1} demand versus 186 cal m^{-2} d^{-1} supply. Recognizing that food availability is likely to be considerably overestimated and that the calculated food requirement for the lucinid biofacies is probably considerably underestimated, planktonic primary production can supply the non-seep biofacies' needs, but cannot supply the vesicomyid biofacies' needs and may not be able to supply the lucinid biofacies' needs. Local enrichment by chemosynthesis is required to support the observed biomass of the vesicomyid biofacies, and probably the lucinid biofacies, either through symbiosis or free-living bacterial production and, of course, all of these clams do have bacterial symbionts. Hindcasting of energy demand based on the observed biomass as preserved and an estimate of sedimentation rate confirms that energy demand exceeds the supply from planktonic rain in these communities. Accordingly, the local enrichment hypothesis, a necessary concomitant of the seep hypothesis, can be confirmed in the death assemblage as well as by observation of live animal physiology and isotopic composition.

5.0 Community Structure and Short-Term Change

I.R. MacDonald

5.1. Introduction

This work component is concerned with describing the patterns in community structure evident in biological assemblages supported by seepage and with documenting natural variation in these patterns. These results will be developed from quantitative analysis of video or photographic images of the seep communities that sample the megafauna, and certain of the abiotic components of the ecosystem. The utility of the images has been extended by use of several photographic techniques. In addition, special analytical methods were used to expand quantifiable coverage of the images over space and time.

5.2. Field Methods

5.2.1. Quantitative Photography

The goals of quantitative photography are to identify the fauna present to the lowest practical taxon and to estimate densities of these fauna in known regions of the study sites. Both video and emulsion photographs were used to obtain images in which seep fauna could be identified and the areal coverage of the image was known. Studio-quality videos were provided by the cameras on the *Johnson Sea-Link.* The emulsion camera used was either a Benthos® 35-mm camera with 28-mm lens or a Photosea® stereo camera, which took photographs stereo-paired as an aid to determining three-dimensional details in the communities. The cameras were oriented vertically and generally took pictures at altitudes of 1 to 3 m above the seafloor. Lasers, mounted on the cameras in parallel arrays of two or four, provided a reliable scale for the photographs by projecting red dots a known distance apart in the final images. Additional analysis of video sequences was occasionally employed to obtain a qualitative characterization of the fauna at sampling stations. In all cases, the time and date were recorded on the imagery, which, together with the navigation records of the support ship and the dive note, provided a reliable means for determining where each photograph was taken.

We deployed durable markers at the sites to facilitate collection of abiotic samples and photographic survey from repeatable locations. A star pattern was flown over the marker at each station. Use of a mosaic form (Fig. 5.1) ensured collection of standardized data sets for each station. Imagery data were collected with both the video camera and, with one exception (GB 386), repetetive photographs were obtained from stations at all of the study sites during JSL-91 and JSL-92. Table 5.1 shows coverage obtained at the study sites during the two cruises. Table 5.2 provides a complete inventory of photographs collected during JSL-91 and JSL-92.

DIVE:_____

SITE:_____

Station _____

	Heading	Start Time	Start Counter	Start Depth	End Time	End Counter	End Depth
1.							
2.							
3.							
4.							
5.							
6.							

Station _____

	Heading	Start Time	Start Counter	Start Depth	End Time	End Counter	End Depth
1.							
2.							
3.							
4.							
5.							
6.							

1. Request a fix
2. Take mosaic photos after sampling has been completed at station.
3. Orient transects with repsect to a central marker—note its number
4. Wait for good visibilty for each transect.
5. Set intervalometer at 7 sec.
6. Make sure lasers are on for camera & video.
7. Have pilot point video down.
8. Try and keep 2 m altitude.
9. Total transect length min. 10, max 15 m
10. Parallel transect spacing 1.5 m--use lasers in video to judge transect spacing.

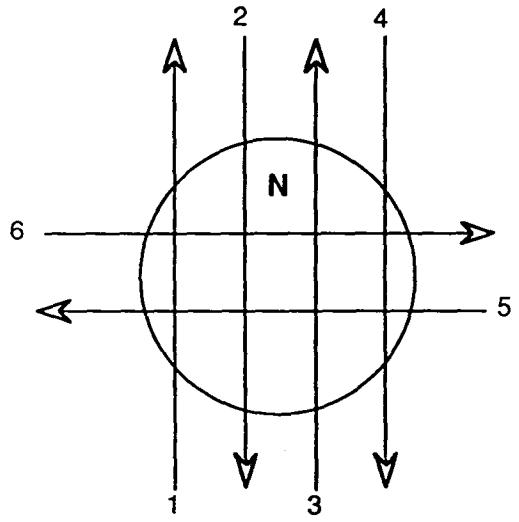

Figure 5.1. Mosaic form used to collect standard data.

Table 5.1. Overview of photographic surveys collected during JSL-91, JSL-92, and ALVIN-92.

Site	Quantitative 1991	Quantitative 1992	Mosaic 1991-92
VK 826	yes	yes	yes
GC 234	yes	yes	yes
GC 233	yes	yes	yes
GC 184/185	yes	yes	yes
GC 386	yes	marginal	no
AC 645	na	yes	potential

Table 5.2. Inventory of color positives (mosaics) from JSL-91.

DIVE	TIMES
3129	10.07.57, 10.08.(07, 16), 11.39.(17, 27, 36, 46, 55), 11.40.(05, 14, 24, 33, 43), 11.46.(07, 17, 26, 36, 45, 55), 11.47.(04, 14, 23, 33, 42, 52), 12.02.(44, 53), 12.03.(03, 12, 22, 31, 41, 50), 12.04.(00, 10)
3129	12.04.(19, 29, 38, 48, 57), 12.05.(07, 16, 26, 35, 45, 55), 12.06.(04, 14, 23, 33, 42, 52), 12.07.(01, 11, 20, 30, 40, 49, 59), 12.08.(08, 18, 27, 37, 46, 56)
3130	16.50.(50, 57), 16.51.(03, 10, 17), 16.52.(04, 11, 17, 24, 31, 37, 44, 51, 58), 16.53.(04, 11), 16.55.(12, 19, 25, 32, 39, 46, 52, 59), 16.56.(06, 13, 19, 26, 33, 39, 46, 53), 16.57.(00, 06, 13)
3130	16.57.(20, 26, 33, 40, 47, 53), 16.58.(00, 07, 14, 20, 27), 17.00.(20, 28, 33, 40, 47, 53), 17.01.(00, 07, 14, 20, 27, 34, 40, 47, 54), 17.02.(01, 07, 14, 21, 28, 34, 41, 48, 54)
3130	17.03.(01, 08, 15, 21), 17.06.(51, 58), 17.07.(04, 11, 18, 25, 31, 38, 45, 56, 58), 17.08.(05, 12, 18, 25, 32, 39, 45, 56, 59), 17.09.(05, 12, 19, 26, 32, 39, 46, 52, 59), 17.10.06
3130	17.10.13, 17.26.(28, 35, 41, 48, 55), 17.27.(01, 08, 15, 22, 28, 35, 42, 48, 55), 17.28.(02, 09, 15, 22, 29, 35, 42, 49, 56), 17.29.(02, 09)
3132	17.30.(26, 33, 39, 46, 53), 17.31.(00, 06, 13, 20, 26, 33, 40, 47, 53), 17.32.(00, 07, 13, 20, 27, 34, 40, 47, 54), 17.33.(00, 07), 17.36.(29, 49, 56), 17.37.(02, 09, 16)
3132	17.37.(22, 29, 36, 43, 49, 56), 17.38.(03, 08, 16, 23, 30), 17.40.(51, 58), 17.41.(04, 11, 18, 25, 31, 38, 45, 51, 58), 17.42.(05, 12, 18, 25, 32), 17.45.(30, 37, 44, 50, 57), 17.46.(04, 11, 17)
3132	17.46.(24, 31, 37, 44, 51, 58), 17.47.(04, 11, 18)
3133	08.45.(44, 50, 57), 08.46.(04, 10, 17, 24, 31, 37, 44), 09.38.(17, 23, 30, 37, 43, 50, 57), 09.39.(09, 10, 17, 24, 30, ?, 44, ?)

Table 5.2. Inventory of color positives (mosaics) from JSL-91 (continued).

DIVE	TIMES
3134	18.18.(51, 57), 18.19.(04, 11, 24, 31, 38, 44, 51, 58), 18.20.(09, 11, 18, 25, 31, 38, 45, 51, 58), 18.21.(05, 12, 18, 25, 32, 38, 45, 52, 59), 18.22.(05, 12, 19, 25, 32, 39)
3134	18.22.(46, 52, 59), 18.23.(06, 12, 19, 26, 32, 39, 46, 53, 59), 18.24.(06, 13, 19, 24, 33, 40, 46, 53), 18.25.(00, 06, 13, 20, 28, 33, 40, 47, 53), 18.26.(00, 07, 13, 20, 27, 34)
3134	18.26.(40, 47, 54)
3136	16.52.(47, 54), 16.53.(00, 07, 14, 21, 27, 34, 41, 47, 54), 16.54.(01, 08, 14, 21, 28, 34, 41, 48, 55), 16.55.(01, 08, 15, 21, 28, 35, 42, 48, 55), 16.52.(02, 08, 15, 22, 29, 35)
3136	16.56.(42, 49, 55), 16.57.(02, 09), 17.00.(29, 35, 42, 49, 56), 17.01.(02, 09, 16, 22, 29, 36, 43, 49, 56), 17.02.(03, 09, 16, 23, 30, 36, 43, 50, 56), 17.03.(03, 10, 17, 23, 30, 37, 43)
3136	17.03.(50, 57), 17.04.(04, 10, 17, 24, 30, 37, 44, 51, 57), 17.05.04, 17.07.(28, 35, 41, 48, 55), 17.08.(01, 08, 15, 22, 28, 35, 42, 48, 55), 17.09.(01, 09, 15, 22, 29, 35, 42, 49, 56)
3136	17.10.(02, 09, 18, 22, 29, 36, 43, 49, 56), 17.11.(03, 09, 16, 23, 29, 36, 43, 50), 17.15.(00, 07, 13, 20, 27, 34, 40, 47, 54), 17.16.(00, 07, 14, 21, 27, 34, 41, 47, 54)
3136	17.17.(01, 07, 14, 21, 28, 34, 41, 48, 54), 17.18.(01, 08, 15, 21, 28, 35, 41, 48, 55), 17.19.(02, 08, 15, 22, 28)
3137	13.00.(37, 44, 51, 57), 13.01.(04, 11, 18, 24, 31, 38, 44, 51, 58), 13.02.(05, 11, 18, 25, 31, 38, 45, 52, 58), 13.03.(05, 12, 18, 25, 32, 38, 45, 52, 59), 13.04.(05, 12, 19, 25)
3137	13.04.(32, 39, 46, 52, 59), 13.05.(06, 12, 19, 26, 33, 39, 46, 53, 59), 13.06.(06, 13, 18, 26, 33), 14.12.(37, 44, 50, 57), 14.13.(04, 10, 17, 24, 30, 37, 44, 51, 57), 14.14.(04, 11, 17)
3137	14.14.(24, 31, 38, 44, 51, 58), 14.15.(04, 11, 18, 24, 31, 38, 45, 51, 58), 14.16.(05, 11, 18, 25, 32, 38, 45, 52, 58), 14.17.(05, 12, 18, 25, 32, 39), 14.46.(24, 31, 38, 45, 51)
3137	14.46.58, 14.47.(08, 11, 18, 25, 32, 38, 45, 52, 58), 14.48.(05, 12, 18, 25, 32, 39, 45, 52, 59), 14.49.(05, 12, 19, 26, 32, 39, 46, 52, 59), 14.50.(06, 12, 19, 26, 33, 39, 46)
3137	14.50.(53, 59), 14.51.(06, 13, 19, 26, 33, 40, 46, 53), 14.52.(00, 06, 13, 20)
3138	11.03.(46, 53, 59), 11.04.(06, 13, 19, 26, 33, 40, 46, 53), 11.05.(00, 06, 13, 20, 27, 33, 40, 47, 53), 11.06.(00, 07, 14, 20, 27, 34), 11.08.(28, 35, 42, 48, 55), 11.09.(02, 08, 15, 22)
3138	11.09.(29, 35, 42, 49, 55), 11.10.(02, 09, 16, 22, 29, 36, 42, 49, 56), 11.11.(02, 09, 16, 23, 29, 36, 43, 49), 11.13.(30, 37, 44, 50, 57), 11.14.(04, 11, 17, 24, 31, 37, 44, 51)
3138	11.14.58, 11.15.(04, 11, 18, 24, 31, 38, 45, 51, 58), 11.16.(05, 11, 18, 25, 32, 38, 45, 52, 58), 11.17.(05, 12), 11.19.(04, 10, 17, 24, 31, 37, 44, 51, 57), 11.20.(04, 11, 18, 24, 31)
3138	11.20.(38, 44, 51, 58), 11.21.(05, 11, 18, 25, 31, 38, 45, 52, 58), 11.22.(05, 12), 11.53.54, 11.54.(00, 07, 14, 20, 27, 34, 41, 47, 54), 11.55.(01, 07, 14, 21, 28, 34, 41, 48, 54), 11.56.01

Table 5.2. Inventory of color positives (mosaics) from JSL-91 (continued).

DIVE	TIMES
3138	11.56.(08, 14, 21, 28, 35, 41, 48, 55), 11.57.(01, 08, 15, 22, 28, 35, 42, 48, 55), 11.58.(02, 08, 15, 22, 29, 35, 42, 49, 55), 11.59.(02, 09, 16, 22, 29, 36, 42, 49, 56)
3138	12.00.(03, 09, 16, 23, 29, 36, 43, 49, 56), 12.01.(03, 10, 16, 23, 30, 36, 43, 50, 57), 12.02.(03, 10, 17, 23, 30, 37, 49, 50, 57), 12.03.(04, 10, 17, 24, 30, 37, 44, 51)
3138	12.03.57, 12.04.(04, 11, 17, 24, 31, 38, 44, 51, 58), 12.05.(04, 11, 18, 24), 12.19.(22, 29, 35, 42, 49, 56), 12.20.(02, 09, 16, 22, 29, 36, 42, 49, 56), 12.21.(03, 09, 16, 23, 29, 36)
3138	12.21.(43, 50, 56), 12.22.(03, 10, 16, 23, 30, 38, 43, 50, 57), 12.23.(03, 10, 17, 23, 30, 37, 44, 50, 57), 12.24.(04, 10, 17)
3142	09.25.(25, 31, 38, 45, 52, 58), 09.26.(05, 12, 18, 25, 32), 09.28.(38, 45, 52, 58), 09.29.(35, 45, 52, 59), 09.30.(05, 12, 19, 26, 32, 39, 46, 52, 59), 09.31.(06, 13, 19, 26, 33, 39, 46)
3142	09.36.58, 09.37.(05, 12, 19, 25, 32, 39, 45, 52, 59), 09.38.(06, 12, 19, 26, 32, 39, 46, 53, 59), 09.39.(06, 13, 19, 26, 33, 40, 46, 53), 09.40.(00, 06, 13, 20, 27, 33)
3142	09.40.(40, 47, 53), 09.41.00
3143	17.25.(27, 34, 41, 48, 54), 17.26.(01, 08, 14, 21, 28, 35, 41, 48, 55), 17.27.(01, 08, 15, 22, 28, 35, 42, 48, 55), 17.28.(02, 09, 18, 22, 29, 35, 42, 49, 56), 17.29.(02, 09, 16)
3143	17.29.(22, 29, 36, 42), 17.33.(16, 23, 30, 36, 43, 50, 56), 17.34.(03, 10, 17, 23, 30, 37, 43, 50, 57), 17.35.(04, 10, 17, 24, 30, 37, 44, 51, 57), 17.36.(04, 11, 17, 24, 31)
3143	17.36.(38, 44, 51, 58), 17.37.(04, 11, 18, 24, 31, 38, 45), 17.40.(21, 28, 35, 42, 48, 55), 17.41.(02, 08, 15, 22, 29, 35, 42, 49, 55), 17.42.(02, 09, 16, 22, 29)
3143	17.42.(36, 42, 49, 56), 17.43.(02, 09, 16, 23, 29, 36, 43, 49, 56), 17.44.(03, 10, 16, 23, 30, 36, 43, 50, 57), 17.45.(03, 10, 17, 23), 17.47.(40, 47, 53), 17.48.(00, 07)
3143	17.48.(13, 20, 27, 34, 40, 47, 54), 17.49.(00, 07, 14, 21, 27, 34, 41, 47, 54), 17.50.(01, 08, 14, 21, 28, 34, 41, 48, 54), 17.51.(01, 08, 15, 21, 28, 35, 41, 48, 55), 17.52.02
3145	17.12.(15, 21, 28, 35, 42, 48, 55), 17.13.(02, 08, 15, 22, 28, 35, 42, 49, 55), 17.14.(02, 09, 15, 22, 29, 38, 42, 49, 56), 17.15.(02, 09, 16, 23, 29, 36, 43, 49, 56), 17.16.03
3145	17.16.(10, 16, 23, 30, 38, 43, 50, 57), 17.17.(03, 10, 17, 23, 30, 37, 44, 50, 57), 17.18.(04, 10, 17, 24, 31, 37, 44, 51, 57), 17.19.(04, 11, 18, 24, 31, 38, 44, 51, 58)
3145	17.20.(05, 11, 18, 25, 31, 38, 45, 52, 58), 17.21.(05, 12, 18, 25, 32, 39, 45, 52, 59), 17.22.(05, 12, 19, 26, 32, 39, 46, 52, 59), 17.23.(06, 13, 19, 26, 33, 39, 46, 53)
3145	17.24.(00, 06, 13), 18.05.(02, 09, 16, 22, 29, 36, 43, 49, 56), 18.06.(03, 09, 16, 23, 30, 36, 43, 50), 18.08.(30, 37, 44, 50, 57), 18.09.(04, 11, 17, 24, 31, 37, 44, 51, 58), 18.10.04
3145	18.10.(11, 18, 24, 31, 38)

Table 5.2. Inventory of color positives (mosaics) from JSL-91 (continued).

DIVE	TIMES
3146	16.33.(28, 36, 43, 50, 56), 16.34.(03, 10, 17, 23, 30, 37, 43, 50, 57), 16.35.(04, 10, 17, 24, 30, 37, 44, 51, 57), 16.36.(04, 11, 18, 24, 31, 38, 44, 51, 58), 16.37.(05, 11)
3146	16.41.(10, 17, 24, 30, 37, 44, 51, 57), 16.42.(04, 11, 18, 24, 31, 38, 44, 51, 58), 16.43.(05, 11, 18, 25, 31, 38, 45, 52, 58), 16.44.(05, 12, 18, 25, 32, 39, 45, 52, 59)
3146	16.47.(53, 59), 16.48.(06, 13, 19, 26, 31, 40, 46, 53), 16.49.((00, 06, 13, 20, 27, 33, 40, 47, 54), 16.50.(00, 07, 14, 20, 27, 34, 41, 47, 54), 16.51.(01, 07, 14, 21, 28, 34, 41)
3146	16.51.(48, 54), 16.52.(01, 08, 15), 16.55.(02, 09, 16, 22, 29, 36, 43, 49, 56), 16.56.(03, 09, 16, 23, 30, 36, 43, 50, 56), 16.57.(03, 10, 17, 23, 30, 37, 43, 50, 57), 16.58.(04, 10, 17)
3146	16.58.(24, 30, 37, 44, 51, 57), 16.59.(04, 11, 17, 24)
3147	16.25.(21, 28, 35, 43, 48, 55), 16.26.(02, 08, 15, 22, 29, 35, 42, 49, 55), 16.27.(02, 09, 16, 22, 29, 36, 42, 49, 56), 16.28.03

Table 5.3 Color positive inventory — JSL-92

DIVE	TIMES	MOSAIC OR STEREO PAIRS
3261	017611250, 018611256, 019611308, 020611311, 021611311, 022611311, 023611312, 024611312	Stereo Pairs
3261	025611312, 026611312, 027611312, 028611312, 029611313, 030611313, 033611313, 034611313 (1/2), 012611248 (DK), 035611314, 036611314, 037611314	Stereo Pairs
3261	038611314, 039611314, 041611315, 042611315, 043611317, 044611317, 045611317, 046611317, 047611318, 048611318, 049611318, 050611318, 051611318	Stereo Pairs--Most shots on this page are extremely dark
3261	053611318, 054611319, 055611319, 056611319, 057611319, 058611319, 059611319, 060611322, 061611322, 062611322, 063611322, 064611322, 065611323	Stereo Pairs--most shots are very dark; about half are scratched
3261	066611323, 067611323, 068611323, 069611323, 070611323, 071611323, 072611324, 073611324, 074611324, 075611324, 076611324, 077611324, 078611325, 079611325	Stereo Pairs--Shots are dark and positives scratched
3261	080611325, 081611325, 082611325, 083611325, 084611326, 085611332(?)	Stereo Pairs--dark and scratched

Table 5.3 Color positive inventory — JSL-92 (continued).

DIVE	TIMES	MOSAIC OR STEREO PAIRS
3262	003621757, 004621757, 007621934, 008621934, 009621934, 010621934, 011621934, 012621934, 013621935, 014621935, 015621935, 016621935, 017621935, 018621935	Stereo Pairs (sampling bucket with 4 inserts)
3262	020621936, 021621936, 022621936, 023621936, 024621936, 025621936, 026621937, 027621937, 028621937, 029621937, 030621937, 033622027, 034622028	Stereo Pairs
3262	035622029, 036622030, 037622030, 038622030, 039622032, 040622033, 041622042, 042622042, 043622043, 044622043, 045622043, 046622043, 047622043, 048622044	Stereo Pairs
3262	049622044, 050622044, 051622044, 052622044, 053622050, 054622051, 055622051, 056622052	Stereo Pairs--053-056 can only see particles floating in water
3263	21.11.25, 21.11.33, 21.11.40, 20.53.02, 20.53.12, 20.53.17, 20.53.27, 20.52.13, 20.52.31, 20.52.39, 20.52.46, 20.52.52, 21.10.98, 21.10.53, 21.11.07, 21.11.13	Mosaic
3265	08.43. (29, 34, 44, 53), 08.44. (03, 12, 22, 32, 41, 51), 08.45. (00, 10), 08.48. (04, 13, 23, 32, 42, 51 (CUT IN 1/2)), 08.49. (01, 11)	Mosaic
3265	08.49. (20, 30, 39, 49, 58), 08.52. (14, 23, 33, 43, 52), 08.53. (02, 11, 21, 30, 40, 50, 59), 08.54. (09, 18, 28, 37, 47), 08.57. (03, 12, 22, 31, 41, 51), 08.58. (00, 10, 19, 29, 38, 48)	Mosaic
3265	08.58.58, 08.59.07, 09.01. (14, 23, 33, 42, 52), 09.02. (02, 11, 21, 30, 40, 48, 59), 09.03. (09, 19, 28, 37, 47, 58), 09.04. (06, 16), 09.06. (08, 18, 27, 37, 47, 56), 09.07. (06, 15, 25, 34, 44), 09.13. (41, 51)	Mosaic--most of the pictures on this page are extremely dark
3268	002681554, 003681555, 004681555, 005681555, 006681555, 007681555, 008681555, 009681556, 010681556, 011681556, 012681556, 013681556, 014681556, 015681557	Stereo Pairs
3268	016681557, 017681557, 018681557, 019681557, 021681557, 022681558, 023681558, 024681558, 025681558, 026681558, 027681558, 028681558, 029681559, 030681559	Stereo Pairs
3268	031681559, 032681559, 033681559, 034681559, 035681600, 036681600, 037681600, 038681600, 039681600, 040681600, 041681601, 042681601, 043681601	Stereo Pairs

Table 5.3 Color positive inventory — JSL-92 (continued).

DIVE	TIMES	MOSAIC OR STEREO PAIRS
3268	044681601, 045681601, 046681601, 047681601, 048681602, 049681602, 050681602, 051681602, 052681602, 053681602, 054681603, 055681603, 056681603, 057681603	Stereo Pairs
3268	058681603, 059681603, 060681604, 061681604	Stereo Pairs
3268	063681604, 064681604 # CUT OFF IS PROBABLY 062681604	Stereo Pairs
3268	065681604, 066681605, 067681605, 068681605, 069681605, 070681605, 071681605, 072681605, 073681606, 074681606, 075681606, 076681606, 077681606	Stereo Pairs
3268	084681607, 085681608, 086681608, 087681608, 088681608, 089681609, 090681609, 091681609, 092681609, 093681609, 094681609, 095681609, 096681610, 097681610 (1/2)	Stereo Pairs
3269	09.14. (38, 47, 57), 09.15. (06, 16, 25, 35, 44, 54), 09.16. (04, 13, 23, 32, 42, 51), 09.17. (01, 10, 20, 30, 39, 49), 09.20. (09, 18, 28, 38, 47, 57), 09.21. (06, 16, 25, 35, 44, 54), 09.22. (04, 13)	Mosaic
3269	09.23. (37, 47, 57), 09.24. (06, 16, 25, 35, 44, 54), 09.25. (03, 13, 23, 32, 42, 51), 09.28. (03, 13, 22, 32, 42, 51), 09.29. (01, 10, 20, 29, 39), 09.31. (11, 20, 30, 98, 49, 59), 09.32. (08, 18), 09.33.40	Mosaic
3269	09.33. (49, 59), 09.34. (08, 18, 28, 37, 47, 56)	Mosaic
3273	11.53. (26, 35, 45, 54), 11.54. (04, 14, 23, 33, 42, 52), 11.55. (01, 11, 20), 11.56.55, 11.57. (04, 14, 23, 33, 42, 52), 11.58. (02, 11, 21, 30, 40, 49, 59), 11.59. (09), 12.01. (28, 37, 47, 56), 12.02. (06, 15)	Mosaic
3273	12.02. (25, 34, 44, 54), 12.03. (03, 13, 22, 32, 41, 51), 12.04.00, 12.05. (22, 32, 42, 51), 12.06. (01, 10, 20, 29, 39, 48, 58), 12.07. (08, 17, 27, 36, 46, 55), 12.08.05, 12.09.51, 12.10. (00, 10, 18, 29, 39)	Mosaic
3273	12.10. (48, 58), 12.11. (07, 17, 26, 36, 46, 55), 12.12. (05, 14)	Mosaic
3274	09.10. (20, 30), 09.11. (02, 11, 21, 30, 40, 49, 59), 09.12. (08, 18, 28, 37, 47, 56), 09.13. (06, 15, 25, 34, 44, 53), 09.14. (03, 13, 22, 32, 41, 51), 09.15. (00, 10, 19, 29, 39, 48, 58), 09.16.07	Mosaic

Table 5.3 Color positive inventory — JSL-92 (continued).

DIVE	TIMES	MOSAIC OR STEREO PAIRS
3274	09.16. (17, 26, 36, 45, 55), 09.18. (03, 13, 22, 32, 41, 51), 09.19. (00, 10, 28, 29, 39, 48, 58), 09.20. (07, 17, 26, 36, 46, 55), 09.21. (05, 14, 24, 33, 43, 52), 09.22. (02, 12, 21, 31, 40)	Mosaic
3274	09.22. (50, 59), 09.23. (09, 18, 28, 37, 47, 57), 09.24. (06, 16, 25, 35, 44, 54), 09.25. (03, 13, 23, 32, 42, 51), 09.26. (01, 10, 20, 29, 39, 48, 58), 09.27. (08, 17, 27, 36, 46, 55), 09.28. (05, 19)	Mosaic
3274	09.28. (24, 34, 43, 53), 09.29. (02, 12, 21, 31, 40, 50), 09.30. (00, 09, 19, 28, 38, 47, 57), 09.31. (06, 16, 26, 35, 45, 54), 09.32. (04, 13, 23, 32, 42, 52), 09.33. (01, 11, 20, 30, 39, 49)	Mosaic
3274	09.33.58, 09.34. (08, 18, 27, 37)	Mosaic
3275	019751732, 021751733, 028751733, 029751734, 030751734, 032751741, 033751753, 034751754, 035751800, 039751820, 040751820	Stereo Pairs
3275	041751820, 042751820, 043751820, 044751821, 045751821, 046751827, 049751842, 050751842, 051751843, 052751843, 053751849, 056751954, 057751954	Stereo Pairs--some pairs very dark
3275	058751954, 059751954, 060751955, 061751955, 062751955, 063751955, 064751955, 065751955, 066751957, 067751957, 068751957, 069751958, 070751958, 071751958	Stereo Pairs--dark
3275	072751958, 073751958, 074751958, 075751958, 076751959, 077751959, 078751959, 079751959, 080751959, 081751959	Stereo Pairs
3277	17.10. (46, 55), 17.11. (05, 15, 24, 34, 43, 53), 17.12. (02, 12, 22, 31, 41), 17.14. (31, 41, 50), 17.15. (00, 10, 19, 29, 38, 48, 58), 17.16.07, 17.18. (15, 24, 34, 43, 53), 17.19. (02, 12, 22, 31, 41, 50).	Mosaic
3277	17.20. (00, 09, 19, 29, 38), 17.22. (16, 25, 35, 44, 54), 17.23. (03, 13, 22, 32, 42, 51), 17.24. (01, 10, 20, 29), 17.26. (07, 17, 26 (1/2), 36 (1/2), 46, 55), 17.27. (05, 14, 24, 33, 43, 52), 17.28.02	Mosaic
3277	17.28. (12, 21, 31), 17.30. (27, 36, 46, 55), 17.31. (05, 15, 24, 34, 43, 53), 17.32. (02, 12, 22), 17.34.13	Mosaic
3280	028801636, 036801638, 040801638, 041801638, 042801638, 043801639, 044801639, 045801640, 046801640, 047801641, 048801641	Stereo Pairs--frame

Table 5.3 Color positive inventory — JSL-92 (continued).

DIVE	TIMES	MOSAIC OR STEREO PAIRS
3280	049801641, 050801642, 051801642, 052801642, 053801642, 054801642, 055801643, 056801643, 057801645, 058801645, 059801645 (1/2), 060801645	Stereo Pairs--frame
3281	018810903, 021810903, 023810903, 029810905, 031810905, 033810905, 034810905, 044810906, 046810906, 048810906, 050810907, 052810907, 054810907	Stereo Pairs--sometimes a number is skipped between consecutive positives
3281	057810907, 058810907, 060810908, 063810908, 064810908, 066810908, 069810908, 072810909, 074810909, 076810909, 078810909, 080810910, 082810910	Stereo Pairs--sometimes a number is skipped between consecutive positives
3281	084810910, 086810910, 088810911, 090810911, 092810911, 094810911, 096810911, 098810911, 100810911, 102810911, 104810912, 106810912, 108810913, 110810913	Stereo Pairs--sometimes a number is skipped between consecutive positives
3281	112810913, 113810917	Stereo Pairs
3283	18.44.(39, 51), 18.45.(02, 14, 25, 37, 48), 18.46.(00, 11, 22, 34, 45, 57), 18.47.(08, 20, 31, 43, 54), 18.48.(06, 17, 28), 18.49.(34, 41, 49, 57), 18.50.(04, 12, 20, 27, 35, 43, 50, 58), 18.51.(06, 13)	Mosaic
3283	18.51.(21, 29, 36, 44, 52, 59), 18.52.(07, 15, 22, 30, 38, 45, 53), 18.53.(01, 08, 16, 24, 31, 39, 47, 54), 18.54.(02, 10, 17, 25, 33, 40, 48, 56), 18.55.(03, 11, 19, 26, 34, 42)	Mosaic--some are very dark
3283	18.55.(49, 57), 18.56.(05, 12, 20, 28, 36, 43, 51, 58), 18.57.(06, 14, 22(?), 29, 37, 49, 52), 18.58.(00, 08, 15, 23, 30, 38, 46, 59), 18.59.(01, 09, 18, 24, 32, 98(?), 47, 55), 19.00.(02, 10)	Mosaic--some are very dark
3283	19.00.(18, 26, 33, 41, 48, 56), 19.01.(04, 12, 19, 27, 35, 42, 50, 58), 19.02.(05, 13, 21, 28, 36, 44, 51, 59), 19.03.(07, 14, 22, 30, 37, 45, 53), 19.04.(00, 08, 16)	Mosaic
3284	08.57.30, 09.02.(14, 23), 09.04.58, 09.05.(28, 52), 09.06.05, 09.07.(37, 51), 09.08.(05, 20, 34, 48), 09.09.02, 09.11.(21, 36, 50), 09.12.(04, 19, 33), 09.13.(06, 20, 34, 48), 09.14.(03, 17, 31, 46), 09.15.(00, 14, 28, 43)	Mosaic--some are very dark
3284	09.37.57, 09.38.58, 10.39.47, 10.40.01	Mosaic
3285	15.50.(41, 55), 15.51.(09, 24, 38, 52), 15.52.(07, 21, 35, 98(?)), 15.53.(04, 18, 32), 15.55.(02, 16, 30, 45, 59), 15.56.(13, 28, 42, 56), 15.57.(11, 25, 39, 53), 16.00.(03, 17, 32, 46), 16.01.(00, 19, 29, 43, 57)	Mosaic--some are very dark

Table 5.3 Color positive inventory — JSL-92 (continued).

DIVE	TIMES	MOSAIC OR STEREO PAIRS
3285	16.02. (12, 26, 40), 16.04. (45, 59), 16.05. (13, 28, 42, 56) 16.06. (10, 25, 39, 53), 16.07.08, 16.09.(11, 25, 39, 54), 16.10.(08, 22, 37, 51), 16.11.(05, 19, 34, 48), 16.13.(18, 32, 47), 16.14.(01, 15, 30, 44, 58), 16.15.13	Mosaic--some are very dark
3285	16.15.(27, 41)	Mosaic
3286	10.07.(37, 46, 53, 59), 10.08.(06,13, 20, 26, 33, 40, 46, 53), 10.09.(00, 07, 13, 20, 27), 10.14.(46, 53, 59), 10.15.(06, 13, 19, 26, 33, 40, 46, 53), 10.16.(00, 06, 13, 20, 27, 33, 40)	Mosaic 10.16.#--pictures are all blue
3286	10.16.(47, 53), 10.17.(00, 07, 14, 20, 27, 34, 40), 10.21.(05, 12, 19, 25, 32, 39, 46, 52, 59), 10.22.(06, 12), 10.23.53, 10.24.(00, 07, 13, 20, 27, 33), 10.26.(46, 53), 10.27.(00, 06, 13, 20, 28, 33)	Mosaic
3286	10.27.(40, 47, 53), 10.28.(00, 07), 10.29.(27, 34, 41, 48), 10.28.14, 10.29.54, 10.30.(01, 08, 14), 10.32.(33, 40, 46, 53), 10.33.(00, 07, 13, 20, 27, 33, 40, 47, 54), 10.34.(00, 07, 14)	Mosaic
3289	010891636, 011891637, 012891637, 021891647, 026891650, 029891650, 032891650, 035891651, 038891651, 039891652, 043891654, 047891654, 051891654, 060891659 (VERY DARK)	Stereo Pairs
3289	066891657, 068891657, 070891657, 072891657, 074891657, 076891657, 080891658, 082891658, 084891658, 086891658, 088891659, 092891701, 094891701	Stereo Pairs--all blue or dark
3289	096891701, 098891701, 100891702, 102891702, 104891702, 106891702, 108891702, 110891702, 112891704, 114891704, 116891704, 118891704, 120891705, 122891705	Stereo Pairs
3289	124891705, 126891705, 128891705, 130891705, 132891705, 134891705, 136891706, 138891706, 140891706, 142891708, 144891708, 146891709, 148891709, 150891709	Stereo Pairs
3289	152891709, 154891709, 156891709, 158891709, 160891711, 165891849, 166891849, 168891850, 169891851, 170891852, 171891852	Stereo Pairs--#160-171 are all dark
3289	16.10.25, 16.18. (10, 15, 17, 24, 29, 39, 49), 18.27. (21, 27, 38, 59), 18.28. (08, 13)	Macro Shots

5.2.2. Navigation

The support ships used by the *Johnson Sea-Link* navigate with LORAN C and GPS Satellite Navigation. During diving operations, the position of the submersible relative to the support ship is continuously monitored by means of a Honeywell Hydrostar doppler sonar (JSL-91) or by a short-baseline acoustic pinger (JSL-92). Obtaining a fix for a specific site on the bottom is accomplished by maneuvering the support ship directly above the submersible (zenith ~5 m) and recording the ship's LORAN C fix at that moment.

5.2.3. Time-lapse Photography

The time-lapse investigations utilized one video system (Autonomous Video Camera System, AVCS) and one emulsion camera (Benthos). A trial deployment of the AVCS camera at a mussel bed during JSL-91 acquired a three-day sequence showing gastropod grazing activity on seep mussels. A second, long-term deployment at a mussle bed and gas seep failed to acquire images due to software failure. A third, short-term deployment of the AVCS during JSL-92 successfully acquired a three-day sequence showing bubbling gas and megafaunal activity on an outcropping hydrate.

The Benthos time-lapse system consisted of a Benthos 388® camera with standard 28 mm Nikonos® lens and a Benthos 389® strobe mounted on a compact pipe frame. The camera was loaded with 400 frames of 35 mm color transparency film, and the intervalometer was set to expose one frame per hour. Two successful deployments of the Benthos system were completed during JSL-91; these recorded a 17-day sequence of a tube worm cluster at GC 184/185 and a five-day sequence of a tube worm cluster in GC 234.

5.3. Analytical Methods

5.3.1. Digitizing

All data interpretation was carried out on digital image files. These files were constructed from the video records by digitizing selected frames with a Targa® video capture board. The 35 mm positive photographs were scanned by use of a Nikon® 3510AF slide scanner. Image file formats are quite diverse and interchange between formats can present problems. Video-capture images were stored as Targa-format files, scanned images were stored as TIF-format files, and both image types were converted to a third format, AGIS-format, for GIS and mosaicking application.

5.3.2. Mosaicking

Construction of accurate, detailed (≥1:100) maps is essential for study of these processes. Previous attempts relied on manual assembly of information traced from 35 mm photographs (Fustec et al., 1987, Hessler et al., 1988) or low-resolution video (MacDonald et al., 1990). These techniques are extremely laborious and provide little assistance for an on-going field effort. We developed a

Small Area Benthic Imaging System (SABIS) to construct mosaics from digitized photographs and to provide preliminary products during the actual field operations from color video images. We tested SABIS during ALVIN-92 (see section 8.3) and have been using the mosaicking software to quantify the video and emulsion images collected during JSL-91 and JSL-92.

Mosaicking is a technique whereby a group of raster images is merged into a continuous image. Raster images are composed of ordered rows and columns of pixels. A pixel is a data element with a fixed row (y) and column (x) coordinate located within a rigidly defined data structure equivalent to Cartesian coordinates. Because the coordinate system of a given raster image is completely independent of any other raster image, the transformation from the coordinate system of one image to a second must be derived. Approaches to mosaicking include the following: 1) independent transformation of each mosaic image to a common coordinate system, such as an earth location coordinate system; and 2) restriction of the image plane for the mosaic to a geocentric Cartesian coordinate system such that the relative position of any pixel in any image is computable.

The present study was concerned with assembling scaled mosaics for areas ~10 sq m and with rapid production of working images. A third mosaicking technique, based on homogeneous coordinates, was appropriate to these requirements with the assumption that differences in the image coordinate systems were attributed to the following: 1) translation due to along-track movement of the imaging platform (submarine); 2) scale change due to minor changes in altitude; and 3) rotation due to bearing changes and yaw of the submarine, executed for full coverage of the scene.

Homogeneous coordinates were used to facilitate matrix computations. In homogeneous coordinates, a Cartesian coordinate, **(x,y)**, is represented as **(W*x, W*y, W)**, where **W** is any scalar and **W≠0**. The Cartesian coordinate can be recovered from the homogeneous coordinate **(X,Y,W)** by **x=X/W** and **y=Y/W**. Herein, we force **W=1**, so for any image coordinate **(x, y)**, the homogeneous coordinate is expressed as **(X, Y, 1)**, and is employed for computation as the homogeneous vector **[x y W]**.

An image coordinate can be transformed by multiplying its homogeneous vector by a 3x3 matrix to produce another homogeneous vector:

$$[X'\ Y'\ W'] = [x\ y\ 1] * \begin{bmatrix} A & B & C \\ D & E & F \\ G & H & I \end{bmatrix}$$

To translate image coordinate **(x, y)** by **Tx** along the x-axis and by **Ty** along the y-axis, one would perform the following matrix operation:

$$[X'\ Y'\ W'] = [x\ y\ 1] * \begin{bmatrix} 1 & 0 & 0 \\ 0 & 1 & 0 \\ Tx & Ty & 1 \end{bmatrix}$$

The homogeneous representations facilitate matrix operations. The term **W'** has no value, and, because **W = 1**, the transformed Cartesian coordinate forms the first two elements of the homogeneous vector. Successive translation operations are additive.

To scale the image coordinate **(x, y)** by **Sx** along the x-axis and by **Sy** along the y-axis, one would perform the following matrix operation:

$$[X' \; Y' \; W'] = [x \; y \; 1] * \begin{bmatrix} Sx & 0 & 0 \\ 0 & Sy & 0 \\ 0 & 0 & 1 \end{bmatrix}$$

Successive scaling operations are multiplicative.

Lastly, to rotate image coordinate **(x, y)** by **q** about the origin, one would perform the following matrix operation:

$$[X' \; Y' \; W'] = [x \; y \; 1] * \begin{bmatrix} \cos\theta & \sin\theta & 0 \\ -\sin\theta & \cos\theta & 0 \\ 0 & 0 & 1 \end{bmatrix}$$

Successive rotation transformations are additive.

In its interactive mode, the mosaicking software presents the user with a split screen; the left side displays a "seed" image, consisting of one or more mosaicked frames, and the right side displays a "candidate" image. The software then prompts the user to select with the mouse cursor two pairs of points in the seed and candidate images that are spatially identical. Here, the arrows painted onto the frames during video capture prove essential for identifying paired points in the two images. The software then offers the choice of pasting the candidate over or under the seed, gives a preview of the joined image, and, if satisfactory, transfers the merged image to disk memory. After a pause for computation, the screen re-displays the newly augmented seed image and prompts the user to select a new candidate from the directory.

6.0 Methods, Collections, and Status of Growth Studies of Chemosynthetic Fauna and Associated Analyses of Animals and Habitats.

C.R. Fisher

6.1. Vestimentiferans

6.1.1. Field Work

1991 The bander was constructed and tested, and modifications made in the tensioning and release mechanisms for the device and in the tags used for the bands. It was then used successfully to band 39 worms without damage. Quality of the video documentation varied with the observer present in the submersible. Review of the videos revealed that 20 worms were adequately videoed for the necessary measurements (Table 6.1). Forty-five *Escarpia* and 22 *Lamellibrachia* were collected for analysis of mass/length relations.

1992 Sixteen of the worms banded and well documented in 1991 were videoed again. No fatalities were noted among banded worms. Four animals not adequately videoed in 1991 were adequately documented in 1992. An additional 20 worms were banded in 1992 and apparently adequately videoed. An additional five *Escarpia* and 57 *Lamellibrachia* were collected for the mass/length relation determinations. One group of animals banded in 1991 were collected for surface inspection of the banding effects. No deleterious effects were noted. These animals were also used in the mass/length relation determinations. Water samples were collected and analyzed from most of the banding stations.

6.1.2. Laboratory Work

Determinations of the one year growth increment for the animals adequately documented in both 1991 and 1992 are still underway. Preliminary results (from cursory examination of the videos and the collected animals) indicate that the animals are growing very slowly compared to their hydrothermal vent relatives (Table 6.1).

Based on wet weight, mass/length relations have been determined for the worms collected in 1991 (Fig. 6.1). When the samples are processed, this relation will be determined for the dry weight of the worms. Since a significant amount of water is unavoidably collected from the tubes along with the animal tissue, the relation will improve with dry weight determination.

Table 6.1 Tubeworm growth studies: status and preliminary results.

Dive / Site	Number Banded Successfully	1991 Good Video	1992 Good Video*	Growth (cm)** Average
3129 / BH	5 of 8	4 of 5	3 of 4 (+1)	
3138 / GC 272	8 of 8	2 of 8	not done	
3140 / BH	7 of 8	4 of 7	2 of 4 (+1)	1.02
3141 / BH	6 of 8	3 of 6	2 of 3 (+2)	
3142 / GC 234	7 of 8	4 of 7	4 of 4	.88
3143 / GC 234	6 of 8	5 of 6	4 of 5 (+1)	1.39

* Numbers in parentheses are individuals not adequately documented in 1991.

** Preliminary data given when available. These analyses are not complete.

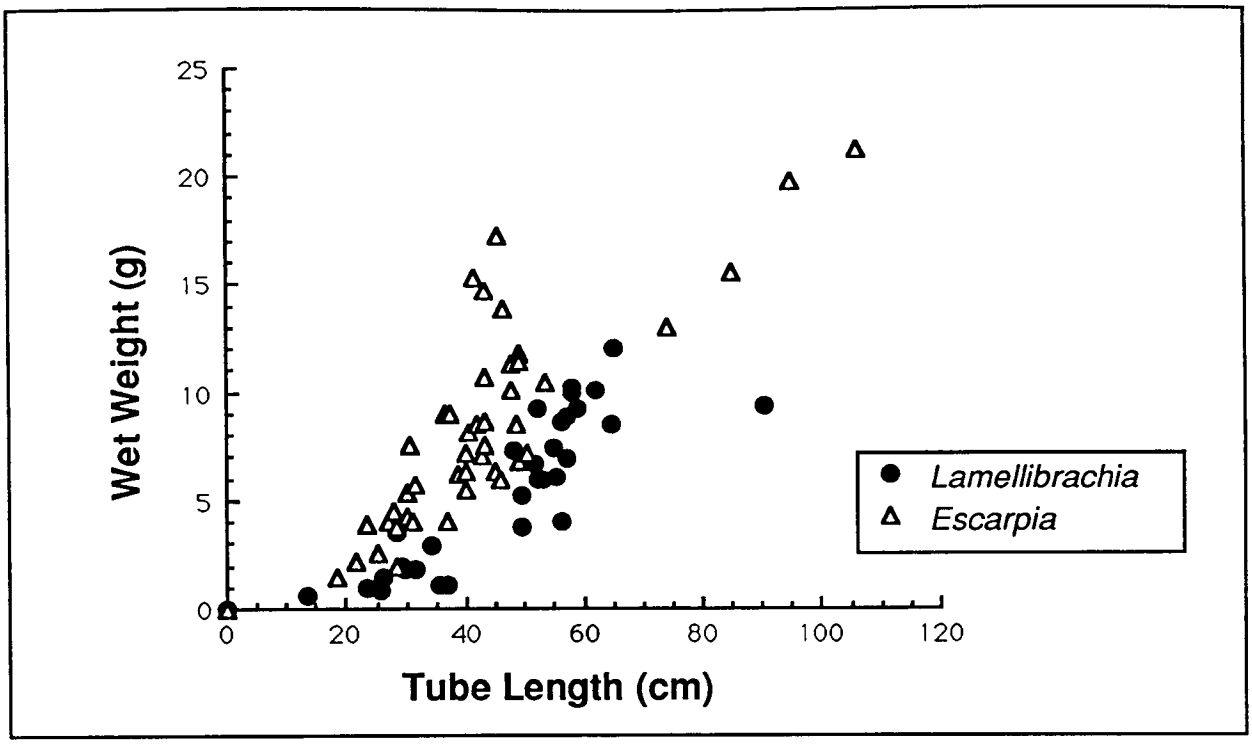

Figure 6.1. Length vs. wet weight for animals collected in 1991.

6.2. Mussels

6.2.1. Field Work

1991 Mussels were collected from four sites for determination of condition index and for re-release for growth studies. Due to loss of dives at the end of the cruise, only three of the growth stations were established. A total of 381 marked mussels were released at these three growth stations. Additional animals from each of the four stations were sampled for subsequent laboratory analysis. Also, two transplant experiments were initiated with mussels deployed in cages.

1992 The three growth stations were re-visited and animals collected at each. A total of 120 marked mussels were collected at the three stations (Table 6.2). Each of the stations was re-established with additional marked mussels. Both marked and unmarked mussels were sampled for laboratory analysis. The transplant cages were collected and the animals sampled for laboratory analysis. Water samples were collected from each of the growth stations. A newly-developed sampling ring was used for quantitative collection of mussels from seven areas. Five additional growth stations were established in connection with these collections.

6.2.2. Laboratory Work

Condition index (CI) was determined for a subsample of animals collected at each of the five 1991 stations (Table 6.2). These collections represent animals

with significantly different CIs. Determination of the CI for the animals collected in 1992 (both marked and unmarked) is partially complete. Growth increments for the individual animals collected at each of the three stations have been determined and the data is currently being fitted to an allometric growth model. The raw data from one of the stations is shown in Figure 6.2. Biomass density and size frequency for the mussels from each ring collection has been determined. Data from the GC 234 ring collection are shown in Figure 6.3. These data will be used to estimate rates of methane oxidation and primary productivity for mussels from each of the areas.

The relation between shell length and tissue wet weight has been determined for the mussels collected in 1991 (Fig. 6.4).

Table 6.2. Condition index (CI) for a subsample of animals collected at each of the five 1991 stations.

Site	1991 Dive (collection)	Condition Index (1991) (±SE)	Growth Studies Number Deployed	Number Recovered
Bush Hill I	3129	0.090 (±0.004, n=50)	--	--
Bush Hill II	3139	0.067 (±0.004, n=18)	116	51
GC 272	3137	0.111 (±0.006, n=20)	115	31
GC 234	3142	0.09 (±0.003, n=20)	150	38
Brine Pool	3145	0.124 (±0.005, n=20)	--	--

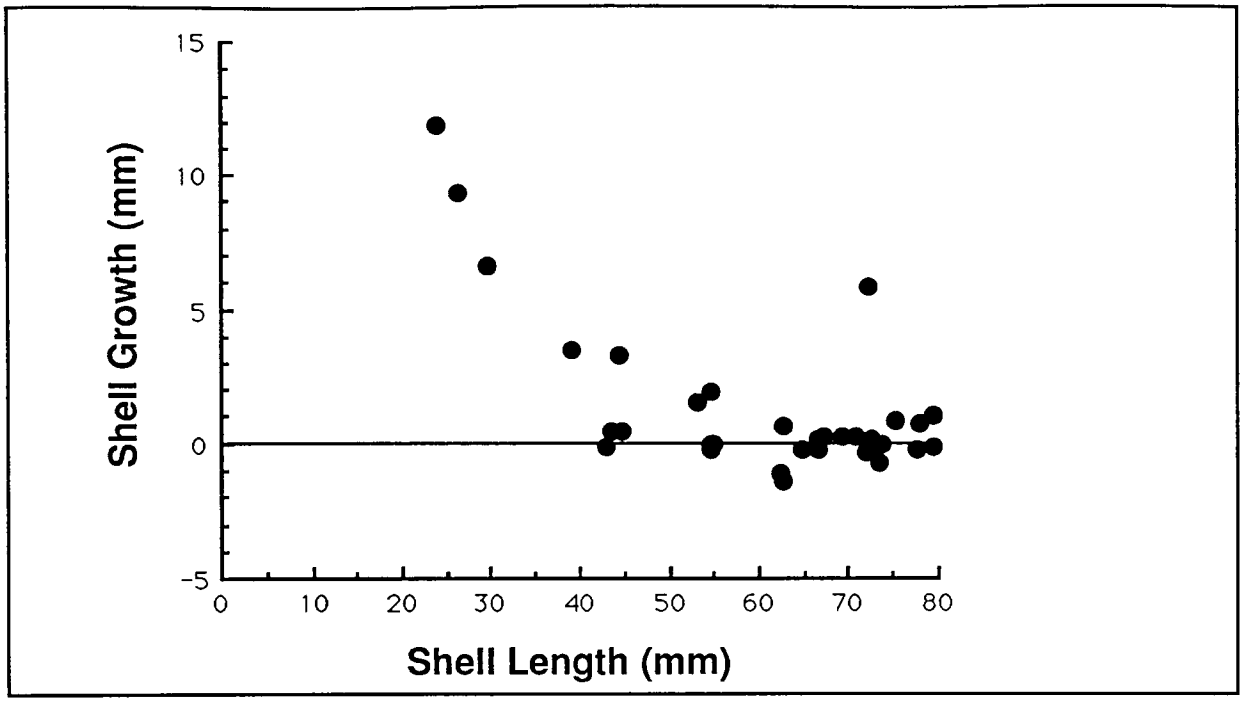

Figure 6.2. One year growth increment of GC 234 mussels as a function of initial size.

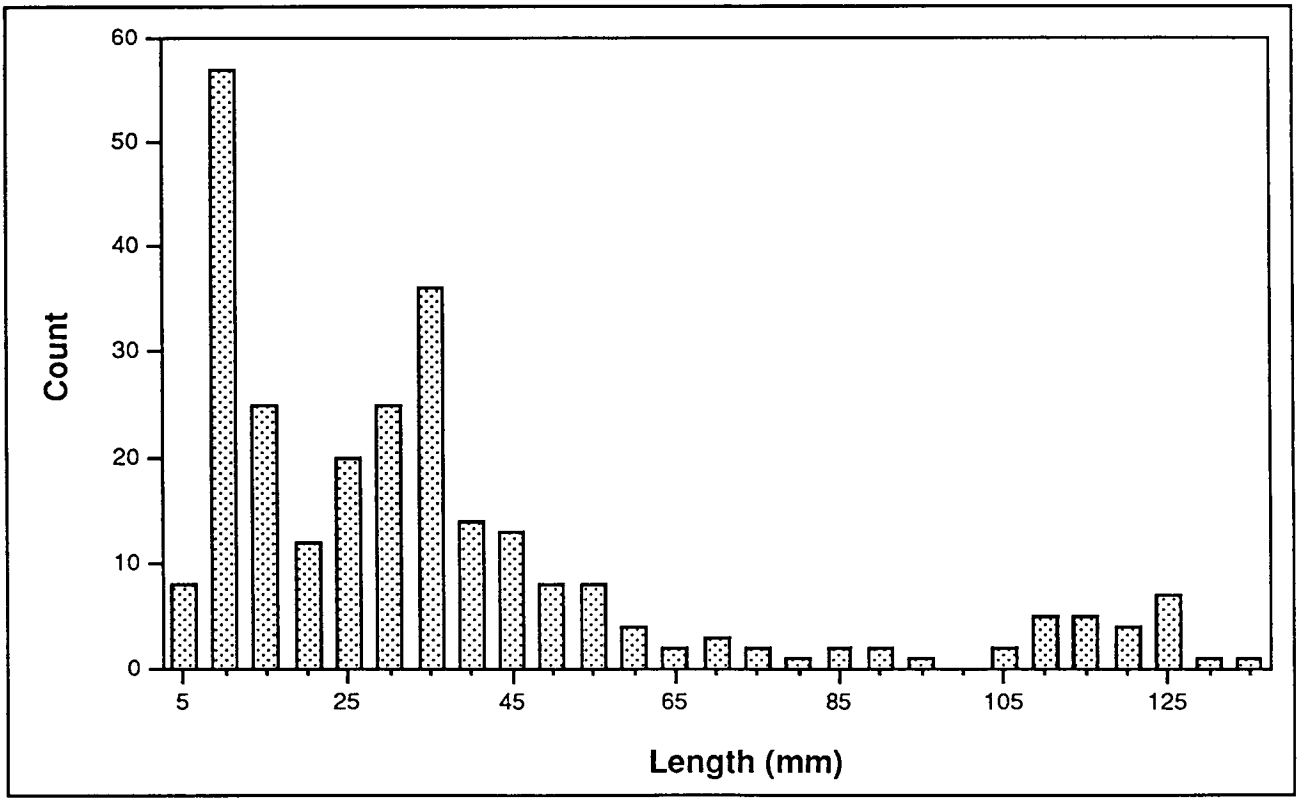

Figure 6.3. Size frequency distribution of 269 mussels collected within 0.5 m diameter ring at GC 234 site. The ring represents a biomass of over 15 kg wet weight of mussel tissue per m^2.

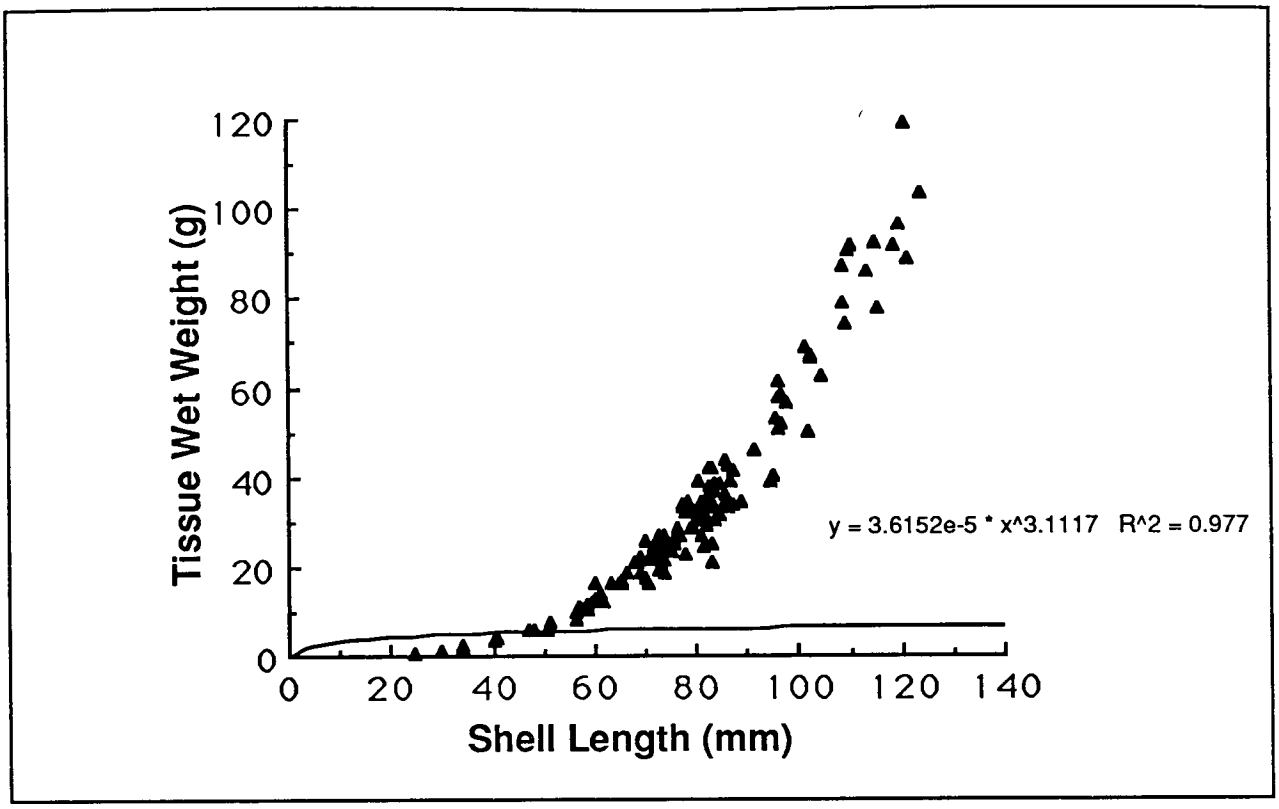

Figure 6.4. Tissue weight vs. shell length, 1992 mussel collection.

6.3. Clams

6.3.1. Field Work

1991 A total of six clam corrals were deployed from the surface and subsequently located on the bottom by the *Johnson Sea-Link*. Four of the corrals were later moved to chosen study sites at GC 272. Twelve clams of each species were collected, marked on the surface, and released into the corrals (six individuals into each corral). Six additional clams were sampled for laboratory analysis of tissue and shell.

1992 Each of the clam corrals was re-visited. In two of the corrals, all of the clams had apparently died immediately after deployment. In the other two, most had died. Clams were collected from one corral where two live clams were seen. Only one live clam was found on the surface. Clams were collected, of which six were immediately re-deployed in one of the corrals. None had moved from their deployment position after two days. Experiments were initiated to determine the cause of death of the clams. Six water samples were taken from among clams to characterize the habitats occupied by the two species, and additional collections were made for blood analyses and determination of condition index. Although most of the clams were dead, the corrals show promise in that none of the surviving clams escaped from the enclosure. The cause of death must be determined, especially since other closely related species from similar depths can be kept alive at surface pressure.

6.3.2. Laboratory Work

Shell volumes have been determined for each of the collected individuals. The condition index of five individuals of each species will be calculated after determination of the soft tissue ash-free dry weight.

6.4. Associated Water Samples

Three new devices were designed and constructed for use in connection with this program. Due to the short lead time before the 1991 field season, only one of them was successfully field tested; the others were built based on that design. All three were standard equipment on every dive in 1992. With these devices, we were able to obtain small volume, high quality water samples from the areas of interest around the three chemosynthetic groups. This included samples from over the clams and mussels, from among the plumes of the vestimentiferans, and at both 5 and 10 cm depths interstitially adjacent or under each of the groups. These water samples were analyzed onboard for sulfide, oxygen, inorganic carbon, methane concentrations, and salinity. This data set provides the only complete description of the chemical microhabitat (with respect to the chemicals of primary interest to the chemosynthetic symbioses) occupied by chemosynthetic organisms at any seep site. A summary of the water samples collected with this apparatus and analyzed onboard is shown in Table 6.3.

Table 6.3. Small volume water samples taken *in situ* and analyzed onboard for sulfide, methane, DIC, and oxygen.

Dive	Site	Number of samples	Samplers used	Sample description
3266		8	5I & 10I	M
3270	BH	8	5I & 10I	TW & M
3271	BH	2	5I & 10I	White Mat
3273	BP	8	5I & 10I	M
3274	BH	6	5I & 10I & B	TW
3275	BH	6	5I & 10I	Hydrate & TW
3276	GC 272	5	5I & 10I	C
3277	GC 272	4	5I & 10I	M
3279	GC 272	5	5I	M
3280	GC 272	5	5I & 10I	Brine & C
3281	GC 234	4	5I & 10I	TW
3283	GC 234	7	5I & 10I	M
3284	GC 234	3	5I & 10I	TW
3285	BP	8	5I & 10I	M
3288	BH	8	5I, 10I & B	M & TW
3289	BH	5	10I	Hydrate & TW

BH = Bush Hill
BP = Brine Pool
5I = 5 cm interstitial
10I = 10 cm interstitial
B = Bottom water
M = Mussel Bed
TW = Tube worm bush
C = Clam bed

6.5. Ongoing Studies

6.5.1. In This Area

As strongly suggested by the scientific review panel during the 1992 meeting, a considerable effort was made to continue the *in situ* growth studies as well as to initiate additional studies where appropriate. There are currently a total of 30 banded vestimentiferans in seven assemblages in the study areas. There are also marked mussels at seven growth stations, including the additional mussels deployed at the original three stations. Each assemblage of tube worms and mussels are marked with permanent floating markers and their location identified on maps of the area. The water chemistry immediately around the animals has been well characterized at over 80% of the sites. These ongoing growth studies will be monitored as opportunity presents. Two grants currently pending with NOAA and NSF may assist in this.

In addition to these fully successful methods, we are still pursuing the use of the "clam corrals" for studies of vesicomyid growth. None of the clams which moved from their deployment positions escaped from the corrals and the corrals appear to be an effective "perimeter" for the proposed studies. We will pursue the possibility that the animals were suffocated during collection by using other collection methods on future cruises, with subsequent deployment of the clams.

6.5.2. Other Sites

Using the same technology, we have banded vestimentiferans for growth studies at two other sites. These studies are related to this project due to their comparative value. One site is the deep-water Gulf of Mexico site at Alaminos Canyon where there are ten banded and documented vestimentiferans. Results from Alaminos must await revisitation of the site. The other site is a hydrothermal-vent site at 13°N on the East Pacific Rise. Several worms banded in October 1991 were collected in April 1992. Preliminary review of the photographic documentation and the collected animals indicates that the tube growth rate of the hydrothermal vent species is about ten times that of the shallow hydrocarbon-seep species.

7.0 Heterotrophic Megafauna of Chemosynthetic Seep Ecosystems

R.S. Carney

7.1. Recovery Experiments

7.1.1. Introduction

This report details progress on the experimental disturbances as proposed in section 6.7.7, subparagraph 2, page 6-56 of the technical proposal. As per the research plan of that proposal, four 0.25 m^2 recovery experiments were deployed in September 1991, and reexamined in August 1992. Preliminary one year observations are presented below and supplemented with observations of marker rods placed in the NR-1 brine pool in September 1989, to extend the duration over which conclusions can be drawn.

Two additional recovery projects have proven less successful due to technical difficulties. Efforts to develop a suitable means of stripping tubeworm clumps off the substrate have had limited success and no experimental stripping has occurred. In conjunction with the clam corral deployments, clams were collected over large areas and the sites revisited one year later. Interpretation of the video is difficult because the effectiveness of the original collecting is unknown, and recognition of live animals in the video images is difficult.

Questions of Sensitivity. From a management perspective, the major ecological questions about hydrocarbon seep communities concern their susceptibility and response to various impacts. When considering the possibilities, conflicting arguments can be made that seep communities are either relatively impervious or especially sensitive. The argument for imperviousness is based upon the observation that the seeps exist in what would normally be considered a chemically hostile environment. The argument for sensitivity is based upon the possibility that communities may require very narrow and easily disturbed chemical gradients. Conflicting arguments can also be put forward that seep communities should be resilient in order to colonize and exploit an ephemeral chemical environment. Or, that they should lack resilience since they exploit a chemical environment which might not be so ephemeral.

It is the purpose of the recovery experiments to provide an initial answer to the question of resilience within quite narrow confines. Mussel clumps were mechanically disturbed, a recovery cage placed over the disturbed portion of bottom, and repopulation by mussels monitored over time. Due to technical and logistical limitations, no effort was made to provide adequate replicates, to test for cage effects, or to determine how chemical seepage might be influenced by disturbance.

Limitations of Method. The visual and taxonomic similarity of seep mussel communities and the mussel mats of the rocky intertidal immediately calls to mind the great success of the experimental application of predator exclusion cages in the shallow water system. The similarities are so apparent that it is important to distinguish the objectives of this present study from the more sophisticated work pioneered by R. Paine at the University of Washington and J. Connell at the

University of California at Santa Barbara. These and related studies have been informatively summarized by Hairston (1989).

The better known intertidal studies sought to examine multispecies competition for the single resource, living space. Typically, an intertidal study subjects an area of intertidal rock to some combination of space modifying (resource opening) and competition/predation modifying treatments. For example, there might be mechanical denuding of the rock surface followed by exclusion of predators and/or competitors by a cage or barrier. Appropriate controls are employed, such as areas left undisturbed and covered by cages or barriers which do not exclude anything.

The hydrocarbon seep situation differs from the intertidal in three very important regards:

1. Space within an invisible chemical gradient of unknown geometry with adequate methane and oxygen is assumed to be the most important resource, not space *per se*. Therefore, we really know neither how the treatment modifies the resource, nor how the geometry of the experiment relates to the geometry of the resource. Compounding the experimental task, it is hard to identify an appropriate control.

2. We do not know enough about seeps to state worthwhile hypotheses about inter-species competition. Eventually, we may find that there are important competitive effects among bacteria, tubeworms, and mussels which are modified by predation and grazing. For now, simply seeing what happens when you scrape off the mussels is an appropriate start.

3. Thirdly, the deep environment is so costly and difficult to work in that even the simplest experimentation can be so expensive and problem-plagued as to discourage more elaborate designs.

Having acknowledged that this experiment lacks appropriate controls and has many unknown and uncontrolled factors, we can state that the results are still informative. If an area is denuded, and it is recolonized by mobile adults and larval recruits, then the communities would seem to be resilient in the face of one type of disturbance. Other results would indicate a lack of resilience in the community or a failure in the design of the experiment.

7.1.2. Material and Methods

Construction of Recovery Cage. A cage design was adopted which would be simple, low cost, and easily observed, deployed, and collected. Since mussel mats can cover several square meters, we selected a cage area of 0.25 m^2 as a practical size. So as to distinguish between settling larvae and crawling adults, an exclusion netting was stretched over half the area and volume of the cage. This netting was intended to allow larvae, small grazers, and predators free access to the disturbed area, but to exclude immigration by mature mussels.

Rectangular recovery frames were constructed of 21 mm outside diameter polyvinyl chloride water pipe. Fifty centimeter lengths were used to make 0.25 m^2 top and bottom sections, and the remaining sides constructed of 20 cm lengths.

Corners were fastened with three-way right angle joints and commercial PVC pipe adhesive. The corners were drilled to allow for flooding of cavities. Half the interior of the cage, across diagonal corners (Fig. 7.1), was enclosed in 3.5 cm stretch mesh plastic fruit tree bird netting. The line of the netting is less than 1 mm in diameter, is easy to see through, and its black color limits obscuring of a video image. Nylon line was stretched across the diagonal of the cage, and then netting was secured with tiewraps to these diagonal lines and adjacent sides. The 50 cm rods used were sanded, chemically deglazed, and painted with white, blue, red, and yellow epoxy-based paint. The 10 cm long color bands provide visual scale, orientation, and color balance in subsequent image analysis.

Cage Deployment. Cages were deployed in conjunction with massive mussel sampling during the 1991 dive series. Two cages were deployed at Bush Hill on dives JSL3129 (Sept. 5, 1991), and JSL3139 (Sept. 20, 1991). Single cages were deployed at Green Canyon 272 on dive JSL3137 (Sept. 19, 1991), and Green Canyon 234 on dive JSL3144 (Sept. 24, 1991).

Disturbance consisted of repeated grabbing of mussels with the *Johnson Sea-Link* manipulator until more than 100 individuals had been collected. Since the contiguous area denuded was typically less than 0.25 m^2, the cages were placed over the denuded area and adjacent bare substrate. The mussels collected were used in other shipboard studies. When marked mussels were returned to the site, they were deployed away from the recovery frames.

Although employing no experimental manipulation of the mussel mat, artificial substrates have been deployed since 1987, commencing with Dive 2053. Since then, 0.5 m long plastic rods have been deployed intermittently at dive sites to serve as simple reference scales. Each rod was cut from 3/4 inch PVC pipe to a length of 0.5 m. It was then sanded, deglazed, and painted with an epoxy-based paint. Three 10 cm-wide primary color bands were painted on each rod. Of special interest is the deployment of both 0.5 m and 3 m rods at the NR-1 Brine Pool site. The shorter rods were placed vertically at the outer edge of the mat in order to monitor that edge. The longer rods were placed a few centimeters from the inner edge at two points in the pool.

Data Extraction. The cages were revisited during the August 1992 dive series, approximately one year after deployment. The cages were visually inspected and then surveyed by panning and zooming the *JSL* video camera. Still frames from this video were printed using a Mitsubishi CP210U video copy processor, and the content and position of biota within the frame recorded. The NR-1 Brine Pool rods have been video surveyed twice since deployment, in 1991 and 1992. At the recommendation of the Scientific Review Board, the cages were not recovered during the 1992 dive series, pending the possibility of long term monitoring. Therefore, only image data is available at this time.

7.1.3. Results at One Year

Bush Hill Site, GC-184/185. Two cages were deployed approximately 40 cm apart at a site of dense mussel and mussel-tubeworm cover (Fig. 7.1). The cages were placed on sediments which had been exposed by the collection of mussels for experimentation. In cage one, approximately 15 large (greater than 7 cm) mussels

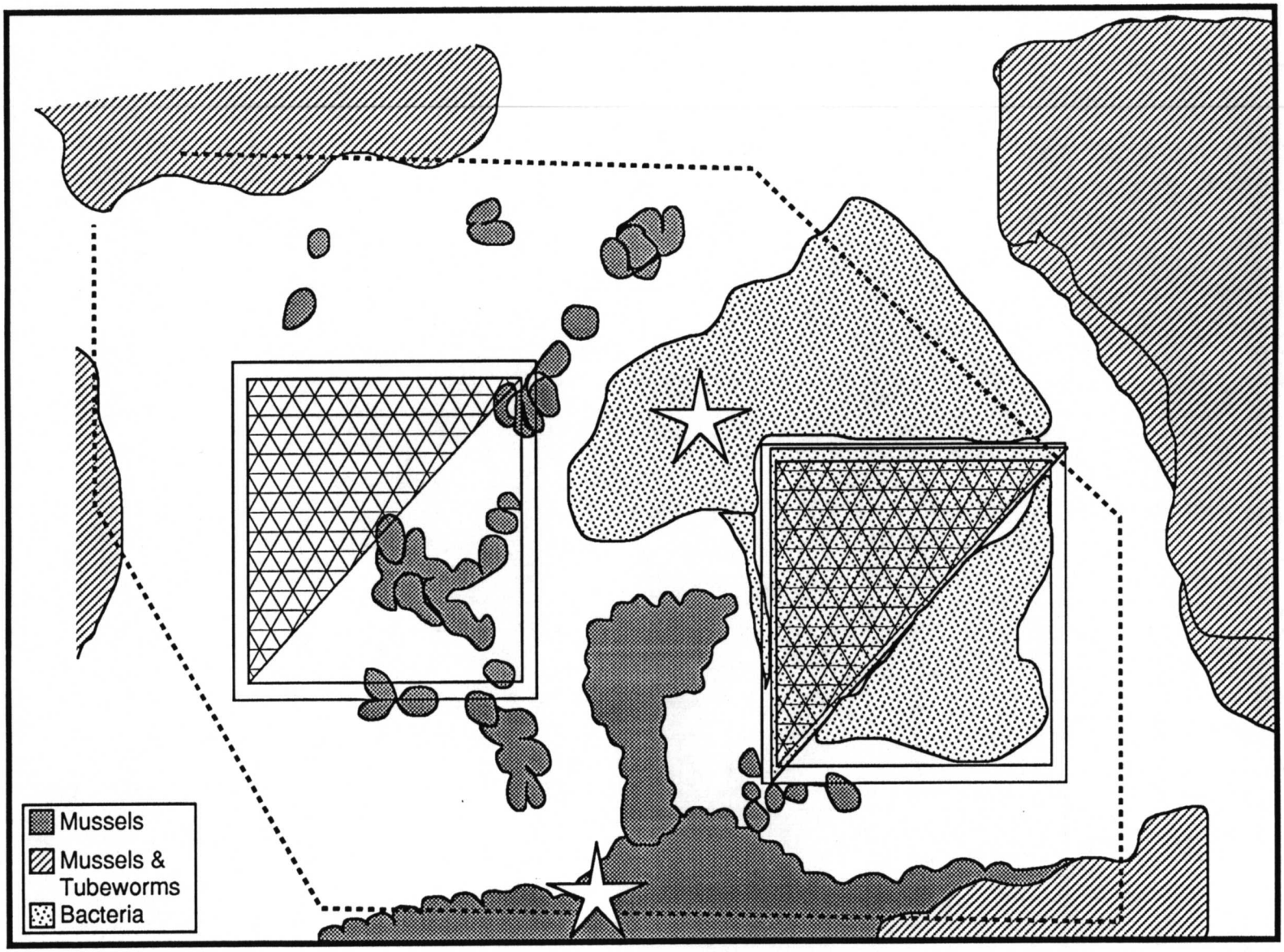

Figure 7.1. Mussel, tubeworm, and bacterial cover at Bush Hill after one year deployment.

occur as a cluster in the open area of the frame. Approximately 10 animals of similar size are attached to the frame of the cage on the open side. The netted side appeared to be devoid of mussels. The crustacea *Munidopsis* and *Alvinocaris* were present in both the open and netted area. The bottom in the open side not occupied by mussels was colored white, suggesting chemical and/or bacterial activity. The bottom on the netted side appeared to have no special coloration.

Cage Two was quite noticeably different. The netted section was completely covered with white *Beggiatoa* film, obscuring observation of any contents. The open side was devoid of mussels, and the bottom was covered with both white and red *Beggiatoa* mats. At least two large mussels were attached to the outer edge of the frame, but none were in the open area. *Munidopsis* and *Alvinocaris* could be seen adjacent to the frame but not within it.

The area between the two cages contained a cluster of approximately 20 large mussel specimens, both clumped and singly. This clump was an extension of a large mussel aggregation located adjacent to the cages. The bottom between the cages also had reddish *Beggiatoa* cover. Two specimens of the seastar *Sclerasterias* were near the two cages.

Site Two, GC-234. A single cage was deployed on an area of mud and exposed low relief carbonates (Fig. 7.2). The site contained both dense mussel aggregations and mussel-tubeworm assemblages. The open section of the cage was whitish due to bacteria or chemical activity. Two mussels were attached to the frame in this section. The netted section contained no mussels, but at least three large specimens appeared to be attached to the exterior of the frame. The netted side contained numerous specimens of *Alvinocaris*, *Munidopsis,* and the gastropod *Buccinium.*

Site Three, GC-272. A single cage was deployed in a field of mussel clumps (Figure 7.3). Tubeworm bushes were in the area, but greater than 2 m from the cage. The cage abuts two mussel clumps. The open side contained a single mussel attached to the inner side of the frame. The bottom of the open side was soft bottom with no distinctive features. The netted side contained two mussels attached to the frame, one under the netting on the bottom and the other attached to the outside of the frame. At the edge of the netting, nearly centered within the frame, was a large burrow approximately 30 cm across. The legs of a large crustacean, possibly an anomuran crab, could be seen within the burrow. During the period of observation, both a hake and a hag fish swam through the open side of the cage.

Brine Pool. The rods in the brine had a coating of "fuzz" which appeared to be hydroids. No other organisms were visible by simple inspection. There were no juvenile mussels obvious at any position on the rods. Rods around the periphery of the mussel mat had little or no such fuzz covering. Rods lying horizontally on the mat appeared to be devoid of a covering.

7.1.4. Discussion

The main conclusion which can be drawn from these initial observations is that recovery from the experimental disturbance does not proceed rapidly. Immigration of adult mussels into a disturbed area is minimal over a year, and

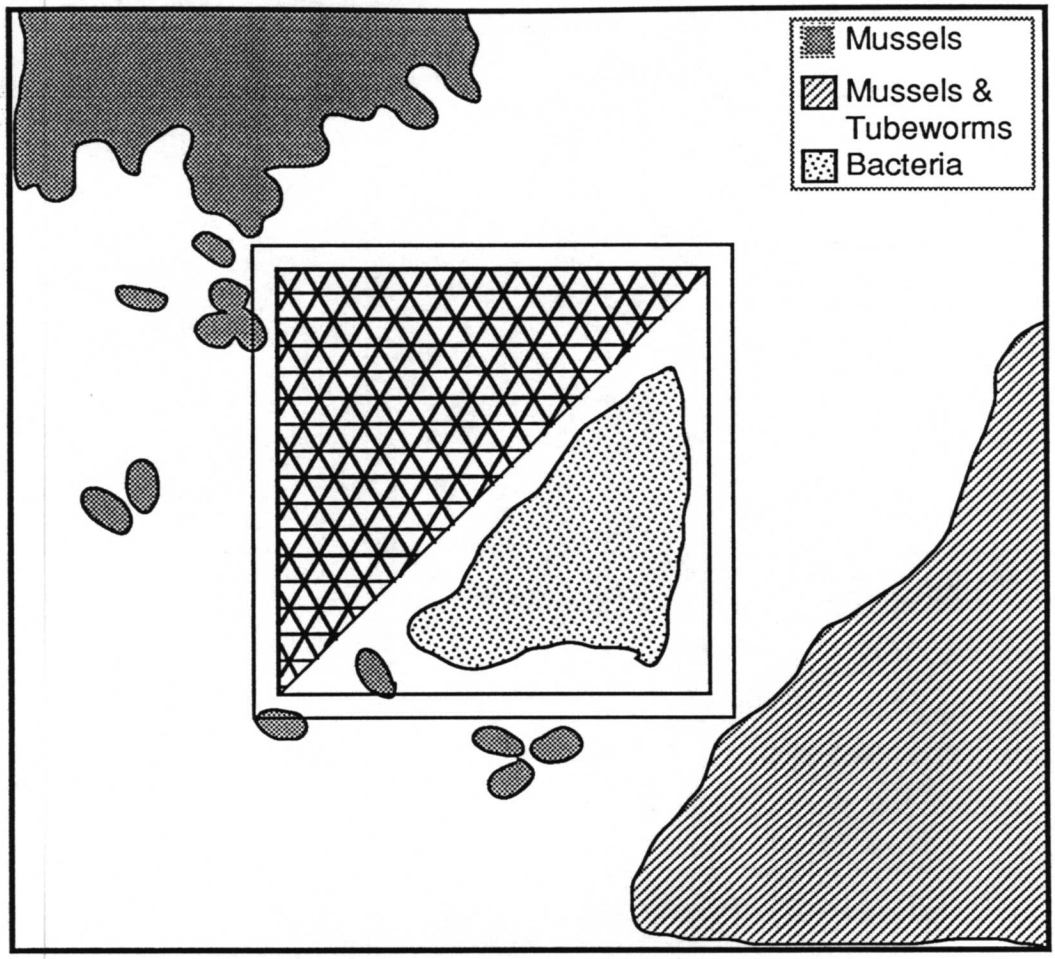

Figure 7.2. GC 234 mussel and bacterial cover after one year.

there is no conspicuous recruitment of juveniles over the period of a year. These results are the same for all three sites with cages. The massive bacterial overgrowth of Cage Two at Bush Hill indicates that development of bacterial mats can take place in less than a year.

The absence of apparent larval recruitment is the most interesting finding. However, the relatively short duration of the experiment, coupled with the lack of any microscopic examination of the caged bottom, limits the certainty of this observation. Mussels may have settled, but field growth rates are so low that recruited individuals are still in the undetectable 1-2 mm size range. Alternately, larvae may not have settled at all. Or, have recruited but failed to survive to a detectable size range.

The observation that mussels have not colonized the brine pool rods for three years supports the conclusion that larval recruitment is a slow, and possibly rare event. This is especially important in the case of rods crossing the brine/seawater interface just a few centimeters from dense mussel clumps. It may be safely assumed that the rods are situated in a chemically suitable environment, yet no mussel clumps have appeared on the rods.

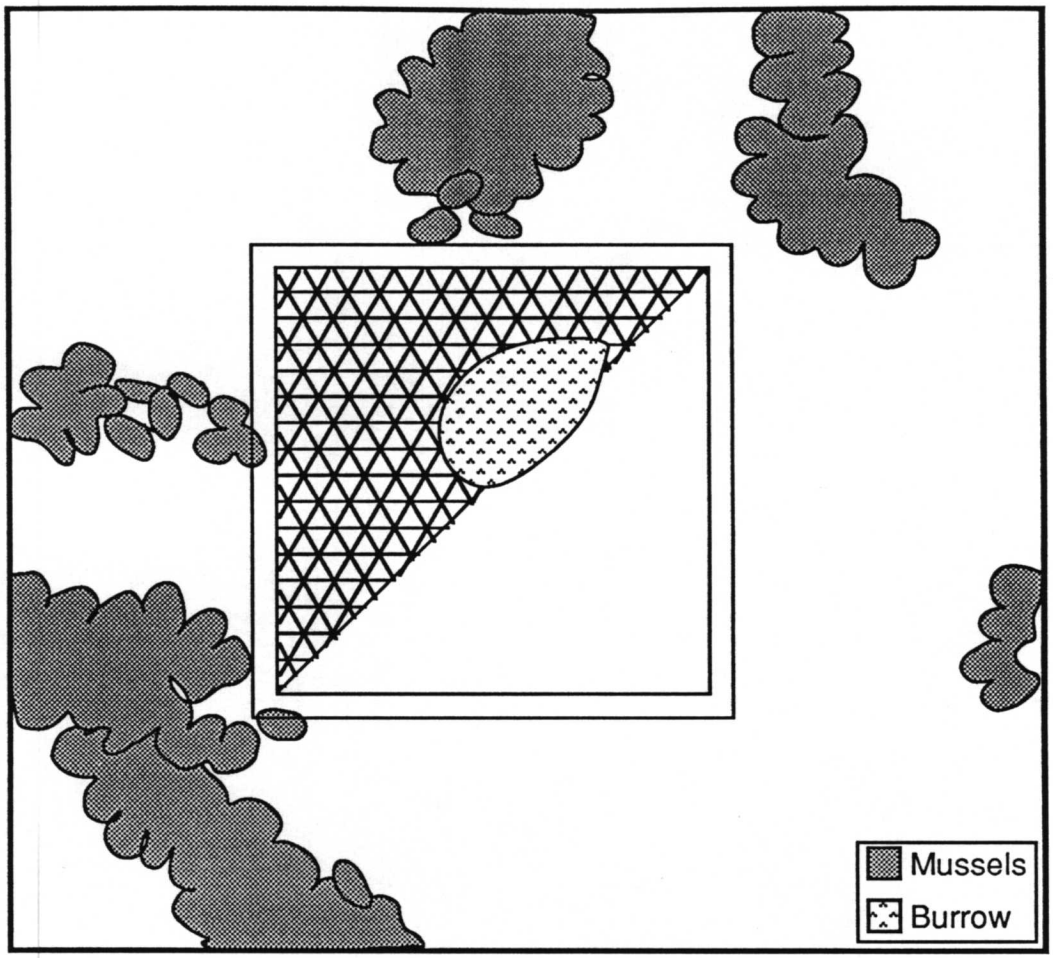

Figure 7.3. GC 272 mussel cover after one year.

In the introductory section, it was mentioned that interspecies competition may be important. The hydroid cover on the brine pool rods is a hint that such processes are in operation. The vertical rods may provide an artificial refuge from predatory browsing by gastropods and crustacea. Isolated from the mussel mat's heterotrophic fauna, the rods in the brine have escaped browsing by gastropods and crustacea and developed a dense hydroid cover. Rods lying horizontally on the mussel mat are exposed to browsing that crops back the hydroids. Similar dense hydroid cover is found on some tubeworms in the Bush Hill area. It may be assumed that some peculiarities of local topography tend to restrict browsers on such bushes. Unfortunately, this grazer control explanation for the hydroids fails to explain the absence of new recruits from all rods at the Brine Pool.

7.1.5. Preliminary Conclusions

Recovery of artificially displaced mussel clumps by migration of mature mussels has begun one year after disturbance. Except for Cage One at Bush Hill, very few specimens participated in this migration. More important to recovery, after one year there was no obvious recruitment of juvenile mussels. At this

preliminary stage, it appears that recovery from disturbance which denudes mussel cover is slow, with successful recruitment of juveniles taking more than three years.

7.2. Macroinfauna Component

7.2.1. Introduction

This section reports on the results of sediment coring and processing with a 300-micron screen at hydrocarbon seep sites. While preliminary examination indicates the seep communities are comprised of megafauna, this task was included for completeness as per the specifications of the RFP. Equipment testing alone was proposed for the 1991 field year, with full sampling planned in 1992.

7.2.2. Methods and Design

The proposed research consisted of two parts. In 1991, the feasibility of using the *JSL* grab in place of the more accepted *ALVIN*-type box core was to be examined by collecting four replicate *JSL* grabs and four replicate *ALVIN*-type box cores. In 1992, five core pairs of the selected coring device were to be from within to 100 m away from a mussel site. Due to the funding limitations and the higher priorities associated with the megafauna tasks, this series would not be replicated. During the pre-dive meeting of the Scientific Review Board in 1992, a greatly reduced design was adopted in which only three paired samples would be taken from adjacent to a mussel mat to within 10 m away.

The *JSL* grab is an integral part of the hydraulic manipulator on the *Johnson Sea-Link*. It consists of two semi-cylindrical 19.2 cm jaws rotating with a radius of 17.8 cm about a common axis to bite into and retain sediments. Under ideal conditions, the bite of the *JSL* grab covers 341 cm^2 of bottom. The *JSL* grab is powerful, extremely easy to use, and can take repeated samples in just a few minutes. The real problem with the grab is that samples must be transferred into the "critter gitter" of the submersible. This is done by positioning the closed grab over a collection chamber and opening the grab so that the sample falls into the chamber. It is obvious that large amounts of sediment are lost during this transfer, and it is suspected that much of the smaller fauna is also lost.

ALVIN-type box cores are manipulator-deployed samplers which are inserted into the sediment, closed, and then returned and sorted aboard the submersible. Since they are not opened until securely on deck, there is no sample loss. The box core covers 232 cm^2 of the bottom, and removes a uniform bite of sediment. However, they are less practical to use; they compete for scientific payload on the sub, are more time consuming than the *JSL* grab, and are prone to mechanical failure. The most common failure is associated with closure of the core. Closure is affected by rotating the handle of the core. If the core is not inserted deeply into cohesive sediments, it tends to rotate rather than close. If the jaws encounter any resistance, such as carbonate gravel, a safety pin shears, preventing damage, but taking no sample and disabling the sampler.

7.2.3 Results

Intercomparison. The intercomparison did not produce useful faunal comparisons, but did point out the difficulty of traditional mega-infaunal sampling in areas of hard substrates. Of four replicate box cores attempted, only two were obtained, with one of dubious quality. In all cases, failure was due to the presence of massive carbonates or carbonate gravels buried under a thin cover of sediments. This prevented penetration or core closure. By contrast, the much more powerful *JSL* grab easily recovered samples from gravel, but lost large amounts of sediment during transfer.

Without replication, no meaningful comparison can be made. However, the one successful *ALVIN*-type core contained ostracods, harpacticoid copepods, and tanaiids totally absent from the *JSL*-Grab. Therefore, it was concluded that the *ALVIN*-type device was needed.

1992 Box Core Sampling. A total of six good cores were collected during the 1992 series. On Bush Hill, two replicate cores were taken within 30 cm, 1 m, and 10 m of a mixed mussel/tubeworm clump. These samples will be processed in the first two quarters of 1993.

7.2.4. Discussion

Discussion must await final analysis.

7.2.5. Preliminary Conclusions

Initial conclusions deal only with sampling matters. Study of the mega-infauna is severely limited by existing technologies. Box cores only work in areas where the sediment cover may be atypical for seeps, and the current submersible sampler has unacceptable sample loss upon transfer. The sample retention abilities of box cores should be combined with the power and shallow sampling capabilities of the *JSL* grab.

7.3. *JSL* Grab-Sampled Megafauna at Mussel Beds

7.3.1. Introduction

This section reports the result of larger fauna collecting with the *JSL* grab, as specified in the Technical proposal. The purpose of this component is to provide a degree of quantification to megafaunal observations with special emphasis upon small scale patterns and chemotroph-heterotroph links.

This component has been reasonably successful with 40 paired *JSL* grabs being collected during the 1991 dive series and 20 in 1992. The 1992 samples were as follows:

JSL3265	CG-234	8 paired *JSL* Grabs
JSL3268	CG-234	4 paired *JSL* Grabs
JSL3269	Bush Hill	4 paired *JSL* Grabs
JSL3274	Bush Hill	4 paired *JSL* Grabs

All 1991 mussel bed samples have been processed except for larger rocks, which need to be broken apart and thoroughly searched. The eight clam bed samples collected in 1991 will be processed in conjunction with the macroinfauna study. All 1992 samples have been removed from field packs, represerved in ethanol, and are being sorted at this time.

Problems. We have encountered two sources of trouble. First, mussel beds are not as simple as initially thought, making prior classifications of "on rock" or "on sediment" less confident. Even identifying an outer edge and inner portion is often difficult. Second, large undisturbed beds are not easily found within the limited cruising range and speed of the *JSL*, rendering equal replication impossible at the different sites.

7.3.2. Methods

Sampling has progressed largely according to plan. Two adjacent *JSL* grabs were taken at the outer edge of a bed and two more were taken within a meter or less from the inner portion of the same bed. If additional beds were nearby, the process was repeated at another bed. If only a single large bed was present, then the sequence of four grabs was repeated on another portion of the same bed. Rather than have a prior classification as to substrate, substrate was assessed from the sample. The inability to pre-classify substrate and to find replicate beds forced abandonment of a balanced design.

Samples were sieved at sea with a 250 micron screen and fixed in 10% seawater formalin. In the lab, the fixative was removed, and the samples water-soaked for five days to dilute residual formalin, and then packed in 80% ethanol. Samples were sieved at 1mm into a large and small fraction and both fractions hand sorted.

7.3.3. Results

General Taxonomic Notes Andres Waren of the Swedish Museum of Natural History has completed a study of vent and seep gastropods of the genus *Provanna*, including those from the Louisiana Continental Slope (Waren and Ponder, 1991). A common species at some hydrocarbon seep sites has been designated *Provanna sculpta*. Unlike the endemic dominant gastropod of the Louisiana seeps, *Bathynerita naticoides* (Clarke, 1989), the genus *Provanna* is widespread in vent and seep systems. Its radular are consistant with a browsing feeding mode.

Publication of *Starfishes of the Atlantic* (Clark and Downey, 1992) has allowed generic identification of the collected starfish. The form common to mussel beds is in the genus *Sclerasterias perrier*. The species that have previously been found in the Gulf of Mexico and West Indies are similar to the material on hand. The morphology of this animal is that of typical *Asteriidae*, which are common bivalve predators. Other genera collected in the area of seeps are *Paragonaster*, and the filter feeding *Novodina*.

Paired Grab Sampling Preliminary results showing the eight most abundant species are presented in Table 7.1. The eight species included represent more than 99% of the specimens collected. These numbers will change slightly as rock fractions are broken up and searched, but they convey the basic patterns.

While Seep Mytilid I and *Bathynerita naticoidea* are the ubiquitous dominants at all sites, there are site-specific patterns in the subdominant gastropods *Provanna sculpta* and *Cataegis meroglypta*. The small *P. sculpta* appears to be very rare at the Brine Pool, uncommon at CG-234, but common and locally abundant at Bush Hill and CG-272. The species *C. meroglypta* is common at Bush Hill, but rare elsewhere. Local patterns of crustacean and polychaete abundance are probably artifacts of sampling. Both crustacea *Alvinocaris* and *Munidopsis* have been observed to flee from the sample as it is pulled from bottom. The locally abundant large polychaete of the family *Orbinidae* appears to have dense clumps which can easily be missed by the relatively small *JSL* grab.

The differences between Edge and Inner samples seem to lie less in the actual species present than in the demographics of the mussels. Edge samples at the Brine Pool and GC-272 often contained few or no live mussels and relatively few associated heterotrophs. This was less the case at Bush Hill, where Edge and Inner were relatively similar. At one site at GC-234, samples judged to have come from the edge at the time of collection show a great abundance of small mussels. Interestingly, these same samples contained large numbers of very small Bathynerita naticoidea. By contrast, the Inner samples were relatively depauperate.

7.3.4. Discussion

Extensive discussion is not justified at this stage of the project. Two observations are, however, worthy of comment. First, mussel beds show marked differences in the abundance of live mussels and heterotrophs on scales less than a meter. This can be interpreted to mean that these communities occupy very narrow and spatially restricted chemical gradients. Second, live heterotrophs and live chemotrophs are quite closely linked. The shell rubble immediately at the edge of beds has markedly fewer browsing gastropods than the live shells just centimeters away. This can be interpreted to mean that productivity, such as free living bacterial production of use to the consumers, is as limited in distribution as the mussel beds.

Table 7.1. Preliminary results showing the eight most abundant species.

Sample	Seep Mytilid I Common Mussel	*Bathynerita naticoides* Snail	*Provanna sculpta* Snail	*Cataegis meroglypta* Snail	*Buccinius canetae* Snail	*Alcinovaris* sp. Shrimp	*Munidopisis* sp. Squat Lobster	Orbiniidae Polychaete
GC-272								
3137.1 Edge	*	*	*	*	0	0	1	0
3137.2 Edge	*	*	3	*	0	0	0	0
3137.3 In	2	10	30	*	0	0	0	0
3137.4 In	*	5	9	*	0	0	0	0
3137.5 In	28	15	32	3	0	0	1	
3137.6 In	19	8	25	1	0	0	0	0
3137.11 Edge	8	0	2	0	0	0	2	0
3137.12 Edge	2	0	3	0	0	0	2	0
Bush Hill								
3139.12 Edge	11	4	8	3	11	1	2	0
3139.1 Edge	15	15	27	8	3	1	0	0
3139.2 In	13	1	9	2	0	2	0	0
3139.3 In	27	30	41	11	2	3	0	0
3139.4 Edge	25	50	27	3	0	3	0	0
3139.5 Edge	10	4	0	2	0	0	1	0
3139.6 In	42	154	14	3	3	4	0	1
3139.7 In	52	149	48	24	4	10	1	3
CG-234								
3142.8 In	11	12	22	0	0	1	0	12
3142.9 In	9	4	1	0	0	0	0	
3142.10 In	20	65	5	2	0	5	2	0
3142.11 Edge	11	34	0	0	*	5	1	42
3142.12 Edge	11	128	1	0	0	4	0	18
3142.1 In	13	20	1	0	0	0	0	0
3142.2 In	22	28	4	0	0	0	1	0
3142.3 Edge	282	588	9	0	0	10	0	12
3142.4 Edge	72	83	*	0	0	0	0	17
Brine Pool								
3145.12 Edge	1	*	*	*	5	0	1	0
3145.1 Edge	4	*	0	2	*	0	1	0
3145.2 In	10	39	0	0	0	2	5	0
3145.3 In	4	15	0	0	0	0	0	0
3145.4 Edge	5	7	0	0	0	0	0	0
3145.5 Edge	*	1	0	0	*	0	0	1
3145.6 In	10	11	0	0	0	9	2	0
3145.7 In	9	8	0	0	0	8	2	0

* Denotes non-living shell

8.0 Ancillary Studies: Topics Not Included in Proposal, but under Consideration for Additional Work

This section describes ancillary data sets and/or research opportunities that have developed since the award of the contract. These descriptions should provide a prospectus for ways the existing contract might be expanded to take advantage of results obtained thus far.

8.1. Microbiological Studies

Much less is known about the ecological and geochemical significance of the microbial community at oil seeps than is known about tube worms, mussels, and clams. Yet, microbial alteration of the seeping hydrocarbons is implicated for both massive accumulation of authigenic carbonates and for sulfide generation (via reduction of seawater sulfate). Hence, the geological character of seeps and the vitality of the biological community is dependent upon how free-living bacteria utilize hydrocarbons. Preliminary studies of the *Beggiatoa* at Bush Hill (GC 184/185) suggested that distinct differences in the nutritional mode may occur at spatial scales <1 m. Direct sampling by submarine can provide additional information needed to understand the regional significance of seeps in the carbon cycle and in maintaining the ecological productivity of seep communities.

Members of the bacterial genus *Beggiatoa* are filamentous and gliding in character and can oxidize reduced sulfur (hydrogen sulfide and thiosulfate) to elemental sulfur, which is deposited within the cells (Kowallik and Pringsheim, 1966). Nelson and Jannasch (1983) demonstrated autotrophic CO_2 fixation and RuBP-carboxylase (RuBPCase) activity in *Beggiatoa*. *Beggiatoa* spp. have been reported to occur as densely populated mats on both coastal (Grant and Bathmann, 1987) and deep sea sediments (Nelson et al., 1989; Jannasch et al., 1989; Jannasch and Wirsen, 1981).

Beggiatoa occur in pigmented and non-pigmented forms in the Gulf seep communities. In September 1991, we collected samples from pigmented and non-pigmented mats with the *Johnson Sea-Link* slurp sampler. The non-pigmented mats occurred over anoxic sediment, which presumably supply reduced sulfur by diffusion to the underside of the mats. In contrast, pigmented mats, which comprise cells morphologically identical to the non-pigmented mats, have been collected over sediments containing high concentrations (≥10%) of extractable oil (MacDonald, personal observation and unpublished data). Primary cell morphology indicated that both white and orange mats comprised *Beggiatoa* spp. Fixation of labeled CO_2 and RuBPCase activities clearly indicated chemoautotrophic activity by the non-pigmented mat cells. These same trials with the pigmented mat material indicated minimal chemosynthetic potential for these cells.

The ability to grow as a facultative autotroph (versatile) as opposed to an obligate autotroph (specialized) can offer advantages for organisms that exist in an environment in which the chemical milieu may change significantly (Gottschal et al., 1979; 1981). Filamentous mats containing gradient organisms such as *Beggiatoa* are dependent on a flux of reduced sulfur (sulfide) from the sediments

below (Nelson et al., 1986). An obligate autotroph may not be as competitive in these situations as one that can switch between heterotrophic and autotrophic nutrition.

We hypothesize that one form of *Beggiatoa* is pursuing an autotrophic existence in which sulfide is plentiful from diffusive processes due to sulfate reduction occurring in the sediment. The other form may be relying primarily on heterotrophic processes utilizing organic compounds from fresh hydrocarbon metabolites diffusing from the sediment. This suggests mat formation controlled by sequential degradation of seeping hydrocarbons.

8.1.1 Mini-Push Core Series

To test this hypothesis, we dissected six representative mats and underlying/adjacent sediment by use of small-diameter push cores. A 1-m frame with rope cross-pieces was used to guide precise placement of the samples and to track which sediment samples came from beneath pigmented or non-pigmented mat material. A video mosaic of the mat, assembled prior to collection, provided additional documentation of sample placement. Analysis of the bacteria will determine their trophic mode, sources of carbon, and pigment characteristics. Geochemical characteristics of spatially synoptic sediment samples and the biodegradation state of extracted oils will show stages in the utilization of seeping hydrocarbons (Kennicutt et al., 1988a). Lipid biomarker analysis of sediment extract will provide a check on the composition of the microbial community.

Mat samples were removed from the individual mini-cores, separated from sediment and other debris, and placed in cryo-vials. These were spun down by use of a microfuge to prevent lysis of the mat proteins, the supernate was poured off, and the pellets were frozen in liquid nitrogen. The cored and bulk mat samples (as appropriate given mat recovery) will be analyzed as follows:

1. RuBPCase and amino acid assay;
2. Pigment extraction and characterization;
3. $\delta^{13}C$ of biomass;
4. Percent elemental sulfur; and
5. $\delta^{34}S$ of elemental sulfur.

Small cores were extruded and sub-sampled for top, middle, and bottom. These samples will be freeze dried, sonicated, and weight extracted for determination of extractable oil percentage. Large sediment samples will be stored frozen in hermetically sealed cans after the addition of sodium azide as a microbial inhibitor. We will extract these sediments for the following analyses:

1. Total Organic Carbon;
2. Extraction and C_{15+} chromatography of saturated hydrogens;
3. $\delta^{13}C$ of extractable organic material (EOM);
4. Percent C_1-C_4 gas in head space;
5. Percent CO_2 in head space;
6. $\delta^{13}C$ of C_1 in head space;
7. $\delta^{13}C$ of CO_2 in head space;

8. Total Scanning Fluorescence (TSF);
9. Percent elemental sulfur; and
10. $\delta^{34}S$ of elemental sulfur.

8.2. Remote Sensing Estimates for Rates and Distribution of Natural Oil Seepage in the Gulf of Mexico

Natural seepage in the Gulf of Mexico causes surface slicks that are visible from space. In a preliminary attempt to use these slicks as a means for remote sensing of seeps and seep communities, we analyzed a photograph of the sun-glint pattern taken from the Space Shuttle *Atlantis* on 5 May 1989, which shows at least 124 slicks, and a Thematic Mapper (TM) image collected by the Landsat orbiter on 31 July 1991, which shows at least 66 slicks. Samples and descriptions made from a surface ship, from aircraft, and from a submarine confirmed that many of the slicks are crude oil and, in three locations, documented the sea-floor source of the oil. The shape and frequency of the slicks argue against anthropogenic sources for the oil.

We derived a mathematical model that simulates formation of slicks based on a parameterization of sea-floor flow rate, down-stream movement on the surface, half-life of floating oil, and threshold thickness for visibility. Results of the model indicate that the size and shape of slicks formed by seepage are determined as much by wind and current as by flow rate. Estimates for local wind velocity and direction on the dates of the imagery (~20 cm/s) determine the prevailing advection velocity. Using this velocity, we fit the model to the lengths and areas of slicks observed in the imagery. We specified a half-life of 48 hours and a threshold thickness of .01 μm for the floating oil, summed the individual seepage rates over the entire imaged area, and extrapolated the rates over one year. This exercise predicts that the slicks in the *Atlantis* photograph and the TM image represent totals of 426,000 bbl/y and 120,000 bbl/y, respectively. Increasing the threshold thickness or decreasing the oil half-life would increase these estimated rates. Periodic fluctuation in seepage might decrease annual discharge.

These findings provide additional evidence for high seepage rates in the northern Gulf of Mexico, they point to extensive seepage in water depths over 1000 m, they considerably increase the area where chemosynthetic communities dependent on seepage may be expected, and they suggest an approach for future study of natural oil seepage by use of remote sensing data that should be of interest to MMS. First, these data could provide a means for estimating the distribution and abundance of seep communities on a regional scale. Second, the area of the slicks will provide an estimate for the total natural input of oil into the Gulf and for the potential value of leasing areas. Finally, there is much current interest in predicting where oil will go in the event of a spill. To study this problem, one could hardly do better than to watch where oil actually does go – if these slicks are indeed persistent features, then we could have a set of natural releases to verify models directly.

To utilize this potential, MMS could undertake a survey of areas of the slope where seeps and seep communities are known to occur using the most cost-effective sensors and sensor platforms available. The Green Canyon/Garden Banks leasing areas are obvious choices to survey. As for sensing data, there are two options. The NASA ER-2 aircraft is outfitted with a Thematic Mapper simulator. This sensor

scans the same spectral wavelengths as the Landsat satellite. The airplane is a refitted U-2 spy plane that flies at 65,000 ft. The plane cruises at 450 knots and scans an 8 nmi swath at an operating cost of $6000/hour. During a typical flight, it could fly pre-determined flight-lines for one to two hours, scanning up to 7200 sq nmi for a cost of about $18,000. The geo-positioning of data from the ER-2 is reportedly accurate to within "a couple of hundred feet" (Gary Sheldon, ER-2 flight manager). With carefully planned flight lines, ER-2 could survey all of the slope between 90° and 93°N and between the 500 and 1000 m isobaths in about three days. This would cover the area where 90% of the known communities occur. The initial evidence suggests that there are many communities we have not yet discovered.

8.3. A 2200 m Seep Community in Alaminos Canyon

Six dives with the submersible *Alvin* were completed at a chemosynthetic community in the Alaminos Canyon region of the Gulf of Mexico near 26°21'N and 94°21'W (Dives 2534-2539, 20-26 May, 1992). This community occupies the crest of a mound at a depth of 2200 m. During this series, 36 permanent markers were carefully photographed with use of quantifiable video techniques. Mosaics covering up to 26 sq m of seafloor were constructed from these data and additional mosaics could be generated. Use of the *Alvin*'s long base line navigation system was integrated in a GIS to document the area explored.

Specimens of tube worms and mussels were collected for taxonomic and physiological study. Insight into the carbonate geology of this area will be obtained from ten rock samples collected from eight different sites. Six sediment cores were collected to document the geochemistry of the pore fluids and the extractable hydrocarbons. With use of a prototype water sampler, discrete, highly targeted samples were collected near mussel siphons and in contact with evident brine seeps. Six tube worms were banded and photographed for determination of growth rates in the event of a future site visit.

Chemosynthetic fauna at the community comprise two species each of vestimentiferans and seep mytilids, which are similar to those found at seeps on the upper slope. Hydrocarbons seepage in the area has been documented in piston cores collected in the vicinity and by preliminary analysis of sediments collected from *Alvin*; however, the correlation between hydrocarbon seepage and community development will require additional study. Elevated salinities observed in water samples, together with shimmering seepage around some of the clusters of fauna, suggests brine seepage. No macro-gas seeps were seen.

9.0 Literature Cited

Aberhan, M. and F.T. Förisch. 1991. Paleoecology and paleoenvironments of the Pleistocene deposits of Bahia la Choya (Gulf of California, Sonora, Mexico). Zitteliana, 18:135-163.

Alexandersson, E.T. 1979. Marine maceration of skeletal carbonates in the Skagerrak, North Sea. J. Sedimentology, 26:845-852.

Anderson, A.L. and W.R. Bryant. 1990. Gassy sediment occurrence and properties; Northern Gulf of Mexico. Geo-Marine Letters, 10:209-220.

Anderson, R.K., R.S. Scalan, P.L. Parker, and E.W. Behrens. 1983. Seep oil and gas in Gulf of Mexico slope sediments. Science, 222:619-621.

Ausich, W.I. and D.J. Bottjer. 1982. Tiering in suspension-feeding communities on soft substrata throughout the Phanerozoic. Science (Washington D.C.), 216:173-174.

Bauer J.E., P.A. Montagna, R.B. Spies, M.C. Prieto, and D. Hardin. 1988. Microbial biogeocchemistry and heterotrophy in sediments of a marine hydrocarbon seep. Limn. and Ocean., 33:1493-1513.

Behrens, E.W. 1988. Geology of a continental slope oil seep, northern Gulf of Mexico. AAPG Bulletin, 72:105-114.

Bernard, B.B., J.M. Brooks, and W.M. Sackett. 1976. Natural gas seepage in the Gulf of Mexico. Earth and Planetary Science Letters, 31:48-54.

Boudreau, B.P. 1991. Modeling the sulfide-oxygen reaction and associated pH gradients in porewaters. Geochim. et Cosmochim. Acta, 55:145-159.

Brooks, J.M., M.C. Kennicutt II, R.R. Fay, T.J. McDonald, and R. Sassen. 1984. thermogenic gas hydrates in the Gulf of Mexico. Science, 226:965-967.

Brooks, J.M., H.B. Cox, W.R. Bryant, M.C. Kennicutt II, R.G. Mann, and T.J. McDonald. 1986. Association of gas hydrates and oil seepage in the Gulf of Mexico. Org. Geochem., 10:221-234.

Brooks, J.M., M.C. Kennicutt, C.R. Fisher, S.A. Macko, K. Cole, J.J. Childress, R.R. Bidigare, and R.D. Vetter. 1987. Deep-sea hydrocarbon seep communities: evidence for energy and nutritional carbon sources. Science, 20:1138-1142.

Brooks, J.M., M.C. Kennicutt II, I.R. MacDonald, D.L. Wilkinson, N.L. Guinasso Jr., and R.R. Bidigare. 1989. Gulf of Mexico hydrocarbon seep communities: Part IV - Description of known chemosynthetic communities. Proceedings 21st Offshore Technology Conference, OTC 5954, pp. 663-667.

Burke, R.A. and W.M. Sackett. 1986. Stable hydrogen and carbon isotopic compositions of biogenic methanes from several shallow aquatic environments. In: Sohn, M.L. (ed.) Organic Marine Geochemistry. *ACS Symp. Ser.*, 305:297.

Callender, W.R. and E.N. Powell, 1992. Taphonomic signature of petroleum seep assemblages on the Louisiana upper continental slope: recognition of autochthonous shell beds in the fossil record. Palaios, 7:388-408.

Callender, W.R. and E.N. Powell. Submitted. Biomass and energy flow of chemoautotrophic petroleum seep death assemblages: implications for the fossil record.

Callender, W.R., G.M. Staff, E.N. Powell, and I.R. MacDonald. 1990. Gulf of Mexico hydrocarbon seep communities; V. Biofacies and shell orientation of autochthonous shell beds below storm wave base. Palaios, 5:2-14.

Carpenter, J. 1965. The accuracy of the Winkler Method for dissolved oxygen analysis. Limnol. Oceanogr., 14:135-140.

Cary, S.C., C.R. Fisher, and H. Felbeck. 1988. Mussel growth supported by methane as sole carbon and energy source. Science, 240:78-80.

Childress, J.J., C.R. Fisher, J.M. Brooks, M.C. Kennicutt, II, R. Bidigare, and A. Anderson. 1986. A methanotrophic marine molluscan symbiosis: mussels fueled by gas. Science, 233:1306-1308.

Clark, A.M. and M.E. Downey. 1992. Starfishes of the Atlantic. Chapman and Hall, London. 794 pp.

Clarke, A.H. 1989. New mollusks from undersea oil seep sites off Louisiana. Malacolgy Data Net, 2:122-134.

Cline, J.D. 1969. Spectrophotometric determination of hydrogen sulfide in natural waters. Limnol. Oceanogr., 14:454-458.

Comfort, A. 1957. The duration of life in molluscs. Proceedings of the Malacological Society of London, 32:219-241.

Davies, D.J., E.N. Powell, and R.J. Stanton, Jr. 1989. Taphonomic signature as a function of environmental process: shells and shell beds in a hurricane-influenced inlet on the Texas coast. Palaeogeography, Palaeoclimatology, Palaeoecology, 72:317-356.

Davies, D.J., G.M. Staff, W.R. Callender, and E.N. Powell. 1990. Description of a quantitative approach to taphonomy and taphofacies analysis: all dead things are not created equal. In: Miller III, W. (ed.) Paleocommunity temporal dynamics: the long-term development of multispecies assemblages. Special Publication (The Paleontological Society), 5:328-350.

De Vernal, A., G. Gilodeau, C. Hillaire-Marcel, and N. Kassou. 1992. Quantitative assessment of carbonate dissolution in marine sediments from foraminifer linings vs. shell ratios: Davis Strait, northwest North Atlantic. Geology (Boulder), 20:527-530.

Denne, R.A. and B.K. Sen Gupta. 1989. Effects of taphonomy and habitat on the record of benthic foraminifera in modern sediments. Palaios, 4:414-423.

Farrow, G.E. and J.A. Fyfe. 1988. Bioerosion and carbonate mud production on high-latitude shelves. Sedimentary Geology, 60:281-297.

Fisher, C.R. 1990. Chemoautotrophic and methanotrophic symbioses in marine invertebrates. Rev. Aquat. Sci., 2:399-436.

Fisher, C.R., M.C. Kennicutt II, and J.M. Brooks. 1990. Stable carbon isotopic evidence for carbon limitation in hydrothermal vent vestimentiferans. Science, 247:1094-1096.

Flessa, K.W. and T.J. Brown. 1983. Selective solution of macroinvertebrate calcareous hard parts: a laboratory study. Lethaia, 16:193-205.

Fustec, A., D. Desbruyères, and S.K. Juniper. 1987. Deep-sea hydrothermal vent communities at 13°N on the East Pacific Rise: microdistribution and temporal variations. Biol. Oceanogr., 4:121-164.

Goldhaber, M.B., R.C. Aller, J.K. Cochran, J.K. Rosenfeld, C.S. Martens, and R.A. Berner. 1977. Sulfate reduction, diffusion and bioturbation in Long Island Sound sediments: report of the FOAM group. Am. J. Sci., 277:193-237.

Gottschal, J.C., A. Pol, and J.G. Kuenen. 1981. Metabolic flexibility of *Thiobacillus* A2 during substrate transitions in the chemostat. Arch. Microbiol., 129:23-28.

Gottschal, J.C., S.D. Vries, and J.G. Kuenen. 1979. Competition between the facultatively chemolithotroph, *Thiobacillus* A2, an obligately chemolithotrophic *Thiobacillus* and a heterotrophic spirillum for inorganic and organic substrates. Arch. Microbiol., 121:241-249.

Grant, J. and U.V. Bathmann. 1987. Swept away: resuspension of bacterial mats regulates benthic-pelagic exchange of sulfur. Science, 236:1472-2474.

Hairston, N.G. 1989. Ecological experiments: purpose, design and execution. Cambridge Univ. Press, Cambridge. 370 pp.

Han, M.W. and E. Suess. 1989. Subduction-induced pore fluid venting and the formation of authigenic carbonates along the Cascadia continental margin: implications for the global Ca-cycle. Palaeogeography, Palaeoclimatology, Palaeoecology, 71:97-118.

Heller, J. 1990. Longevity in molluscs. Malacologia, 31:259-295.

Herbert, T.D., W. B. Curry, J.A. Barron, L.A. Codispoti, R. Gersonde, R.S. Keir, A.C. Mix, B. Mycke, H. Schrader, R. Stein, and H.R. Thierstein. 1989. Group report geological reconstructions of marine productivity, pp. 409-428. In: Berger, W.H., V.S. Smetacek, and G. Wefer (eds.), Productivity of the ocean: present and past. John Wiley and Sons Ltd., New York.

Herguera, J.C. and W.H. Berger. 1991. Paleoproductivity from benthic foraminifera abundance: glacial to postglacial change in the west-equitorial Pacific. Geology (Boulder), 19:1173-1176.

Hessler, R.R., W.M. Smithey, and C.H. Keller. 1985. Spatial and temporal variation of giant clams, tubeworms and mussels at deep-sea hydrothermal vents. Bulletin Biological Society Washington, 6:411-428.

Hessler, R., P. Lonsdale, and J. Hawkins. 1988. Patterns on the ocean floor. New Scientist, 24:47-51.

Hilly, A., M. le Pennec, D. Prieur, and A. Fiala-Médioni, 1986. Anatomie et structure du tractus digestif d'un Mytilidae de source hydrothermales profondes de la ride du Pacifique Oriental. Cahiers de Biologie Marine, 27:235-241.

Hoffman, A. 1977. Synecology of macrobenthic assemblages of the Korytnica Clays (Middle Miocene; Holy Cross Mountains, Poland). Acta Geologica Polonica, 27:227-280.

Hofmann, E.E., J.M. Klinck, E.N. Powell, S. Boyles, and M. Ellis. Submitted. Modeling oyster populations II. Adult size and reproductive effort.

Jannasch, H.W. and C.O. Wirsen. 1981. Morphological survey of microbial mats near deep-sea thermal vents. Appl. Environ. Microbiol., 41:528-538.

Jannasch, H.W., D.C. Nelson, and C.O. Wirsen. 1989. Massive natural occurrence of unusually large bacteria (*Beggiatoa* sp.) at a hydrothermal deep-sea vent site. Nature, 342:834-836.

Johnson, H.P., and M. Helferty. 1990. The geological interpretation of side-scan sonar. Reviews of Geophysics, 28(4):357-380.

Jørgensen, N.O. 1992. Methane-derived carbonate cementation of marine sediments from the Kattegat, Denmark; Geochemical and geological evidence. Marine Geology, 103:1-13.

Kammer, T.W., C.E. Brett, D.R. Boardman II, and R.H. Mapes. 1986. Ecological stability of the dysaerobic biofacies during the Late Paleozoic. Lethaia, 19:109-121.

Kennicutt II, M.C., J.M. Brooks, and G.J. Denoux. 1988a. Leakage of deep, reservoired petroleum to the near surface on the Gulf of Mexico continental slope. Mar. Chem., 24:39-59.

Kennicutt II, M.C., J.M. Brooks, R.R. Bidigare, and G.J. Denoux. 1988b. Gulf of Mexico hydrocarbon seep communities-I. Regional distribution of hydrocarbon seepage and associated fauna. Deep-Sea Res., 35:1639-1651.

Kennicutt II, M.C., J.M. Brooks, and R.A. Burke, Jr. 1989. Hydrocarbon seepage, gas hydrates, and authigenic carbonate in the northwestern Gulf of Mexico. Proceedings 21st Offshore Technology Conference, OTC 5952, pp. 649-654.

Kennicutt II, M.C., R.A. Burke, Jr., I.R. MacDonald, J.M. Brooks, G.J. Denoux, and S.A. Macko. 1992. Stable isotope paritioning in seep and vent organisms: chemical and ecological significance. Chem. Geol., 101:293-310.

Khripounoff, A. and P. Alberic. 1991. Settling of particles in a hydrothermal vent field (East Pacific Rise 132N) measured with sediment traps. Deep-Sea Res., 38:729-744.

Kowallik, U. and E.G. Pringsheim. 1966. The oxidation of hydrogen sulfide by *Beggiatoa*. Am. J. Bot., 53:801-806.

Lapenis, A.G., N.S. Os'kina, M.S. Barash, N.S. Blyum, and Y.V. Vasikeva. 1990. Late Quaternary changes in productivity of the oceanic biota. Oceanology, 30:69-75.

Le Pennec, M., and A. Fiala-Médioni. 1988. The role of the digestive tract of *Calyptogena laubieri* and *Calyptogena phaseoliformis*, vesicomyid bivalves of the subduction zones of Japan. Oceanologica Acta, 11:193-199.

Lutz, R.A., L.W. Fritz, and R.M. Cerrato. 1988. A comparison of bivalve (*Calyptogena magnifica*) growth at two deep-sea hydrothermal vents in the eastern Pacific. Deep-Sea Res., 35:1793-1810.

Lyle, M. and N. Pisias. 1990. Ocean circulation and atmospheric CO2 changes: coupled use of models and paleoceanographic data. Paleoceanography, 5:15-41.

MacDonald, I.R., G.S. Boland, J.S. Baker, J.M. Brooks, M.C. Kennicutt II, and R.R. Bidigare. 1989. Gulf of Mexico hydrocarbon seep communities; II. Spatial distribution of seep organisms and hydrocarbons at Bush Hill. Marine Biology, 101:235-247.

MacDonald, I.R., N.L. Guinasso Jr., J.F. Reilly, J.M. Brooks, W.R. Callender, and S.G. Gabrielle. 1990. Gulf of Mexico hydrocarbon seep communities; VI. Patterns in community structure and habitat. Geo-Marine Letters, 10:244-252.

Majewske, O.P. 1969. Recognition of invertebrate fossil fragments in rocks and thin sections. E.J. Brill, London, 101 pp.

Miller III, W. 1982. The paleoecological history of Late Pleistocene estuarine and marine fossil deposits in Dare County, North Carolina. Southeastern Geology, 23:1-13.

Montagna, P.A., J.E. Bauer, M.C. Prieto, D. Hardin, and R.B. Spies. 1986. Benthic metabolism in a natural coastal petroleum seep. Mar. Ecol. Prog. Ser., 34:31-40.

Montagna, P.A., J.E. Bauer, J. Toal, D. Hardin, and R.B. Spies. 1987. Temporal variability and the relationship between benthic meiofaunal and microbial populations of a natural coastal petroleum seep. J. Mar. Res., 45:761-769.

Nelson, D.C. and H.W. Jannasch. 1983. Chemoautotrophic growth of a marine Beggiatoa in sulfide-gradient cultures. Arch. Microbiol., 136:262-269.

Nelson, D.C., B.B. Jorgensen, and N.P. Revsbech. 1986. Growth pattern and yield of a chemoautotrophic *Beggiatoa* sp. in oxygen-sulfide microgradients. Appl. Environ. Microbiol., 52:225-233.

Nelson, D.C., C.O. Wirsen, and H.W. Jannasch. 1989. Characterization of large autotrophic *Beggiatoa* abundant at hydrothermal vents of the Guaymas Basin. Appl. Environ. Microbiol., 55:2909-2917.

Neurauter, T.W., and W.R. Bryant. 1990. Seismic expression of sedimentary volcanism on the continental slope, northern Gulf of Mexico. Geo-Marine Letters, 10:225-231.

Odé, H. 1975-1988. Distribution records of the marine Mollusca in the northwest GUlf of Mexico. Texas Conchologist, 11:52-63; 12:40-56, 79-84, 108-124; 13:52-68, 74-81, 84-88, 106-107, 114-122; 14:10-11, 14-24, 41-52, 64-75, 93-104; 16:71-80; 19:54-63; 20:28-32; 24:59-82, 94-107.

Ovsyannikov, V.M., V.S. Lebedev, V.M. Bogdanove, and G.A. Mogilevskii. 1973. Fractionation of carbon isotpes by microorganisms during oxidation of gaseous hydrocarbons. Mikrobiologiya, 42:589.

Parsons, T.R., M. Takahashi, and B. Hargrave. 1984. Biological oceanographic processes. Pergamon Press, New York, 330 pp.

Pilkey, O.H., B.W. Blackwelder, L.J. Doyle, and E.L. Estes. 1969. Environmental significance of the physical attributes of calcareous sedimentary particles. Transactions Gulf Coast Association of Geological Societies, 19:113-114.

Powell, E.N. and H.C. Cummins. 1985. Are molluscan maximum life spans dominated by long-term cycles in benthic communities? Oecologia (Berlin), 67:177-182.

Powell, E.N. and D.J. Davies. 1990. When is an "old" shell really old? J.Geol., 98:823-844.

Powell, E.N. and R.J. Stanton, Jr. 1985. Estimating biomass and energy flow of molluscs in paleo-communities. Palaeontology (London), 28:1-34.

Powell, E.N., G.M. Staff, D.J. Davies, and W.R. Callender. 1989. Macrobenthic death assemblages in modern marine environments: formation, interpretation and application. Critical Reviews in Aquatic Science, 1:555-589.

Rau, G.H. 1981. Hydrothermal vent clam and tube worm $^{13}C/^{12}C$: further evidence of non-photosynthetic food sources. Science, 213:338-340.

Rau, G.H. 1985. $^{13}C/^{12}C$ and $^{15}N/^{14}N$ in hydrothermal vent organisms: Ecological and biogeochemical implications. Bull. Biol. Soc. Wash., 6:243-248.

Rau, G.H. and J.I. Hedges. 1979. Carbon-13 depletion in a hydrothermal vent mussel: Suggestion of a chemosynthetic food source. Science, 203:648-649.

Rosman, I., G.S. Boland, and J.S. Baker. 1987. Epifaunal aggregations of Vesicomyidae on the continental slope off Louisiana. Deep-Sea Res., 34:1811-1820.

Roux, M., M. Rio, E. Schein, R.A. Lutz, L.W. Fritz, and L.M. Ragone. 1989. Mesures in situ de la croissance des bivalves et des vestimentifères et de la corrosion des coquilles au site hydrothermal de 13°N (dorsale du Pacifique oriental). Comptes Rendus des Seances de l'Academie des Sciences Serie III, 308:121-127.

Rowe, G., M. Sibuet, J. Deming, A. Khripounoff, J. Tietjen, S. Macko, and R. Theroux. 1991. Total sediment biomass and preliminary estimates of organic carbon residence time in deep-sea benthos. Marine Ecology Progress Series, 79:99-114.

Ruby, E.G., H.W. Jannasch, and W.G. Deuser. 1987. Fractionation of stable carbon isotopes during chemoautotrophic growth of sulfur-oxidizing bacteria. Appl. Envir. Micro., 53:1940.

Scott, R. 1978. Approaches to trophic analysis of paleocommunities. Lethaia, 11:1-14.

Simberloff, D. and T. Dayan. 1991. The guild concept and the structure of ecological communities. Annual Review of Ecology Systematics, 22:115-143.

Silverman, M.P. and V.I. Oyama. 1968. Automatic apparatus for sampling and preparing gases for mass spectral analysis in studies of carbon isotope fractionation during mathane metabolism. Analytical Chem., 40:1833.

Staff, G., E.N. Powell, R.J. Stanton, Jr., and H. Cummins. 1985. Biomass: is it a useful tool in paleocommunity reconstruction? Lethaia, 18:209-232.

Stanton Jr., R.J. and P.C. Nelson. 1980. Reconstruction of the trophic web in paleontology: community structure in the Stone City Formation (Middle Eocene, Texas). Journal of Paleontology, 54:118-135.

Stanton Jr., R.J., E.N. Powell, and P.C. Nelson. 1981. The role of carnivorous gastropods in the trophic analysis of a fossil community. Malacologia, 20:451-469.

Troutman, B.M. and G.P. Williams. 1987. Fitting straight lines in the earth sciences. In: Size, W.B., ed., Use and abuse of statistical methods in the earth sciences. New York: Oxford University Press. pp. 107-128

Waren, A. and W.F. Ponder. 1991. New species, anatomy, and systematics position of the hydrothermal vent and hydrocarbon seep gastropod family *Provaidae fam.*n (Caenogastropoda). Zoologica Scripta, 20:27-56.

Williams, G.P. and B.M. Troutman. 1987. Algebraic manipulation of equations of best-fit straight lines, pp. 129-141. In: W.B. Size (ed.), Use and abuse of statistical methods in the earth sciences. Oxford University Press, New York.

As the Nation's principal conservation agency, the Department of the Interior has responsibility for most of our nationally-owned public lands and natural resources. This includes fostering sound use of our land and water resources; protecting our fish, wildlife, and biological diversity; preserving the environmental and cultural values of our national parks and historical places; and providing for the enjoyment of life through outdoor recreation. The Department assesses our energy and mineral resources and works to ensure that their development is in the best interests of all our people by encouraging stewardship and citizen participation in their care. The Department also has a major responsibility for American Indian reservation communities and for people who live in island territories under U.S. administration.